Robust Nonlinear Control Design with Proportional-Integral-Observer Technique

Von der Fakultät für Ingenieurwissenschaften,
Abteilung Maschinenbau und Verfahrenstechnik der
Universität Duisburg-Essen
zur Erlangung des akademischen Grades

DOKTOR–INGENIEURIN

genehmigte Dissertation

von

Yan Liu
aus
Liaoning, VR China

Referent: Univ.-Prof. Dr.-Ing. Dirk Söffker
Korreferent: Univ.-Prof. Dr.-Ing. Steven Liu
Tag der mündlichen Prüfung: 13. Januar 2011

Preface

This doctoral thesis presents parts of the results from my research at the Chair Dynamics and Control (SRS) at the University of Duisburg-Essen during 2006-2010.

First of all, I would like to thank my supervisor Univ.-Prof. Dr.-Ing. Dirk Sffker for offering me this chance to work on my dissertation at the Chair SRS in Germany, which is not only significant for my scientific career but also very important for my personal life. I really appreciate his valuable input and comments related to my thesis, his zeal to engage me in intense scientific discussions and for his guidance in my chosen career path.

Secondly, I would like to thank Univ.-Prof. Dr.-Ing. Steven Liu, my second supervisor, for assisting me with helpful discussions and giving me generous advice for my life after graduation.

I would also like to use this opportunity to give my thanks to all my longterm and short-term colleagues at the Chair SRS, with whom I have had many scientific and non-scientific conversations, allowing me to have a wonderful time at the chair and in Duisburg and for helping me learn interesting cultures, especially from my dear arabic friends.

Special thanks to our secretaries Mrs. Doris Schleithoff and Yvonne Vengels for assisting me in my daily life at SRS; to Mr. Kurt Thelen for teaching me the fundamentals in hydraulics and with test rigs; and to my colleagues Kai Dettmann, Dennis Gamrad, Frank Heidtmann, Marcel Langer, Markus zbek, and Fan Zhang for the careful proof-reading of my thesis and presentation.

In remembrance of Dr. Wend, I would like to acknowledge him for his support and guidance.

Most importantly, I would like to thank my parents, Guanglan Zhang and Yuejun Liu, as well as my husband Shen Wang for their love and encouragement which gave me the strength to complete this thesis.

Duisburg, March 2011 Yan Liu

Dedicated to my father

Liu, Yuejun
1954 - 2009

Contents

Abbreviations

API-Observer	Advanced Proportional-Integral-Observer
EFL-Lue	the classical Exact Feedback Linearization method combined with Luenberger observer
EFL-PIO	the proposed robust control approach as a combination from Exact Feedback Linearization and PI-Observer
EKF	Extended Kalman Filter
FDI	Fault Detection and Isolation
KF	Kalman Filter
LMI	Linear Matrix Inequality
LQR	Linear Quadratic Regulator
LTR	Loop Transfer Recovery
MIMO	Multi-Input Multi-Output
PI-Observer	Proportional-Integral-Observer
PLC	Programmable Logic Controller
SISO	Single-Input Single-Output
SHM	Structural Health Monitoring
UIO	Unknown Input Observer
UKF	Unscented Kalman Filter

1 Introduction

Control technique is one of the most important techniques which has received significant attentions in the last century. Its rapid development changes people's way of life and evokes an age of automation. Along the history of control technique, the observer technique, as an essential basic to realize the control design on practical systems due to the expensive or inaccessible measurements, has been a key research focus and shows great potentials in the area of fault diagnosis and fault detection. Observer-based control and observer-based fault diagnosis are still current key research areas. In this part, the idea motivating this thesis is introduced with the review of observer technique and robust nonlinear control.

1.1 Development of observer technique

In the classical control theory, the observer technique is known as a method for reconstructing system states by using measured inputs and outputs of the system and can also assist in fault detection, etc. The standard classical state observer was first proposed and developed by Luenberger in [85–87] in the early sixties of the last century. Since then, observer technique has been developing rapidly and continuously. Several different directions of observer design are evolved, for example, optimal observer design [83, 100] and nonlinear observer design [61, 71, 99]. According to their structures, orders, observer gains, or considered classes of systems, observers can be classified as:

- linear and nonlinear observer;
- full-order, reduced-order, and minimal-order observer;
- high gain observer, sliding mode observer, and adaptive observer; and
- observer design for time-varying systems[122, 123], nonlinear systems [17, 27, 133], stochastic systems [16, 132], etc.

In the following parts of the thesis, the observer design for time invariant systems will be considered.

1.1.1 Review of observer technique

In order to reduce the complexity of the introduction and to avoid unnecessary repetition of fundamentals in control technique, the review of observer design is made within certain interested aspects.

During the development of observer technique, one of the current research directions is the observer design for systems with both known and unknown inputs, the so-called Unknown Input Observer (UIO), because external inputs to the system are not always available from measurements. In this context, disturbances or modeling errors can be considered as unknown inputs as well. Most of the representative contributions [8, 21, 30, 40, 45, 46, 127] focus on plausible state estimation with unknown inputs, where the UIO proposed in [8] uses geometric theory, the one in [30] applies a well-known strategy to decouple the effects from the disturbance, and the UIO in [46] introduces a sliding mode unknown input observer for the state estimation. Furthermore, Proportional-Integral-Observer (PI-Observer) is proposed in [130] as an UIO with a simple structure, which is developed and applied by many researchers [6, 57, 110] also to improve the robustness of the state estimations.

In addition to the mentioned state observers as UIOs, state and disturbance observers [19, 31, 39, 70, 76, 102, 118, 120] have also been developed to estimate states and unknown inputs as disturbances simultaneously. In [39], the disturbance is assumed to satisfy differential equations with arbitrary characteristic roots. Stein and Park also proposed in [102, 120] a state and disturbance observer based on singular value decomposition, where the differentiation of the output measurement is needed in the algorithm. In [19], a state and disturbance observer is designed based on the same concept as in [102], but no derivatives of the outputs are required, here the unknown inputs have to satisfy some additional bounds. Later in [115, 118], it is shown that the PI-Observer can be used as a high-gain observer to estimate both the original states and the extended states (the unknown inputs/disturbances), if high observer gains are used. Additionally, no strong or special restrictions of the disturbances are required. Another kind of state and disturbance observer is introduced in [76] based on inverse dynamics and derivatives of output signals. To solve the problem with noise using direct differentiation of measurements, the proposed observer is adjusted by introducing a new design parameter [77]. A nonlinear state and disturbance observer is proposed in [70] based on the concept of nonlinear state observer design from [61, 71]. Here, a nonlinear transformation of the states and disturbances satisfying certain singular partial differential equations is required. A nonlinear observer is also proposed in [31] to estimate the state and disturbance simultaneously. In this thesis, the nonlinearity of the system has to be a Lipschitz function of the states, inputs, disturbances, and uncertainties.

Furthermore, UIOs only estimating disturbances in order to realize disturbance rejection and attenuation are outlined in [38, 51]. The disturbance observer in [38] is based on inverse dynamics in frequency domain and it is applied for servo systems [72, 124]. The same observer is compared in [108] with another disturbance observer proposed and developed in [18, 51, 105], which is also designed in frequency domain. According to the comparison, the filter structure in the disturbance observer from [38] is not trivial, while a model for the dynamics of disturbance is preconditioned for the observer in [51].

After the review and discussion of the different kinds of UIOs, it can be seen that UIOs designed for different types of specific systems have been proposed and no UIO design is generally applicable. Therefore, this thesis is focusing on the observer designs for broader applications and taking full effect of their functions.

Besides UIOs, Kalman Filter (KF) techniques have to be mentioned as well. The KF (firstly introduced in [58]) can also be seen as a special type of observer, which can estimate state variables of a system with white and Gaussian disturbances and noises. Due to its special properties in consideration of the noises, it has been used in numerous engineering areas. For nonlinear systems, the Extended Kalman Filter (EKF) based on first-order linearization at each time step is proposed in [20, 65]. Both the KF and the EKF algorithms are based on the propagation of a Gaussian random variable through the system dynamics, which can lead to errors in the posterior mean and covariance. Therefore, the Unscented Kalman Filter (UKF) for nonlinear estimation is proposed later by [54] to achieve better accuracy of the estimations (to the 3rd order in Taylor series expansion). The EKF and UKF can also be used for dual estimation (the state and parameter estimation).

1.1.2 Analysis of observer technique development

After the short review of observer techniques, the purpose of observer design will be discussed as follows. When the realization of efficient measurements is technically too difficult or economically too expensive, estimations may be obtained instead of measurements from the considered systems by different kinds of observers. Usually, an observer can be applied for two major goals. Firstly, the estimations obtained from observers are widely applied to realize observer-based control for practical systems as standard observer-based state feedback for linear systems or more complicated observer-based control for specific systems. For example, in [73] an observer-based adaptive fuzzy-neural control is designed for unknown nonlinear dynamical systems, in [15] a fuzzy observer-based robust fuzzy control for nonlinear systems, and in [107] an observer-based control for piecewise-affine systems. Secondly, the application of observer technique is naturally extended to the research area of monitoring sensors and systems, fault diagnosis, and Fault Detection and Isolation (FDI) in the early development of observers in [7, 53] besides the observer-based control. The development of the observer-based FDI has been summarized in [22].

For both of the two major application goals, state and disturbance observers show advantages over the observers with unique estimation purpose. As discussed, among the state and disturbance observers the PI-Observer as high-gain observer, which can be classified as in Figure 1.1, has the simplest structure and needs no derivatives of the measurements or nonlinear transformation. The widely applied KF technique and its extensions are also known as an alternative solution for dual estimation task. In comparison, the EKF can estimate the states and parameters of the system but the focus is to get good estimation quality considering the existence of measurement noise and process noise as with known covariance and zero mean, where nonrandom disturbances and modeling errors are not considered. More generally, the PI-Observer assumes bounded disturbances but no other limitations with respect to the dynamics of disturbances.

The advantages of high gain PI-Observer are summarized as follows: The high gain

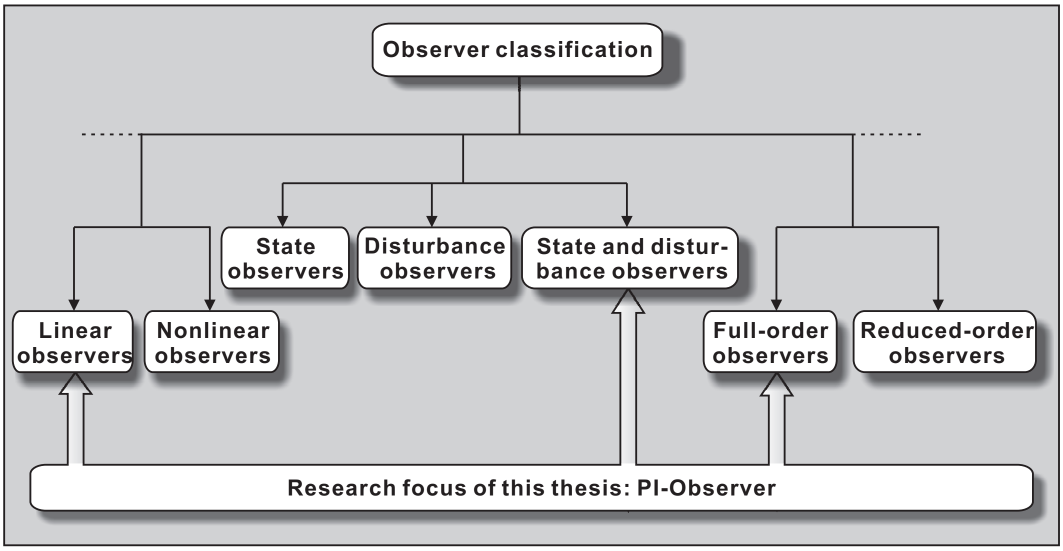

Figure 1.1: Classification of observers

PI-Observer

- has a simple linear structure in contrast to nonlinear observers;
- is robust against disturbances and noise compared with Luenberger observer or observers without the integral part in the feedback of estimation errors;
- estimates the states and unknown inputs simultaneously in comparison with state or disturbance observers;
- requires no special limitations on the type of disturbances compared with other kinds of state and disturbance observers; and
- assumes no statistic information from process and measurement noise in contrast with EKF.

The disadvantages and limitations of PI-Observer are that

- the location where the unknown inputs affect the system is assumed as known;
- at least a nominal linear state space model of system has to be available, so that the nonlinear or unknown parts can be considered as unknown inputs; and
- to estimate both the states and the unknown inputs, more independent measurements could be required than for a state observer.

Since the PI-Observer is applied as a state and disturbance observer in [118], many applications have been done to realize robust control or fault diagnosis, in [67] for elastic mechanical systems modeled by finite element method and in [60] for a hydraulic system with simplified linear model. But no robust control or fault diagnosis of complex systems with nonlinear models have yet been considered using the PI-Observer technique. Therefore, the focus of this thesis is chosen on the advanced high-gain PI-Observer design and its application to observer-based robust nonlinear control. In the next part, the development and state of the art of robust nonlinear control approaches will be discussed.

1.2 Development of robust nonlinear control

Due to the inevitable nonlinearities in real systems, many nonlinear control methods are developed. In remarkable textbooks as [47, 62, 114] several classical nonlinear control methods (e.g., feedback linearization, sliding mode control, backstepping approach) are described in detail. For the exact feedback linearization method all the states and a precise model from the system to be controlled are required and the robustness of the closed-loop system is not guaranteed due to parameter uncertainties or modeling errors. With sliding mode control uncertainties and modeling errors in system models can be handled, but it can only be applied, when chattering in the control input is acceptable. According to the situation in nonlinear control, researchers have struggled for decades to realize robust and practical solutions for nonlinear systems by proposing different approaches or mostly improving classical control methods. Considering the availability of the states and the most commonly used full state feedback, observer-based robust nonlinear control approaches have also been discussed in a large number of research works to achieve this goal.

In [32] an exact feedforward linearization approach based on differential flatness for nonlinear system control is proposed, which has also robustness problem as the classical feedback linearization method. Hence, the authors discuss later in [33] its robustness with respect to uncertainties and disturbances. In [34], a robust nonlinear predictive control based on exact feedforward linearization is introduced. It demonstrates that the nonlinear flatness-based control methods are applicable and rational. Unfortunately, the assumptions with respect to disturbances and the availability of all the states are not discussed.

In [28, 89, 91, 101, 104] different methods are developed and applied to solve the robustness problem of the exact feedback linearization method. However, the modeling errors or the disturbances are considered with known bounds and/or known dynamical properties within most of the methods [89, 101, 104]. Robust feedback linearization methods are proposed by improving the design of the nonlinear feedback in [28, 91].

Robust nonlinear H_∞ control approaches have been introduced in [48, 49] also to solve the problem in nonlinear control with external disturbances and uncertainties. With this method, a nonlinear partial differential equation (a Hamilton-Jacobi equation) has to be solved, which is not a trivial task and in some cases not possible.

Besides the robustness, availability of the states has also been considered in nonlinear control design. Of course, observer-based control design, especially controllers based on state and disturbance observers or only disturbance observers, have been studied to improve the robustness of classical nonlinear control and realize tasks like fault diagnosis, e.g., in [13–15, 25]. The discrete-time method in [13, 14] can solve the robust control problem of linear Multi-Input Multi-Output (MIMO) systems with mismatched disturbances that do not change significantly in two consecutive sampling instances. That means the rate of disturbances is limited. In [25] a robust control is proposed for a class of uncertain nonlinear systems without assumption of passifiability. The proposed control approach in [25] is based on an adaptive observer design and can partially linearize considered systems. Considering no disturbances, the adaptive control approach is suitable for a general class of nonlinear systems. However, it can only be applied to nonlinear systems with a basic linear time-invariant state space representation and additive nonlinearities, when external disturbances and especially measurement noise exist.

From 2007, the International Journal of Robust and Nonlinear Control offers regularly literature surveys [1] introducing the current research results in nonlinear and robust control as well as in monitoring and fault detection. In the surveys, it can be found that the robust H_∞ methods [29, 44, 103, 131], the Linear Matrix Inequality (LMI) based approaches [106, 126], and the methods as combinations of different approaches are discussed frequently for the application on different kinds of systems (e.g., time-delay systems, descriptor systems, etc.) besides the classical nonlinear control methods, for instance the flatness-based methods, sliding mode control, and adaptive control. The H_∞ technique and the rapidly developed LMI-based method [9] (since successfully solving LMIs by computer convex programming in the 1980's) are both based on realizing optimization problems of the control loop. The difficulties in the design with the two methods lie in the problem formulation, which should be appropriate addressed to make the relevant and important properties of the closed-loop optimized. Nonlinear constraints such as saturation are generally difficult to be handled. The level of mathematical understanding is also an obstacle for their practical application.

On the other hand, the high-gain PI-Observer as a state and disturbance observer can be applied to design an observer-based nonlinear robust control. Due to the simple linear structure of the PI-Observer, the best complementary method for the PI-Observer in nonlinear control design is the exact feedback linearization approach. The PI-Observer can offer the estimations of the states and unknown inputs for the exact feedback linearization. The linearized model generated by the feedback linearization is appropriate for the PI-Observer design. The combination of the two approaches may be a potential robust nonlinear control method for the class of nonlinear systems that is suitable for the classical exact feedback linearization method. Although the combined approach is also concentrated on a small part of nonlinear systems, the simple structure of the PI-Observer and the classical design of the exact feedback linearization ensure that the approach is easily understood by engineers and therefore a wide application in industry may be possible.

Until today, there is still no standard control design process for nonlinear systems. All the proposed approaches can only partially solve the control problem of a certain class of nonlinear systems; but from the directions and trends of the development it can be concluded that the observer-based methods have advantages in getting unmeasured system states (and disturbances with disturbance observer) and are of great interest. That motivates the research about the PI-Observer-based nonlinear robust control.

1.3 Motivation and tasks of the thesis

In the research areas in mechanical engineering, control design for mechanical systems is a very important branch. In order to avoid nonfeasible measurements or to save costs, observers are usually utilized to augment or replace sensors in a control system. As discussed, observer-based control has been widely applied and well developed. From the review of the observer technique, it can be clearly seen that the state and disturbance observers have advantages in relation to state observers and disturbance observers in reconstructing the state and disturbance simultaneously and are therefore appropriate for disturbance attenuation, disturbance rejection, and fault diagnosis in control systems. Among the state and disturbance observers, the high-gain PI-Observer is the one with almost the simplest structure and design process. Although there are already some development and applications based on the high-gain PI-Observer, the general problem of high gains that leads to large overshoot and strong influence from measurement noise in the control and estimation performance is not solved. On the other hand, due to the linear structure of the PI-Observer, its application on complicated nonlinear systems is limited and has not been studied. Weighing the advantages and disadvantages of PI-Observer and considering its development history, it can be concluded that there is still space for future development of PI-Observer in optimal design of the observer gains and in the area of robust nonlinear control for mechanical systems. Based on this starting point, the focus of this work is chosen to improve the high gain design process for the PI-Observer and to develop a robust nonlinear control based on the PI-Observer for possible general application in nonlinear systems.

After introducing the basic ideas and motivations of the work, the tasks of this work are arranged in the following points:

- analyzing the design of PI-Observer, especially the observer gain design;
- developing an adaptive algorithm to determine the gains automatically according to the current dynamics of the system;
- searching for a possible application of PI-Observer in nonlinear control to improve the robustness of the control loop; and
- studying the applicability of PI-Observer in mechanical systems, especially in nonlinear mechanical systems.

1.4 Organization of the thesis

After the introduction, PI-Observer design especially the high-gain PI-Observer design is systematically discussed and the online adjustment of the PI-Observer gains proposed as an Advanced PI-Observer (API-Observer) is detailed in the second chapter. At the same time, the implementation of the addressed adjustment algorithm is included showing the adaption of the PI-Observer gains to the current situation of system dynamics and disturbances on a practical system with simulation results and real measurements respectively.

Secondly, a high gain PI-Observer-based nonlinear control method is proposed as a combination of the classical Exact Feedback Linearization method and the PI-Observer (EFL-PIO). Directly after it, the applicability on mechanical systems is surveyed. Numerical examples of mechanical systems are given to illustrate the application of the EFL-PIO approach in the third chapter.

In the fourth chapter, the implementation of the proposed PI-Observer-based nonlinear control method is illustrated in detail on a hydraulic cylinder system for its position control. Besides that, the position control for the cylinder system without direct position measurement is realized with the PI-Observer applied as virtual sensor. Here a discrete-time control algorithm is developed and programmed to satisfy the normal industrial requirement.

The last chapter summarizes the whole thesis and gives suggestions for future work.

2 Advanced PI-Observer Design

PI-Observers have been developed for several decades. The general PI-Observer design will be shortly reviewed, new improvements and analysis of the PI-Observer design will be discussed in this part.

2.1 Review of PI-Observer technique

PI-Observer was firstly introduced as a term by Wojciechowski in [130] for single-input single-output systems and then applied by others in [57, 110] for multivariable systems. It has an additional integral loop in the feedback of estimation error in comparison with a Luenberger observer, which has a similar structure as the extended state observer proposed by [97] for disturbance estimations. The integral part in feedback besides the proportional feedback leads to the special structure as well as the name of PI-Observer and offers additional degrees of freedom for the estimation task in two aspects, the one in improving robustness of estimations or observer-based control [110] and the other in estimations of both the states and the unknown inputs as a state and disturbance observer [97]. That leads to the development of PI-Observers in two main directions summarized below with literatures, where the term PI-Observer for the observer with integral loop in the feedback of estimation error additionally to the proportional loop is applied.

One direction is mainly to improve the robustness of control loops and state estimations. Robust control based on PI-Observer is discussed in [6, 128], robust loop transfer recovery in [98] and robust state estimation by attenuating both measurement noise and modeling errors in [12]. A robust output derivative estimation method based on PI-Observer is recently introduced in [111] as well. Besides the classical PI-Observer design, some new estimators inspired by the concept of the additional integral loop are proposed to improve the robustness of different control and estimation tasks. One of them is proportional integral KF addressed in [63] to increase the robustness of KF with inaccurate models of measurement and process noise. In [75] it is developed as a proportional fading-integral KF to increase the stability margin and allow the rejection of unknown transitory disturbances. In [63, 75], the filter gains are designed by trial and error process. An optimal design strategy for the filter gains based on Riccati equation to get minimum error variance is given in [4] and a LMI-based design method for the filter gains is introduced in [55] for a class of stochastic linear systems. Furthermore, a proportional integral adaptive observer is proposed in [74] and developed in [56, 113, 125] systematically for disturbance rejection with unknown system parameters.

In the other direction, the PI-Observer is used as state and disturbance observer with high observer gains to estimate both the original states and the unknown inputs as extended states as introduced in [97]. The proposed extended observer in [97] is also classified as PI-Observer due to its structure and can be applied to estimate nonlinearities [92, 93] and unknown inputs for quantitative disturbance rejection or fault diagnosis [68, 118]. The application of PI-Observer to estimate disturbances and nonlinearities as unknown inputs has been realized in many areas. For example it is applied to robust control of robotic systems with unknown nonlinearities from kinematics or friction [5, 42, 94]. It is also discussed for dynamical systems in [118] and later for mechanical systems in [67, 68, 115] for example to estimate the contact force [67] and to estimate unmeasured states and disturbance force as virtual sensors [35, 60]. The estimations from PI-Observer are utilized for monitoring elastic structures in [36] and for fault identification in [37] as well.

Both of the two directions of PI-Observer development still catch attentions from researchers. The classical PI-Observer and its variants (e.g., proportional integral adaptive observer) are one of the possibilities to improve the robustness of control design but do not show dominant advantages in relation to other methods. PI-Observer as high gain observer is able to estimate the disturbances and unknown effects of systems as unknown inputs together with the states. This gives the possibility for its application in a quantitative fault diagnosis and at the same time in an observer-based robust control design. Hence this thesis work concentrates on the development of the high gain PI-Observer design and its applications.

Although the high gain PI-Observer has been applied in different areas to estimate disturbances and to detect faults as mentioned above, the basic problem of high observer gains still has to be considered. The high observer gains should be kept as low as possible within performance allowance. In other words, the current observer gains should be chosen according to a compromise between the desired estimation performance and resulting negative effects. The design of PI-Observer gains has been discussed since its first application. Classical pole placement method is used in [41, 109, 118], which can not solve the high gain design task directly. The observer gains are chosen based on a H_∞ norm minimization in [90, 112] and minimum estimation error variance approaches in [4, 75], whereby high gain PI-Observer is not considered. Eigenstructure assignment for PI-Observer is discussed in [23, 24], where a complete parameterization for the gains and the left eigenvectors is established based on a set of design parameters (eigenvalues of the observer system, parameter vectors with certain dimension, and the integral gain matrix) to offer more degrees of freedom for the design. However, the integral gain matrix is very important for the PI-Observer design especially for the high-gain PI-Observer design and should not be chosen without any care. In [67, 115], the high gains in PI-Observer are designed based on the Linear Quadratic Regulator (LQR) and Loop Transfer Recovery (LTR) method, but the order of magnitude for the observer gains is determined with previous analysis qualitatively; no systematic/analytical approach has been developed for the determination of high PI-Observer gains.

The task to design high gain observer suitably is explored in [2, 26]. Solutions are recommended for the high gain design with variable observer gains between two fixed observer gains (usually one high gain and one low gain) according to distinguished switching conditions. Of course using two gains to be switched is under the consideration of the clarity of the programming and the simplification of the structure. However, the problem choosing suitable observer gains for the high gain PI-Observer can only be roughly solved with approaches using two fixed observer gains, because the level of the high and low gains is difficult to be determined to match every case of the changing unknown inputs. For example, in [26] the observer gains are switched only once regarding the transient time, but for high gain PI-Observer design the dynamics of the unknown inputs (also of modeling disturbances) may strongly change along the time and several switches with different transient time intervals may be necessary. In [2] the observer gains are also switched regarding to pre-defined transient time, but more generally the switch is not limited as only once. However, both the two given observer gains have to be suitably chosen in advance. That means the high observer gains have to be determined based on assumed situations which can not match every requirement during the whole working time and this approach is not a suitable one to solve the mentioned problem to choose suitable gains for the high gain PI-Observer. To solve the design problem of observer gains for the high gain PI-Observer, one design method adapting the high gains to different situations and requirements will be discussed after the introduction of the general high gain PI-Observer design. The proposed observer with adaptive gains is named as Advanced PI-Observer (API-Observer).

2.2 General high gain PI-Observer design

In this part, the PI-Observer applied and developed in [118] is introduced.

For a class of systems described by

$$\dot{\boldsymbol{x}}(t) = \boldsymbol{A}\boldsymbol{x}(t) + \boldsymbol{B}\boldsymbol{u}(t) + \boldsymbol{N}\boldsymbol{d}(\boldsymbol{x},t) + \boldsymbol{E}\boldsymbol{g}(\boldsymbol{x},t), \tag{2.1}$$

$$\boldsymbol{y}(t) = \boldsymbol{C}\boldsymbol{x}(t) + \boldsymbol{h}(t), \tag{2.2}$$

with the state vector $\boldsymbol{x}(t) \in \mathbb{R}^n$, the input vector $\boldsymbol{u}(t) \in \mathbb{R}^l$, the measurement vector $\boldsymbol{y}(t) \in \mathbb{R}^m$, the time variant and unknown inputs $\boldsymbol{d}(\boldsymbol{x},t) \in \mathbb{R}^r$, the measurement noise $\boldsymbol{h}(t) \in \mathbb{R}^m$, and the unmodeled dynamics $\boldsymbol{E}\boldsymbol{g}(\boldsymbol{x},t)$ with $\boldsymbol{g}(\boldsymbol{x},t) \in \mathbb{R}^p$ and $\boldsymbol{E} \in \mathbb{R}^{n\times p}$. Here, the information about the dynamics of $\boldsymbol{d}(\boldsymbol{x},t)$ is assumed as unavailable. Only the matrix $\boldsymbol{N}$ denoting the position of the unknown inputs acting to the system is assumed as known. The aim is, with the given information of the system model, the matrices $\boldsymbol{A} \in \mathbb{R}^{n\times n}$, $\boldsymbol{B} \in \mathbb{R}^{n\times l}$, $\boldsymbol{C} \in \mathbb{R}^{m\times n}$, and $\boldsymbol{N} \in \mathbb{R}^{n\times r}$, to estimate the dynamical behavior of the system and the dynamics of the unknown inputs. The system matrix $\boldsymbol{A}$ is assumed stable.

The basic idea for the estimation of time dependent unknown inputs in [51, 92, 97] is to approximate the dynamics of the unknown inputs $\boldsymbol{d}(t)$[1)] by a fictitious linear dynamical

[1)] Note that the unknown inputs $\boldsymbol{d}$ is allowed to be a function of known inputs $\boldsymbol{u}(t)$ and states $\boldsymbol{x}(t)$ as system

$$\dot{\boldsymbol{v}}(t) = \boldsymbol{V}\boldsymbol{v}(t), \tag{2.3}$$

where the unknown inputs are described by

$$\boldsymbol{d}(t) \approx \boldsymbol{H}\boldsymbol{v}(t). \tag{2.4}$$

Considering the states in (2.3) as extended states of system (2.1), an extended system description is set up by

$$\begin{bmatrix} \dot{\boldsymbol{x}}(t) \\ \dot{\boldsymbol{v}}(t) \end{bmatrix} = \underbrace{\begin{bmatrix} \boldsymbol{A} & \boldsymbol{N}\boldsymbol{H} \\ \boldsymbol{0} & \boldsymbol{V} \end{bmatrix}}_{\boldsymbol{A_e}} \begin{bmatrix} \boldsymbol{x}(t) \\ \boldsymbol{v}(t) \end{bmatrix} + \underbrace{\begin{bmatrix} \boldsymbol{B} \\ \boldsymbol{0} \end{bmatrix}}_{\boldsymbol{B_e}} \boldsymbol{u}(t) + \begin{bmatrix} \boldsymbol{E}\boldsymbol{g}(t) \\ \boldsymbol{0} \end{bmatrix} \tag{2.5}$$

$$\boldsymbol{y}(t) = \underbrace{\begin{bmatrix} \boldsymbol{C} & \boldsymbol{0} \end{bmatrix}}_{\boldsymbol{C_e}} \begin{bmatrix} \boldsymbol{x}(t) \\ \boldsymbol{v}(t) \end{bmatrix}, \tag{2.6}$$

with the same assumption for unmodeled dynamics $\boldsymbol{E}\boldsymbol{g}(\boldsymbol{x}, t)$ as for the unknown inputs $\boldsymbol{d}(\boldsymbol{x}, t)$. Appropriate matrices $\boldsymbol{V}$ and $\boldsymbol{H}$ can be easily determined (e.g., in [50–52, 84]), if the dynamical behavior of disturbances $\boldsymbol{d}(t)$ is known or the disturbances are constant or slowly varying. However, the task considered here does not assume that the dynamical behavior of $\boldsymbol{d}(t)$ is known. With this consideration, it is discussed and shown theoretically in [92, 117] and with practical application examples in [64, 66, 116, 118] that the choice $\boldsymbol{V} = \boldsymbol{0}$ or $\boldsymbol{V} \to \boldsymbol{0}$ and $\boldsymbol{H} = \boldsymbol{I}$ for the estimation of time dependent unknown inputs is appropriate. The extended system can be described by

$$\begin{bmatrix} \dot{\boldsymbol{x}}(t) \\ \dot{\boldsymbol{d}}(t) \end{bmatrix} = \underbrace{\begin{bmatrix} \boldsymbol{A} & \boldsymbol{N} \\ \boldsymbol{0} & \boldsymbol{0} \end{bmatrix}}_{\boldsymbol{A_e}} \begin{bmatrix} \boldsymbol{x}(t) \\ \boldsymbol{d}(t) \end{bmatrix} + \underbrace{\begin{bmatrix} \boldsymbol{B} \\ \boldsymbol{0} \end{bmatrix}}_{\boldsymbol{B_e}} \boldsymbol{u}(t) + \begin{bmatrix} \boldsymbol{E}\boldsymbol{g}(t) \\ \boldsymbol{0} \end{bmatrix} \tag{2.7}$$

$$\boldsymbol{y}(t) = \underbrace{\begin{bmatrix} \boldsymbol{C} & \boldsymbol{0} \end{bmatrix}}_{\boldsymbol{C_e}} \begin{bmatrix} \boldsymbol{x}(t) \\ \boldsymbol{d}(t) \end{bmatrix}, \tag{2.8}$$

with $\boldsymbol{d}(t) \approx \boldsymbol{v}(t)$. The choice of $\boldsymbol{V} = \boldsymbol{0}$ and $\boldsymbol{H} = \boldsymbol{I}$ results in an integral part in the classical PI-Observer shown in Figure 2.1.

2.2.1 Structure of a high gain PI-Observer

In this part, the general high-gain PI-Observer design described in [115] for the considered class of systems (2.1)-(2.2) will be introduced briefly. The purpose of the approach is the robust estimation of unknown inputs without any assumptions about their dynamics. For

$\boldsymbol{d}(\boldsymbol{x}, \boldsymbol{u}, t)$. Due to the fact that no information of the dynamical behavior is available, it is written as $\boldsymbol{d}(t)$ without loss of generality.

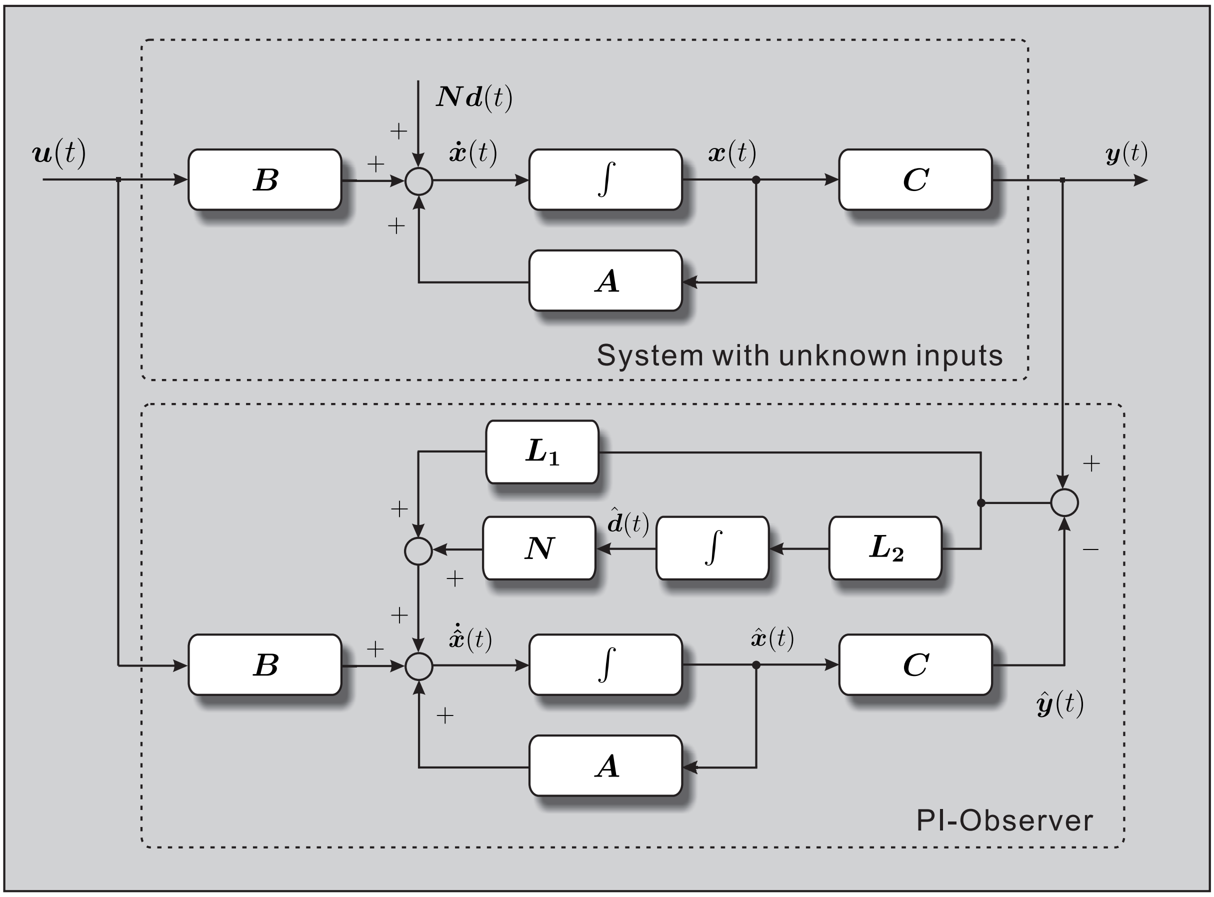

Figure 2.1: Structure of PI-Observer [118]

the PI-Observer design, the system in (2.1)-(2.2) is considered as a system described in (2.7)-(2.8) with extended states.

The states $\boldsymbol{x}(t)$ and the unknown inputs $\boldsymbol{d}(\boldsymbol{x}, t)$ in (2.1) can be estimated by a high-gain observer design

$$\begin{bmatrix} \dot{\hat{\boldsymbol{x}}}(t) \\ \dot{\hat{\boldsymbol{d}}}(t) \end{bmatrix} = \underbrace{\begin{bmatrix} \boldsymbol{A} & \boldsymbol{N} \\ \boldsymbol{0} & \boldsymbol{0} \end{bmatrix}}_{\boldsymbol{A_e}} \begin{bmatrix} \hat{\boldsymbol{x}}(t) \\ \hat{\boldsymbol{d}}(t) \end{bmatrix} + \underbrace{\begin{bmatrix} \boldsymbol{B} \\ \boldsymbol{0} \end{bmatrix}}_{\boldsymbol{B_e}} \boldsymbol{u}(t) + \underbrace{\begin{bmatrix} \boldsymbol{L_1} \\ \boldsymbol{L_2} \end{bmatrix}}_{\boldsymbol{L}} (\boldsymbol{y}(t) - \hat{\boldsymbol{y}}(t)), \tag{2.9}$$

$$\hat{\boldsymbol{y}}(t) = \underbrace{\begin{bmatrix} \boldsymbol{C} & \boldsymbol{0} \end{bmatrix}}_{\boldsymbol{C_e}} \begin{bmatrix} \hat{\boldsymbol{x}}(t) \\ \hat{\boldsymbol{d}}(t) \end{bmatrix}. \tag{2.10}$$

The concept of the high gain PI-Observer is similar to the parameter estimation with Extended Kalman Filter (EKF) technique. But the goal here is to use the extended integral parts in the observer to estimate the unknown inputs. In parameter estimation with KF technique, unknown parameters in a system model with well-known structure are estimated and in contrast the time-dependent unknown inputs or nonlinearities without special assumptions are considered as additional extended states to be estimated by high gain PI-Observer. EKF additionally allows the estimation of unknown parameters.

2.2.2 Conditions for the PI-Observer design

A necessary requirement for the PI-Observer design, the full observability of the extended system $(\boldsymbol{A_e}, \boldsymbol{C_e})$

$$rank \begin{bmatrix} \lambda I_n - \boldsymbol{A} & -\boldsymbol{N} \\ \boldsymbol{0} & \lambda \boldsymbol{I}_r \\ \boldsymbol{C} & \boldsymbol{0} \end{bmatrix} = n + r \tag{2.11}$$

for all the eigenvalues λ of A_e, has to be fulfilled to get the estimations of $\boldsymbol{x}(t)$ and $\boldsymbol{d}(t)$, because the PI-Observer is designed for the estimation of the states in the extended system. This condition includes that the dimension of the unknown input vector $\boldsymbol{n}(t)$ has to be less than or equal to the number of independent measurements, namely $r \leq m$ (Proofs refer to [97, 115]). It reflects simultaneously that the measurements/the outputs include indirectly the information of all the states.

2.2.3 Convergence of estimation errors

Based on Eq. (2.9) and Eq. (2.10), considering the estimation errors as $\boldsymbol{e}(t) = \hat{\boldsymbol{x}}(t) - \boldsymbol{x}(t)$ and $\boldsymbol{f_e}(t) = \hat{\boldsymbol{d}}(t) - \boldsymbol{d}(\boldsymbol{x}, t)$, the error dynamics of the extended system becomes

$$\begin{bmatrix} \dot{\boldsymbol{e}}(t) \\ \dot{\boldsymbol{f}}_{\boldsymbol{e}}(t) \end{bmatrix} = \underbrace{\begin{bmatrix} \boldsymbol{A} - \boldsymbol{L}_1\boldsymbol{C} & \boldsymbol{N} \\ -\boldsymbol{L}_2\boldsymbol{C} & \boldsymbol{0} \end{bmatrix}}_{\boldsymbol{A_{e,obs}}} \begin{bmatrix} \boldsymbol{e}(t) \\ \boldsymbol{f_e}(t) \end{bmatrix} - \begin{bmatrix} \boldsymbol{E}\boldsymbol{g}(\boldsymbol{x}, t) \\ \dot{\boldsymbol{d}}(\boldsymbol{x}, t) \end{bmatrix} + \underbrace{\begin{bmatrix} \boldsymbol{L_1} \\ \boldsymbol{L_2} \end{bmatrix}}_{\boldsymbol{L}} h(t). \tag{2.12}$$

The convergence of estimation errors have been discussed in several former research publications [64, 66, 95, 117, 118].

In [95] it is shown that the condition

$$\boldsymbol{C} A^{k-1} \boldsymbol{N} = \boldsymbol{0}, \text{ with } k = 2, ..., n, \tag{2.13}$$

is necessary for the convergence. Detailed discussions and important conclusions both in time domain and frequency domain will be repeated in this part.

Convergence of estimation errors in frequency domain

For a suitable observer design, the feedback matrix $\boldsymbol{L}$ has to be chosen in such a way that the estimation errors tend to zero ($\boldsymbol{e} \to \boldsymbol{0}$, $\boldsymbol{f_e} \to \boldsymbol{0}$). The error dynamics (2.12) is affected by the term $\dot{\boldsymbol{d}}(\boldsymbol{x}, t)$. In [66, 115], the approximative decoupling $\dot{\boldsymbol{d}}(t)$ to $\boldsymbol{e}(t)$, $\boldsymbol{f_e}(t)$ by applying high gains matrix $\boldsymbol{L}$ is introduced and will be repeated here briefly. The error dynamics (2.12) for stationary behavior can be described by

$$\begin{aligned} \boldsymbol{e}(s) &= \boldsymbol{G}^{-1}\boldsymbol{N}\boldsymbol{f_e}(s) - \boldsymbol{G}^{-1}\boldsymbol{E}\boldsymbol{g}(s) + \boldsymbol{G}^{-1}\boldsymbol{L}_1\boldsymbol{h}(s)\,, \qquad (2.14)\\ \boldsymbol{f_e}(s) &= -[s\boldsymbol{I} + \boldsymbol{L}_2\boldsymbol{C}\boldsymbol{G}^{-1}\boldsymbol{N}]^{-1}s\,\boldsymbol{d}(s)\\ &\quad +[s\boldsymbol{I} + \boldsymbol{L}_2\boldsymbol{C}\boldsymbol{G}^{-1}\boldsymbol{N}]^{-1}\boldsymbol{L}_2\boldsymbol{C}\boldsymbol{G}^{-1}\boldsymbol{E}\boldsymbol{g}(s)\\ &\quad +[s\boldsymbol{I} + \boldsymbol{L}_2\boldsymbol{C}\boldsymbol{G}^{-1}\boldsymbol{N}]^{-1}\boldsymbol{L}_2(\boldsymbol{I} - \boldsymbol{C}\boldsymbol{G}^{-1}\boldsymbol{L}_1)\boldsymbol{h}(s), \qquad (2.15) \end{aligned}$$

with $\boldsymbol{G} = [s\boldsymbol{I} - (\boldsymbol{A} - \boldsymbol{L}_1\boldsymbol{C})]$. The state estimation error $\boldsymbol{e}(s)$ and the estimation error of unknown inputs $\boldsymbol{f_e}(s)$ are considered separately. The feedback matrices $\boldsymbol{L}_1$ and $\boldsymbol{L}_2$ are required to stabilize the extended system described by the matrix $\boldsymbol{A_{e,obs}}$ and are also required to minimize the influence from the disturbance $\dot{\boldsymbol{d}}(t)$ as unknown inputs to the estimations $\boldsymbol{e}(t)$ and $\boldsymbol{f_e}(t)$. The two requirements

- $\mathrm{Re}\{\lambda_i\} < 0$, for all the eigenvalues of matrix $\boldsymbol{A_{e,obs}}$, and
- $\|\boldsymbol{L}_2\|_F \gg \|\boldsymbol{L}_1\|_F$.

for the PI-Observer gain matrices design have to be fulfilled. The necessity of the first requirement is comprehensible. The introduction of the second requirement will be explained in the following discussion. From Eq. (2.15), it can be seen that the transfer function from $s\boldsymbol{d}(s)$ to $\boldsymbol{f_e}(s)$ should satisfy $\left\|[\boldsymbol{I}s + \boldsymbol{L}_2\boldsymbol{C}\boldsymbol{G}^{-1}\boldsymbol{N}]^{-1}\right\|_\infty \le \gamma,\ \ \gamma \longrightarrow Minimum$ to minimize the influence from the disturbance $\boldsymbol{d}$ to the estimation error $\boldsymbol{f_e}$.

Assuming without loss of generality a full rank of matrix $\boldsymbol{G}$ and high gains of $\boldsymbol{L}_2$, the values of $\boldsymbol{L}_1$ in $\boldsymbol{G}$ are smaller relative to $\boldsymbol{L}_2$ ($\|\boldsymbol{L}_2\|_F \gg \|\boldsymbol{L}_1\|_F$[2)]), so that γ becomes very small. Assuming that the unknown inputs $\|s\,\boldsymbol{d}(s)\|_F$ are bounded, the estimation error $\|\boldsymbol{f_e}(s)\|_F$ can be reduced to an arbitrarily small value (but not to zero), if the measurement noise and the unmodeled dynamics are not taken into account.

From the two other parts in Eq. (2.15), large $\|\boldsymbol{L}_2\|_F$ will increase the influence from measurement noise $\boldsymbol{h}(s)$ and unmodeled dynamics $\boldsymbol{g}(s)$ to the estimation error $\|\boldsymbol{f_e}(s)\|_F$. In [66, 115] detailed proofs and further applications are given.

Convergence of estimation errors in time domain

Sufficient conditions for an asymptotic stable PI-Observer design are given in [96] as $\left\|\dot{\boldsymbol{d}}\right\| \le g$ and related to the high gains $\boldsymbol{L}_1 \to a\boldsymbol{L}_{10}$, $\boldsymbol{L}_2 \to a\boldsymbol{L}_{20}$, $a \to \infty$. Furthermore, bounds of estimation errors $\|\boldsymbol{e}\|$ and $\|\boldsymbol{f_e}\|$ are discussed [96]. For a given bound of

$$\left\|e^{\boldsymbol{A_e} - \boldsymbol{L}\boldsymbol{C_e}}\right\| \le ce^{-bt}, \quad \text{with } c,\ b > 0, \qquad (2.16)$$

the errors $\boldsymbol{e}$ and $\boldsymbol{f_e}$ are bounded by

$$\|\boldsymbol{e}\| \le ce^{-bt}\,\|\boldsymbol{e_0}\| + \frac{c}{b}(1 - e^{-bt})\left\|\dot{\boldsymbol{d}}\right\| \quad \text{and} \quad \|\boldsymbol{f_e}\| \le \frac{c}{b}g, \ \text{ for } \ t \to \infty. \qquad (2.17)$$

---

2) The norm $\|\cdot\|_F$ denotes here the Frobenius norm, $\|A\|_F = \sqrt{\sum_{i=1}^{m}\sum_{j=1}^{n} a_{ij}^2} = \sqrt{trace(A^*A)}$ for A in $R^{m\times n}$.

In [64], estimation errors in special cases are analyzed in detail. The estimations can be stated by

$$\lim_{t\to\infty}\left[\begin{bmatrix}\hat{\boldsymbol{x}}(t)\\ \hat{\boldsymbol{d}}(t)\end{bmatrix}-\left(\begin{bmatrix}\boldsymbol{x}(t)\\ \mathbf{0}\end{bmatrix}+\sum_{i=1}^{z}\left((\boldsymbol{A_e}-\boldsymbol{LC_e})^{-1}\right)^{i}\begin{bmatrix}\boldsymbol{N}\\ \mathbf{0}\end{bmatrix}\boldsymbol{d}^{(i-1)}(t)\right)\right]=0, \qquad (2.18)$$

if the disturbance is a polynomial of degree $z-1$. Considering constant disturbances $\boldsymbol{d}=\boldsymbol{k}$ and $\boldsymbol{V}\neq 0$, the remaining estimation errors can be set up by

$$\lim_{t\to\infty}\begin{bmatrix}\boldsymbol{e}(t)\\ \boldsymbol{f_e}(t)\end{bmatrix}=(\boldsymbol{A_e}-\boldsymbol{LC_e})^{-1}\begin{bmatrix}\mathbf{0}\\ \boldsymbol{V}\end{bmatrix}\boldsymbol{k}. \qquad (2.19)$$

The estimation results with $\boldsymbol{d}=\boldsymbol{k}$ and $\boldsymbol{V}=0$ are described by

$$\lim_{t\to\infty}\begin{bmatrix}\hat{\boldsymbol{x}}(t)\\ \hat{\boldsymbol{d}}(t)\end{bmatrix}=\begin{bmatrix}\boldsymbol{x}(t)\\ \boldsymbol{k}\end{bmatrix}. \qquad (2.20)$$

For a special case introduced in [64] with a single constant disturbance $d=k$ acting to the b-th state $\boldsymbol{N}=\boldsymbol{i}_b$ and one measured state (the a-th state) $\boldsymbol{C}=\boldsymbol{i}_a^T$, using displacement measurements and the condition $\boldsymbol{CN}=\mathbf{0}$ are necessary for a disturbance model with $V\neq 0$ to achieve minimized estimation errors.

2.3 New analysis of PI-Observer design

For the development and application of PI-Observer, the basic problem using high observer gains still has to be accounted, namely the conflict between the time behavior/quality of estimation and the sensitivity to measurement noise/unmodeled dynamics. In this part, this problem as well as the influence from high observer gains will be analyzed and a solution strategy will be given.

2.3.1 Problem in the design of PI-Observer gains

As discussed in Chapter 2.2.3, the problem in the high gain PI-Observer design lies in the determination of suitable high observer gains. The reasons are at first high observer gains evaluated here by $\|\boldsymbol{L_2}\|_F$ will lead to non-negligible influence from measurement noise and unmodeled dynamics to the estimation quality due to the increasing of the second and third terms as shown in (2.15). On the other hand, the ratio between $\|\boldsymbol{L}_2\|_F$ and $\|\boldsymbol{L}_1\|_F$, $\delta=\|\boldsymbol{L}_2\|_F/\|\boldsymbol{L}_1\|_F$, should be large to compensate the effect from the unknown input dynamics, as shown in (2.14) and (2.15).

2.3.2 Analysis of observer gains

The LQR method can be applied to design the high-gain PI-Observer feedback matrices. For the time-invariant case this task can be realized by solving the algebraic matrix Riccati equation.

For an asymptotic observer, suitable observer gains can be calculated, if for given positive definite matrices $\boldsymbol{Q}$, $\boldsymbol{R}$ the Riccati equation

$$\boldsymbol{A}_e\boldsymbol{P} + \boldsymbol{P}\boldsymbol{A}_e^T + \boldsymbol{Q} - \boldsymbol{P}\boldsymbol{C}_e^T\boldsymbol{R}^{-1}\boldsymbol{C}_e\boldsymbol{P} \;\; = \;\; \boldsymbol{0} \tag{2.21}$$

has a unique positive definite solution matrix $\boldsymbol{P}$. The observer feedback matrix is calculated with $\boldsymbol{L} = \boldsymbol{P}\boldsymbol{C}_e^T\boldsymbol{R}^{-1}$.

To illustrate the conflict/the problem clearly and tersely, here without loss of generality the weighting matrices in Eq. (2.21) are chosen as

$$\boldsymbol{Q} = \begin{bmatrix} \boldsymbol{I}_n & \boldsymbol{0}_{n\times r} \\ \boldsymbol{0}_{r\times n} & q\boldsymbol{I}_r \end{bmatrix}, \quad \boldsymbol{R} = \boldsymbol{I}_m, \tag{2.22}$$

with one scalar design parameter $q > 0$.

It will be shown that the parameter q can reflect almost all the important aspects which should be considered. Using the given definitions of the weighting matrices, the solution of the Riccati equation and the observer gain matrix can be calculated by

$$\boldsymbol{P} = \begin{bmatrix} \boldsymbol{P}_{11} & \boldsymbol{P}_{12} \\ \boldsymbol{P}_{12}^T & \boldsymbol{P}_{22} \end{bmatrix}, \tag{2.23}$$

$$\boldsymbol{L} = \boldsymbol{P}\boldsymbol{C}_e^T = \begin{bmatrix} \boldsymbol{P}_{11}\boldsymbol{C}^T \\ \boldsymbol{P}_{12}^T\boldsymbol{C}^T \end{bmatrix}, \tag{2.24}$$

$$\boldsymbol{A}\boldsymbol{P}_{11}+\boldsymbol{P}_{11}\boldsymbol{A}^T-\boldsymbol{P}_{11}\boldsymbol{C}^T\boldsymbol{C}\boldsymbol{P}_{11}=-(\boldsymbol{I}_n+\boldsymbol{N}\boldsymbol{P}_{12}^T+\boldsymbol{P}_{12}\boldsymbol{N}^T), \tag{2.25}$$

$$\boldsymbol{P}_{12}^T\boldsymbol{C}^T\boldsymbol{C}\boldsymbol{P}_{12} = q\boldsymbol{I}_r, \tag{2.26}$$

$$\boldsymbol{A}\boldsymbol{P}_{12} + \boldsymbol{N}\boldsymbol{P}_{22} = \boldsymbol{P}_{11}\boldsymbol{C}^T\boldsymbol{C}\boldsymbol{P}_{12}. \tag{2.27}$$

For the design/proof, the relation among the preferred design parameter q, the norm $\|\boldsymbol{L_2}\|_F$, and the ratio δ is considered [78].

Theorem 1. *For increasing design parameter q, the ratio δ, and the norm $\|\boldsymbol{L_2}\|_F$ will increase correspondingly.*

Mathematical description:

For two general design parameters q_a and q_b, the corresponding solution matrices $\boldsymbol{P^a}$ and $\boldsymbol{P^b}$ are denoted by

$$\boldsymbol{P^a} = \begin{bmatrix} \boldsymbol{P}_{11}^a & \boldsymbol{P}_{12}^a \\ \boldsymbol{P}_{12}^{a\,T} & \boldsymbol{P}_{22}^a \end{bmatrix} \text{ and } \boldsymbol{P^b} = \begin{bmatrix} \boldsymbol{P}_{11}^b & \boldsymbol{P}_{12}^b \\ \boldsymbol{P}_{12}^{b\,T} & \boldsymbol{P}_{22}^b \end{bmatrix}. \tag{2.28}$$

Similarly,

$\boldsymbol{L}^a = \begin{bmatrix} \boldsymbol{L}_1^a \\ \boldsymbol{L}_2^a \end{bmatrix} = \begin{bmatrix} \boldsymbol{P}_{11}^a\boldsymbol{C}^T \\ \boldsymbol{P}_{12}^{a\,T}\boldsymbol{C}^T \end{bmatrix}$, *and* $\boldsymbol{L}^b = \begin{bmatrix} \boldsymbol{L}_1^b \\ \boldsymbol{L}_2^b \end{bmatrix} = \begin{bmatrix} \boldsymbol{P}_{11}^b\boldsymbol{C}^T \\ \boldsymbol{P}_{12}^{b\,T}\boldsymbol{C}^T \end{bmatrix}$ *are defined.*

With assumed parameters $q_a > q_b > 0$, it follows that

i) $\|\boldsymbol{L}_2^a\|_F > \|\boldsymbol{L}_2^b\|_F$ *and correspondingly* *ii)* $\delta^a = \|\boldsymbol{L}_2^a\|_F / \|\boldsymbol{L}_1^a\|_F > \delta^b = \left\|\boldsymbol{L}_2^b\right\|_F / \left\|\boldsymbol{L}_1^b\right\|_F$.

Proof. i) The matrices $\boldsymbol{P^a}$ and $\boldsymbol{P^b}$ are solution matrices of the Riccati equation (2.21), satisfying the equation (2.26), which can be rewritten by

$$\boldsymbol{P}_{12}^T\boldsymbol{C}^T\boldsymbol{C}\boldsymbol{P}_{12} = (\boldsymbol{C}\boldsymbol{P}_{12})^T(\boldsymbol{C}\boldsymbol{P}_{12}) = q\boldsymbol{I}_r. \tag{2.29}$$

Considering the trace of the matrices in (2.29), it follows

$$tr((\boldsymbol{C}\boldsymbol{P}_{12})^T(\boldsymbol{C}\boldsymbol{P}_{12})) = tr(\boldsymbol{L_2}\boldsymbol{L_2}^T) = tr(q\boldsymbol{I}_r) = rq, \tag{2.30}$$

so each expression is described using r. Considering the above obtained results, the norm of the gain matrix can also be expressed by

$$\|\boldsymbol{L_2}\|_F = \left\|\boldsymbol{L_2}^T\right\|_F = \sqrt{tr(\boldsymbol{L_2}\boldsymbol{L_2}^T)} = \sqrt{rq}. \tag{2.31}$$

With the assumption $q_a > q_b > 0$ and r as constant, it holds

$$\|\boldsymbol{L}_2^a\|_F = \sqrt{rq_a} > \sqrt{rq_b} = \left\|\boldsymbol{L}_2^b\right\|_F. \tag{2.32}$$

$$\Rightarrow \|\boldsymbol{L}_2^a\|_F > \left\|\boldsymbol{L}_2^b\right\|_F. \tag{2.33}$$

ii) From (2.25)

$$\boldsymbol{P}_{11}\boldsymbol{C}^T\boldsymbol{C}\boldsymbol{P}_{11} = \boldsymbol{A}\boldsymbol{P}_{11} + \boldsymbol{P}_{11}\boldsymbol{A}^T + (\boldsymbol{I}_n + \boldsymbol{N}\boldsymbol{P}_{12}^T + \boldsymbol{P}_{12}\boldsymbol{N}^T), \tag{2.34}$$

it can be obtained

$$\begin{aligned}\|\boldsymbol{L}_1\|_F^2 &= \left\|\boldsymbol{P}_{11}\boldsymbol{C}^T\right\|_F^2 = tr(\boldsymbol{P}_{11}\boldsymbol{C}^T\boldsymbol{C}\boldsymbol{P}_{11}) \\ &= tr(\boldsymbol{A}\boldsymbol{P}_{11} + \boldsymbol{P}_{11}\boldsymbol{A}^T) + n + tr(\boldsymbol{N}\boldsymbol{P}_{12}^T + \boldsymbol{P}_{12}\boldsymbol{N}^T) \\ &= 2tr(\boldsymbol{A}\boldsymbol{P}_{11}) + n + 2tr(\boldsymbol{N}\boldsymbol{P}_{12}^T).\end{aligned} \tag{2.35}$$

Therefore, it follows

$$\|\boldsymbol{L}_1^a\|_F^2 - \left\|\boldsymbol{L}_1^b\right\|_F^2 = 2tr(\boldsymbol{A}(\boldsymbol{P^a}_{11} - \boldsymbol{P^b}_{11})) + 2tr(\boldsymbol{N}(\boldsymbol{P^a}_{12} - \boldsymbol{P^b}_{12})^T). \tag{2.36}$$

It is obvious that the matrices $\boldsymbol{Q_a} \geq \boldsymbol{Q_b}$ [3)] for $q_a > q_b > 0$. If the algebraic Riccati equation (2.21) is considered, then it can be obtained that $\boldsymbol{P^a} \geq \boldsymbol{P^b}$, because of the monotonicity of maximal solutions of algebraic Riccati equations [129].

Due to the assumed stability of the matrix A, the extended system matrix A_e is also stable. Considering the condition $\boldsymbol{P^a} \geq \boldsymbol{P^b}$, the following statement

$$(\boldsymbol{P^a} - \boldsymbol{P^b})\boldsymbol{A}_e + (\boldsymbol{P^a} - \boldsymbol{P^b})\boldsymbol{A}_e^T = \tilde{\boldsymbol{H}} = \begin{bmatrix} \tilde{\boldsymbol{H}}_1 & \tilde{\boldsymbol{H}}_2 \\ \tilde{\boldsymbol{H}}_3 & \tilde{\boldsymbol{H}}_4 \end{bmatrix} \geq 0 \tag{2.37}$$

[3)] Note that if the matrices A and $A - B$ are positive semidefinite, it is written here $A \geq 0$ and $A \geq B$ or $B \leq A$ respectively. Matrices A and B are assumed to be hermitian matrices.

holds, where

$$\begin{aligned}\tilde{\boldsymbol{H}}_1 = \boldsymbol{A}(\boldsymbol{P^a}_{11} - \boldsymbol{P^b}_{11}) + (\boldsymbol{P^a}_{11} - \boldsymbol{P^b}_{11})\boldsymbol{A}^T \\ +\boldsymbol{N}(\boldsymbol{P^a}_{12} - \boldsymbol{P^b}_{12})^T + (\boldsymbol{P^a}_{12} - \boldsymbol{P^b}_{12})\boldsymbol{N}^T \geq 0,\end{aligned} \tag{2.38}$$

because $\tilde{\boldsymbol{H}}_1 \in R^{n\times n}$ is one of the principal submatrices of $\tilde{\boldsymbol{H}}$. It follows that

$$\begin{aligned} tr(\tilde{H}_1) &= 2tr(\boldsymbol{A}(\boldsymbol{P^a}_{11} - \boldsymbol{P^b}_{11}) + \boldsymbol{N}(\boldsymbol{P^a}_{12} - \boldsymbol{P^b}_{12})^T) \\ &= \|\boldsymbol{L}_1^a\|_F^2 - \left\|\boldsymbol{L}_1^b\right\|_F^2 \leq 0. \end{aligned} \tag{2.39}$$

That means $\|\boldsymbol{L}_1^a\|_F \leq \left\|\boldsymbol{L}_1^b\right\|_F$. With the result from i), it can be stated that the following inequality

$$\delta^a = \|\boldsymbol{L}_2^a\|_F/\|\boldsymbol{L}_1^a\|_F > \delta^b = \left\|\boldsymbol{L}_2^b\right\|_F/\left\|\boldsymbol{L}_1^b\right\|_F \text{ holds.} \tag{2.40}$$

□

2.3.3 Strategy for suitable PI-Observer gain design

Based on the analysis above, a compromise has to be reached between the influence from the two aspects on the estimation quality, namely the measurement noise and the unknown inputs.

According to Theorem 1 with increasing design parameter q the estimation quality will be improved regarding the increasing ratio δ but be more sensitive to the measurement noise and unmodeled dynamics considering the increasing norm $\|\boldsymbol{L_2}\|_F$. The relations are shown in Figure 2.2[4)] qualitatively, where the curves are drawn by way of example. At different time points, the minimal levels of the estimation error are different, because all the variables are time dependent. However, it is obvious that the minimal level of estimation error can be obtained by adapting the design parameter q to the current situation. In the following parts of this chapter, an algorithm for online adjustment of the parameter q is presented as an Advanced PI-Observer (API-Observer) based on the contributions in [78, 82].

2.4 Advanced PI-Observer design

In this part, the Advanced PI-Observer (API-Observer) is introduced with online adaption of the observer gain matrix. The structure and the design process of API-Observer is given below in detail.

[4)] Note that the estimation error of the states $\boldsymbol{e}(t)$ and of the unknown inputs $\boldsymbol{f_e}(t)$ are coupled together as mentioned in Chapter 2.2.3 and one of them can represent the quality of the estimations.

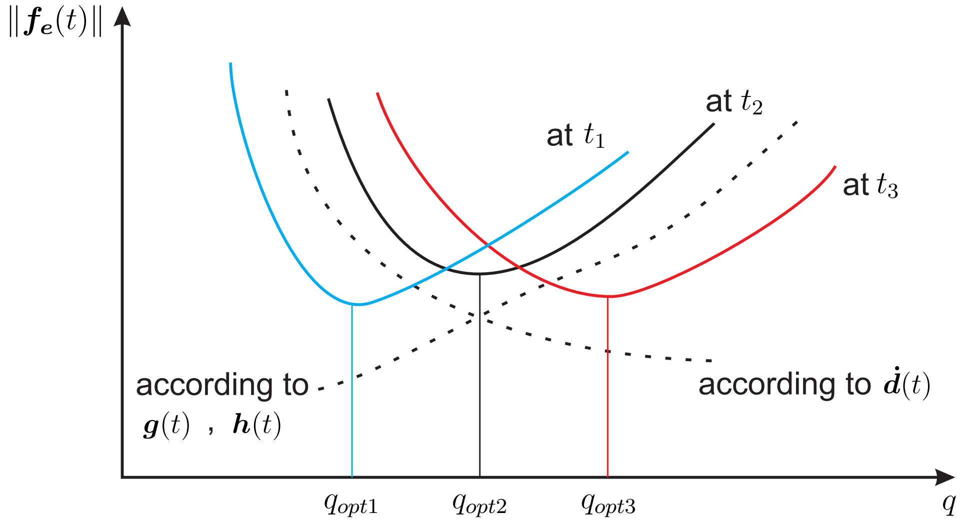

Figure 2.2: Relations between estimation error $\|\boldsymbol{f_e}(t)\|$ and design parameter q

2.4.1 Concept of the API-Observer

Based on the analysis in Chapter 2.3.2, the search for compromise is described by the cost function

$$J(q), \quad J = \mu \frac{1}{h} \int_{t-h}^{t} \boldsymbol{e_y}(\tau)^T \boldsymbol{e_y}(\tau) d\tau + q, \tag{2.41}$$

where the parameter μ is used for normalization (a suggested way to determine it is to choose it as the inverse of acceptable tolerance of estimation error) and the variable h denotes the current step size of the numerical time integration of the observer. The measurable estimation error $\boldsymbol{e_y}(t) = \boldsymbol{y}(t) - \hat{\boldsymbol{y}}(t)$ in the first part of (2.41), which is implicitly dependent on the parameter q, represents the output estimation error, which is influenced by measurement noise. On the other hand, the second part of the cost function $J(q)$ is taken into account for the evaluation of effects from unmodeled dynamics and measurement noise. The description of the compromise $J(q)$ is to some extent proportional to the estimation quality from the PI-Observer according to the former discussion. The goal here is not to reach the absolute minimal level of the estimation error, but to get acceptable relative minimal levels of the estimation error over the time. Therefore, the search for the local/relative minimal value of the cost function $J(q)$

$$\arg\min_{q} \quad J(q), \quad J = \mu \frac{1}{h} \int_{t-h}^{t} \boldsymbol{e_y}(\tau)^T \boldsymbol{e_y}(\tau) d\tau + q \tag{2.42}$$

is the suitable process for adapting the parameter q to get rational relative minimal levels of the estimation error.

2.4.2 Structure of the API-Observer

A sketch of the API-Observer with online adaption of observer gains process is given in Figure 2.3. The adaptive scheme shown in Figure 2.3 deciding the observer gains to be applied is based on a bank of PI-Observers, where the variables $\hat{x}_m$, $\hat{x}_l$, and $\hat{x}_r$ represent the estimations (for states and unknown inputs) from different PI-Observers in the observer bank. The API-Observer is constructed with three parallel running PI-Observers. The

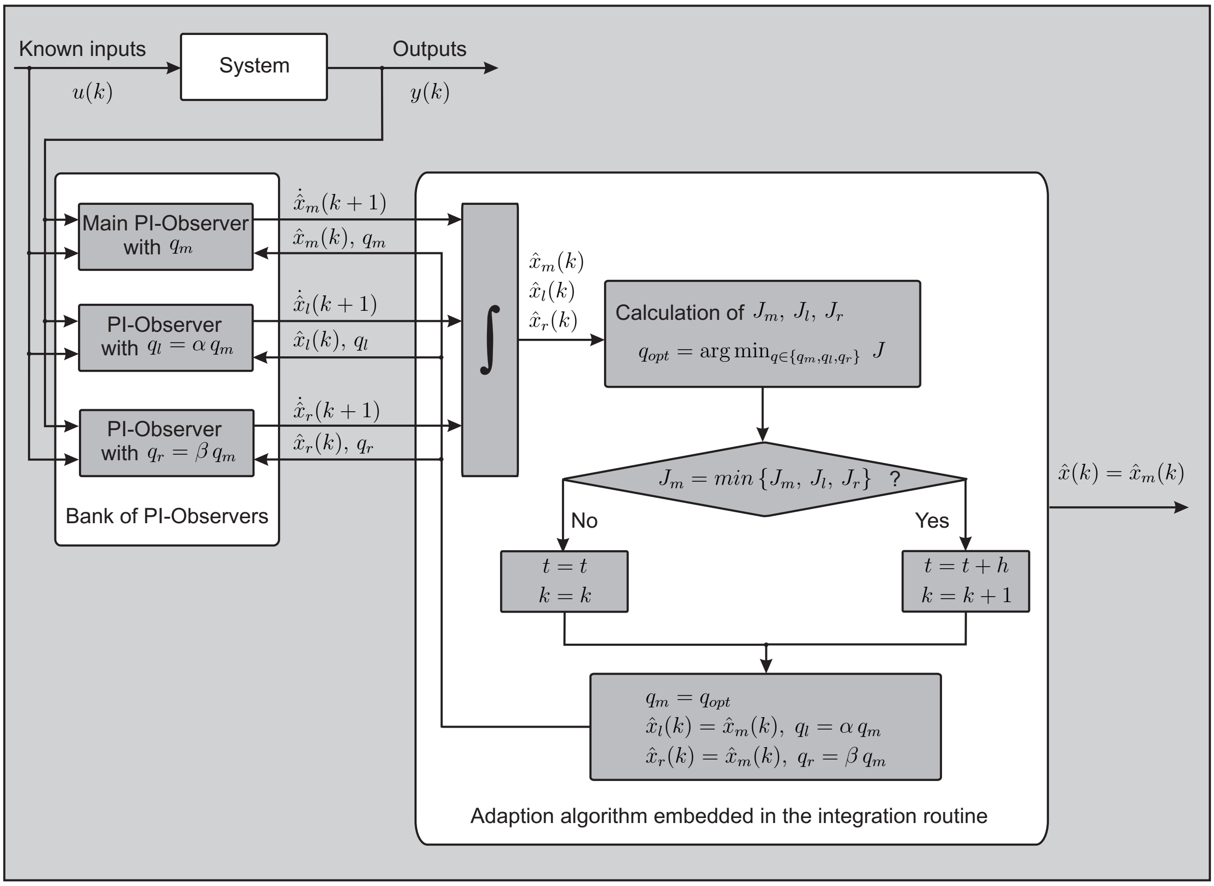

Figure 2.3: Sketch of proposed adaption algorithm

main PI-Observer with the design parameter q_m is the observer which generates the final valid estimation. To realize the optimization, two parallel running PI-Observers which use different design parameters $q_l = \alpha q_m$ and $q_r = \beta q_m$ $(0 < \alpha < 1 < \beta)$ respectively are included to compare the cost functions J_m, J_l, and J_r for the last step. If the cost function J_m is the smallest one, namely $q_m = q_{opt}$, where $q_{opt} = \arg\min_{q\in\{q_m,\, q_l,\, q_r\}} J$, then the estimation results will be taken as valid and the integration will go on.

Otherwise the estimation results will not be taken and the integration will be repeated with new defined $q_m = q_{opt}$, $q_l = \alpha q_m$, and $q_r = \beta q_m$. The integration will go on for the next step until it fulfills $q_m = q_{opt}$. The step size h is controlled inside the integral algorithm with the integrated step-size control. As a matter of experience, the range of the parameter q for the searching is taken within the interval $q \in [1, 10^{30}]$.

Briefly speaking, the task of the optimization is to keep the design parameter q_m of the main PI-Observer always having the relative minimal value of the cost function.

2.4.3 Stability of estimation error dynamics

According to the algorithm in Figure 2.3, the observer gain may change stepwise, as shown in Figure 2.4. In general, the changing observer gains can lead to an unstable total estimation error dynamics even if every observer gain matrix is designed to make the error dynamics converge asymptotically to a small value.

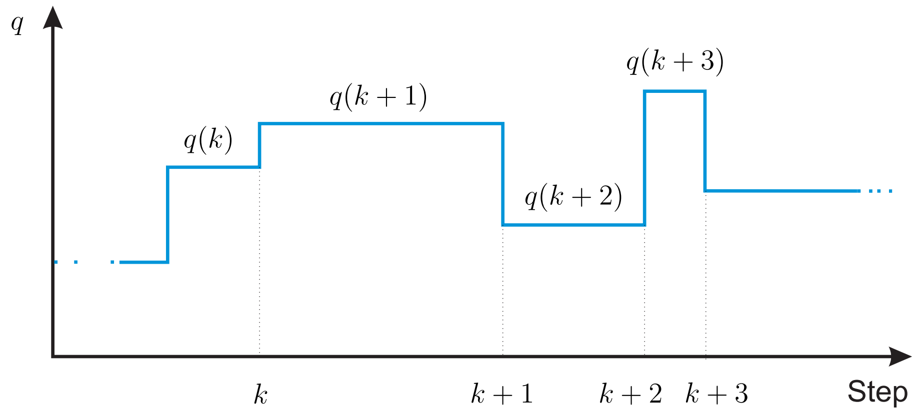

Figure 2.4: Illustration of changing gains

The stability condition for switching observers has been already addressed in many literatures, e.g., in [88]:

If all the observer gains are chosen/designed to have the Euclidean norm of the estimation error as a Lyapunov function of the error dynamics, then the total estimation error will vanish asymptotically.

For the case which is considered in this paper, the observer matrix $\boldsymbol{L}$ is designed using LQR method for different design parameters q. That indicates that a piecewise Lyapunov function of the estimation error dynamics may exist, but it can not ensure the convergence of the estimation error during the change of observer gains. However, taking the change conditions into account the estimation error of API-Observer can be proven to converge towards zero. The reason is that the observer gain respectively the parameter q is changed only if the cost function J from the current observer gains, which is to some extent proportional to the norm of the estimation error, is no more the local minimal one. That is to say, the change is towards the direction that makes the cost function J smaller, which ensures the convergence of the estimation error.

In order to explain it more clearly, an adaption example of the API-Observer among three parameters q_i, q_{ii}, and q_{iii} is shown in Figure 2.5.

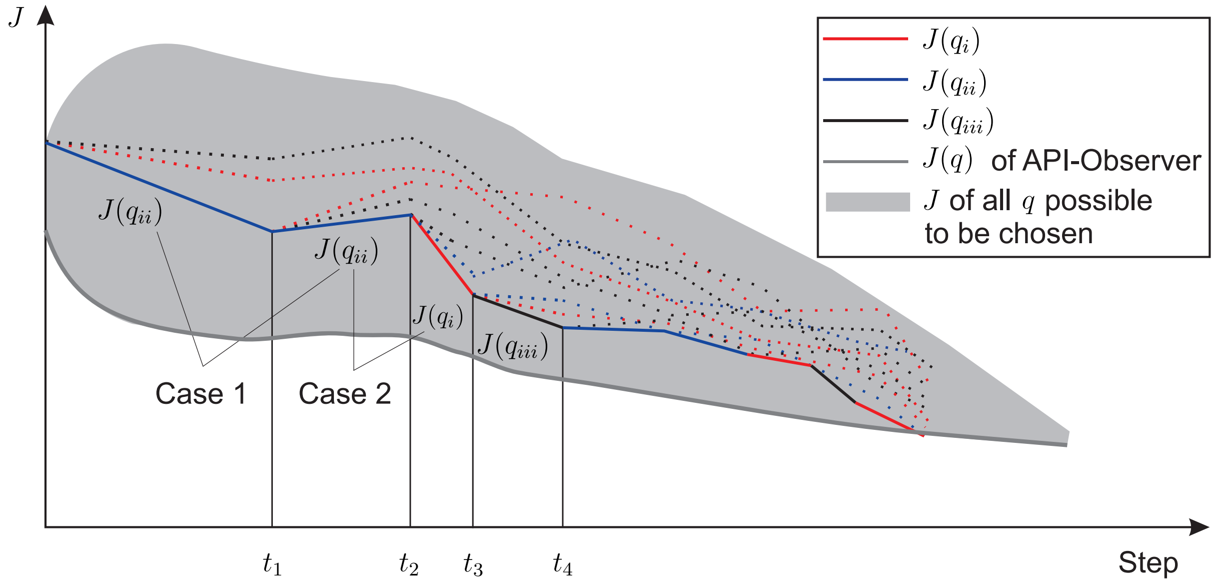

Figure 2.5: Cases of changing parameter q illustrated by cost function J

It is known that if the change of parameter q is arbitrary among the three parameters, the whole trajectory of the cost function J as well as the estimation error of API-Observer may diverge in case that the switch is alway towards the direction of a larger J, although the observer design is Hurwitz stable for every parameter. However, in the considered example with the given three parameters the variable parameter q is chosen with the proposed adaptive scheme to keep the cost function J at a minimal level as marked with the colored solid line in Figure 2.5. The adaptive parameter q in this example is $q(k_1) = q(k_2) = q_{ii}$, $q(k_3) = q_i$, and $q(k_4) = q_{iii}$. The convergence of the estimation error is discussed as follows. There exist two possible cases for the change of parameter q: the first possibility is the one as shown by Case 1 that the cost function J from one design parameter q_{ii} is the minimal one for two consecutive steps t_1 and t_2, namely $J_{min}(k_1) = J(q_{ii}, k_1)$ and $J_{min}(k_2) = J(q_{ii}, k_2)$; the second case is that the minimal cost function in the last step is no more the minimal one in the following step as shown by Case 2 with $J_{min}(k_2) = J(q_{ii}, k_2)$ and $J_{min}(k_3) = J(q_i, k_3)$. For Case 1, the convergence of the cost function J as well as the estimation error is guaranteed by the asymptotic PI-Observer design with parameter q_{ii}. For Case 2, the estimation error converges towards zero, because the change of parameter q is made to get a smaller cost function ($J(q_i, k_3) < J(q_{ii}, k_3)$) where the speed of convergence is even faster than with the parameter $q(k_3) = q_{ii}$. This discussion can be extended to the general case of API-Observer with uncertain number of parameters q for choosing. Considering the shaded area in Figure 2.5 as all possible values of J, the final trajectory of the cost function from an API-Observer with uncertain number of parameters q for choosing will be the gray solid line that ensures the convergence of the estimation error towards zero.

2.4.4 Discrete-time realization

In order to show the broad applicability of the API-Observer especially in industrial areas, the discrete-time realization is given here. The adaption algorithm shown in Figure 2.3, which is embedded in the numerical integration routine for the continuous design, is programmed in a simple loop in the discrete-time realization of API-Observer. The only difference is that the design of the PI-Observers should be transformed into discrete-time description by using the transformations

$$\begin{aligned} \boldsymbol{A}_{dis} &= e^{\boldsymbol{A}T_{dis}}, \\ \boldsymbol{B}_{dis} &= \left(\int_0^{T_{dis}} e^{\boldsymbol{A}t}dt\right)\boldsymbol{B}, \\ \boldsymbol{C}_{dis} &= \boldsymbol{C}, \\ \boldsymbol{D}_{dis} &= \boldsymbol{D}, \end{aligned}$$

where $(\boldsymbol{A}, \boldsymbol{B}, \boldsymbol{C}, \boldsymbol{D})$ are the matrices in a continuous time state space representation and $(\boldsymbol{A}_{dis}, \boldsymbol{B}_{dis}, \boldsymbol{C}_{dis}, \boldsymbol{D}_{dis})$ are those from the corresponding discrete-time description. T_{dis} is the discretization step size.

2.5 Validation of the API-Observer on an elastic beam

In this part, the validation of the introduced API-Observer design both in continuous time and discrete-time realization is given based on node displacements estimation of an elastic beam system.

2.5.1 Simulation results with an elastic beam model

An elastic beam example [115] shown in Figure 2.6 is given here to illustrate the proposed approach.

The elastic beam system is modeled using the Finite Element Method. The length of each element is 98 mm, the cross-sectional area is 125 mm^2. The displacements z_i and the angles θ_i $(i = 1, \cdots, 5)$ as well as the corresponding velocities and angular velocities are considered as the system states.

The system model can be described in state space form as

$$\dot{\boldsymbol{x}}(t) = \boldsymbol{A}\boldsymbol{x}(t) + b(t) + \boldsymbol{N}d(x,t), \tag{2.43}$$

$$\boldsymbol{y}(t) = \boldsymbol{C}\boldsymbol{x}(t) + \boldsymbol{C}_h\boldsymbol{h}(t), \tag{2.44}$$

with the state vector

$$x(t) = \begin{bmatrix} z_1 & \theta_1 & \cdots & z_5 & \theta_5 & \dot{z}_1 & \dot{\theta}_1 & \cdots & \dot{z}_5 & \dot{\theta}_5 \end{bmatrix}^T, \tag{2.45}$$

one known input $b(t)$, one unknown input $d(x,t)$ acting at the moment of contact between vibrating beam and contact device. Two measurements, the displacements at the third

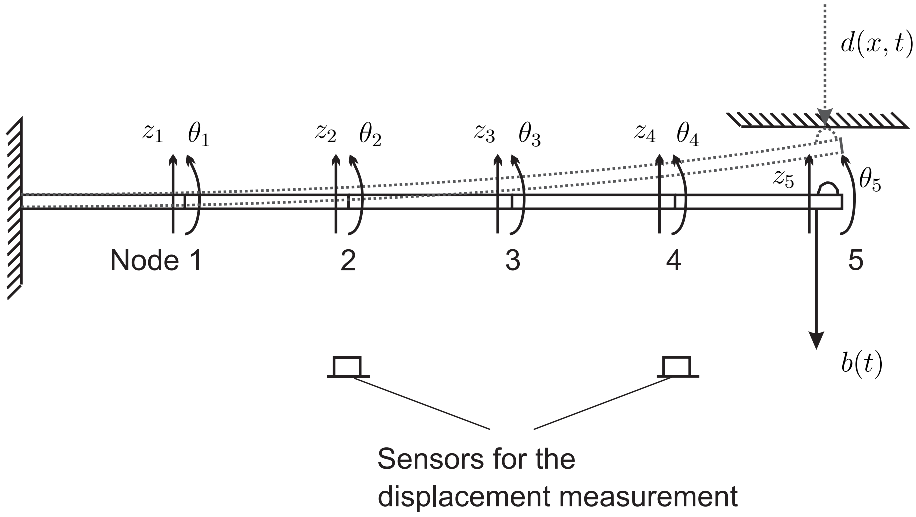

Figure 2.6: Structure of an elastic beam

and the fourth nodes ($y_1(t) = x_3(t)$, $y_2(t) = x_7(t)$), are taken. The task is to estimate the unknown and not measured contact force $\boldsymbol{d}(x,t)$ acting on the last node of the beam.

The relevant matrices are the system matrix $\boldsymbol{A} = \begin{bmatrix} \mathbf{0}_{10\times10} & \boldsymbol{I}_{10\times10} \\ -\boldsymbol{M}^{-1}\boldsymbol{K} & -\boldsymbol{M}^{-1}\boldsymbol{D} \end{bmatrix}$, input matrix $\boldsymbol{N} = \begin{bmatrix} \mathbf{0}_{18\times1} \\ 1 \\ 0 \end{bmatrix}$, the output matrix $\boldsymbol{C} = \begin{bmatrix} \mathbf{0}_{1\times2} & 1 & \mathbf{0}_{1\times17} \\ \mathbf{0}_{1\times6} & 1 & \mathbf{0}_{1\times13} \end{bmatrix}$, and $\boldsymbol{C_h} = \begin{bmatrix} c_{x3} \\ c_{x7} \end{bmatrix}$, where in the simulation it is assumed that $c_{x3} = 0.3$ and $c_{x7} = 1$.

The stiffness matrix $\boldsymbol{K}$ and the mass matrix $\boldsymbol{M}$ are calculated using finite element theory. The damping matrix is taken as $\boldsymbol{D} = \xi\boldsymbol{K}$, where ξ is suitably chosen (using Raleigh damping hypothesis).

For the simulation, the contact force calculation is realized by

$$d(x,t) = -3.8 \times 10^6 (x_9(t) - 1 + 5 \times 10^{-4})^2, \tag{2.46}$$

if the displacement of the last node fulfills $x_9(t) \geq 1$ representing a nonlinear and stiff elastic contact, which is unknown in structure and parameters to the observer.

Results with API-Observer design in continuous time

At first, the simulation results from the API-Observer design in continuous time are shown and discussed in detail.

Simulation results without consideration of measurement noise and modeling error

At first, the model for the elastic beam is assumed as perfect and no modeling errors are considered. Simulation results from the API-Observer are shown in Figure 2.7 and Figure 2.8 in comparison with two PI-Observers with invariant observer gains under the same conditions (without measurement noise and modeling errors). In the case without consideration of measurement noise and modeling error (Figure 2.7 and Figure 2.8), it can be seen that the design parameter q has to be suitably chosen (relative large, e.g., 10^{16} rather than 10^{10}) to get sound estimations of contact force and unmeasured states, if a general high-gain PI-Observer with invariant observer gains is applied to estimate unknown inputs. As known, it is difficult to determine the suitable level of the design parameter q in practical applications.

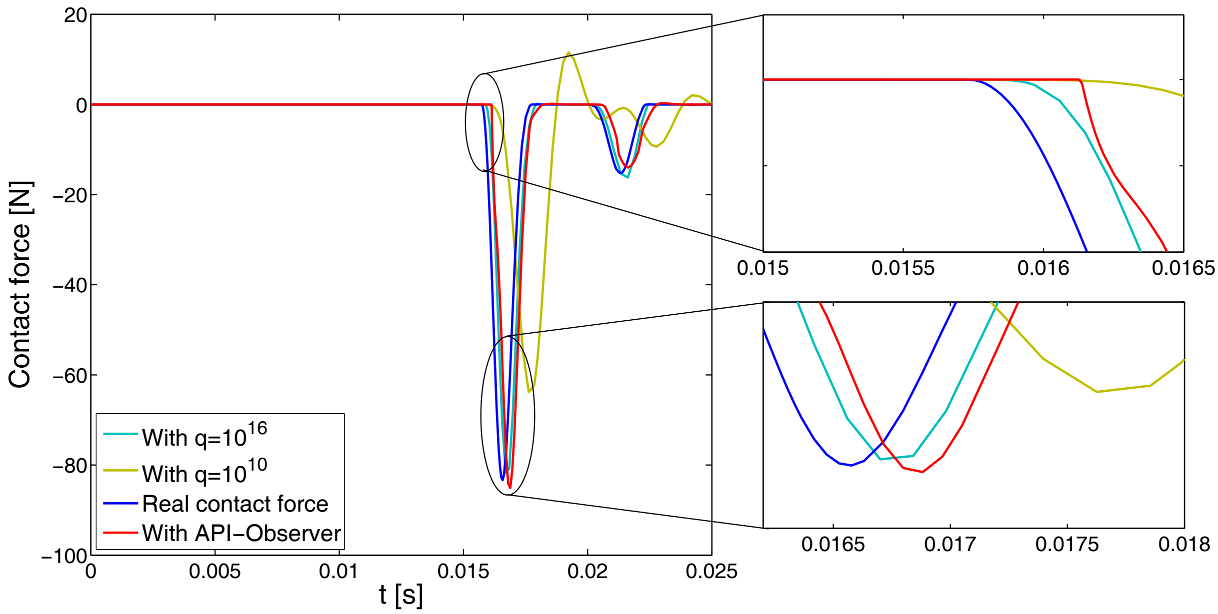

Figure 2.7: Estimation results of contact force I

Correspondingly, the estimations from the API-Observer given in Figure 2.9 are almost as good as the results with constant parameter 10^{16}, where the design parameter q is setting to high levels only when the contact appears. The feature from API-Observer with online adjusted design parameter q as well as observer gains gives the possibility for API-Observer to have a robust performance in the situation when measurement noise and modeling errors are not negligible.

Simulation results with consideration of measurement noise and modeling error In this part, the performance of API-Observer will be compared with general high-gain PI-Observers under the consideration of measurement noise and modeling errors. Here, white noise $\boldsymbol{h}(t)$ with amplitudes of 0.5% of the measurements and some model uncertainty, where the real damping coefficient ξ is 10% larger than the nominal value, are considered in the simulation.

In Figure 2.10 and Figure 2.11, the estimations of the contact force and the displacement at node 5 from the API-Observer are compared with the estimations of two normal PI-Observers with constant design parameters $q = 10^{10}$ and $q = 10^{14}$ respectively. It is

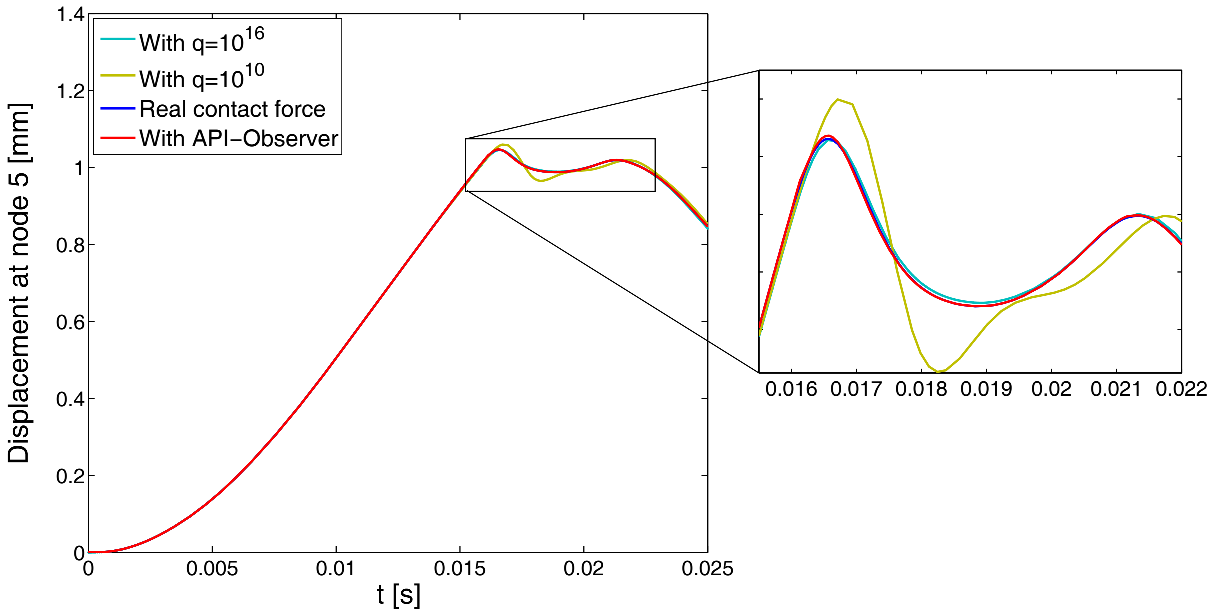

Figure 2.8: Estimation results of displacement (at node 5) I

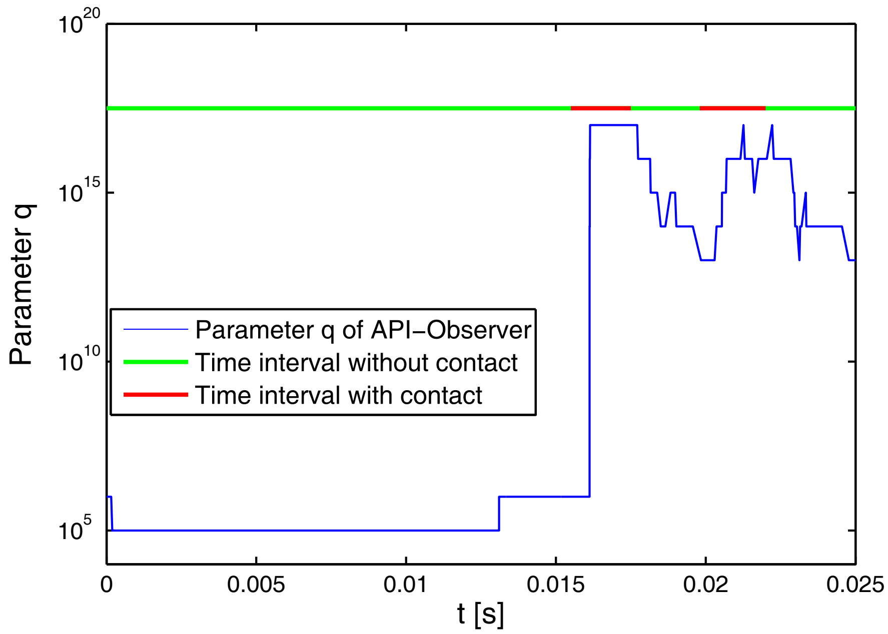

Figure 2.9: Online optimized parameter q I

clearly shown that with a large constant design parameter $q = 10^{14}$ the estimation of the unknown input is strongly influenced by the measurement noise. In contrast, the estimation from the PI-Observer with low design parameter $q = 10^{10}$ shows almost no effect from the measurement noise and model uncertainty, but still a large delay time and a non precise amplitude of the estimated contact force as in the situation when no measurement noise and modeling errors are considered.

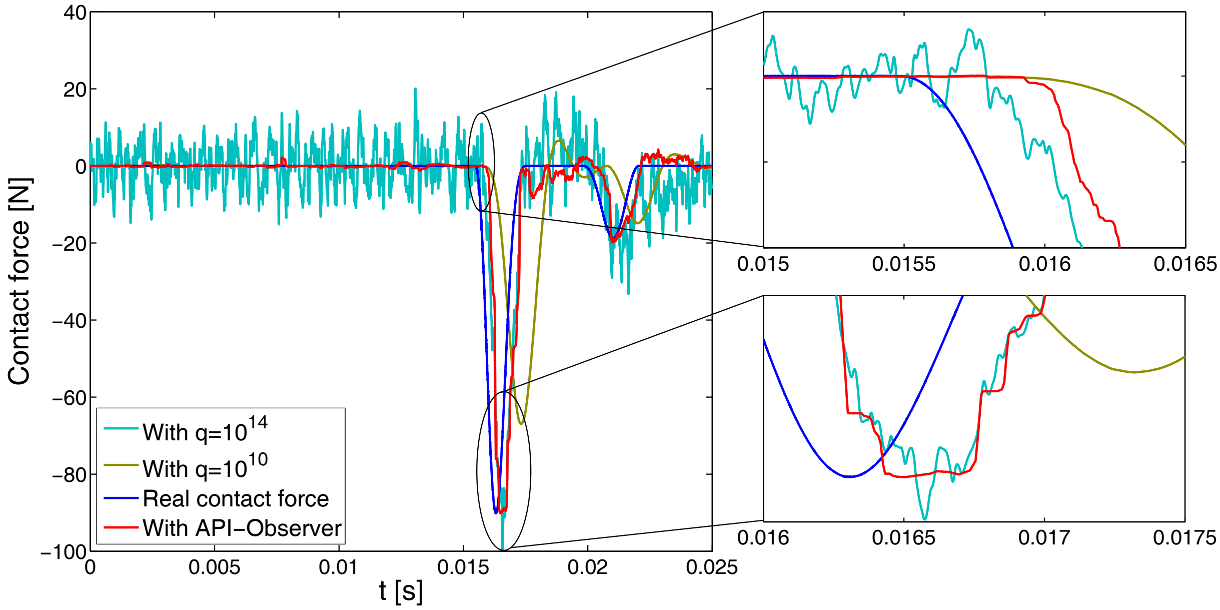

Figure 2.10: Estimation results of contact force II

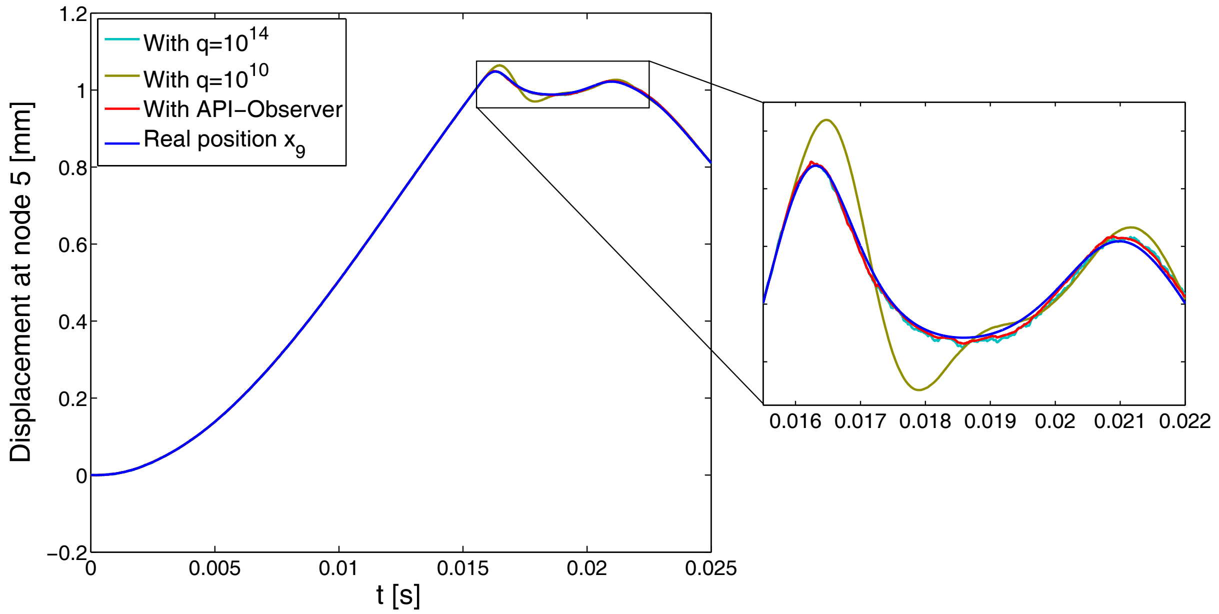

Figure 2.11: Estimation results of displacement (at node 5) II

The estimations from the API-Observer combine the advantages of both the high and low parameters for q. The estimated contact force from the API-Observer reacts rapidly as with a high design parameter q and shows no strong influence from the measurement noise and the unmodeled dynamics. The same performance can also be found in the estimation of the displacement x_9. The changing design parameter q of the API-Observer is given in Figure 2.12, where it can be found that during the time intervals when the contact exists the design parameter q is adjusted to be larger than without contact. Exactly the changing parameter q leads to better performance from API-Observer.

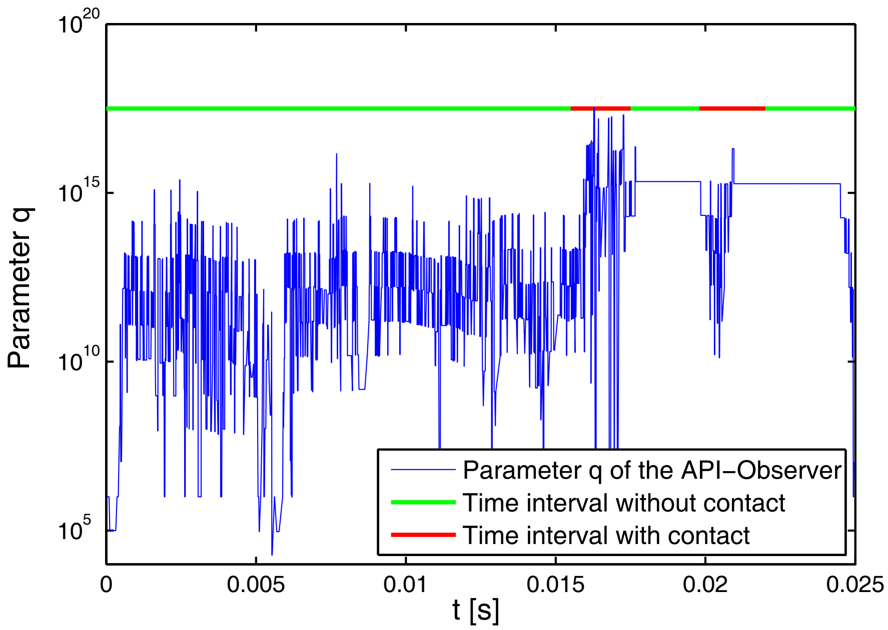

Figure 2.12: Online adapted parameter q II

It can be stated as a conclusion that the online adaption in the API-Observer design is necessary for estimation improvement and can be realized by the proposed approach as shown.

Results with API-Observer design in discrete-time

Due to the fact that the results from the API-Observer design in discrete-time are similar with the ones given above in continuous time, only part of the results in the second case with consideration of measurement noise and modeling error is illustrated in Figure 2.13, Figure 2.14, and Figure 2.15 and no detailed discussion are given here to avoid repetition.

The results show that the discrete-time design of the API-Observer is also easily realizable and no evident difference between the continuous time and discrete-time designs exists. The API-Observer can be applied in discrete-time applications.

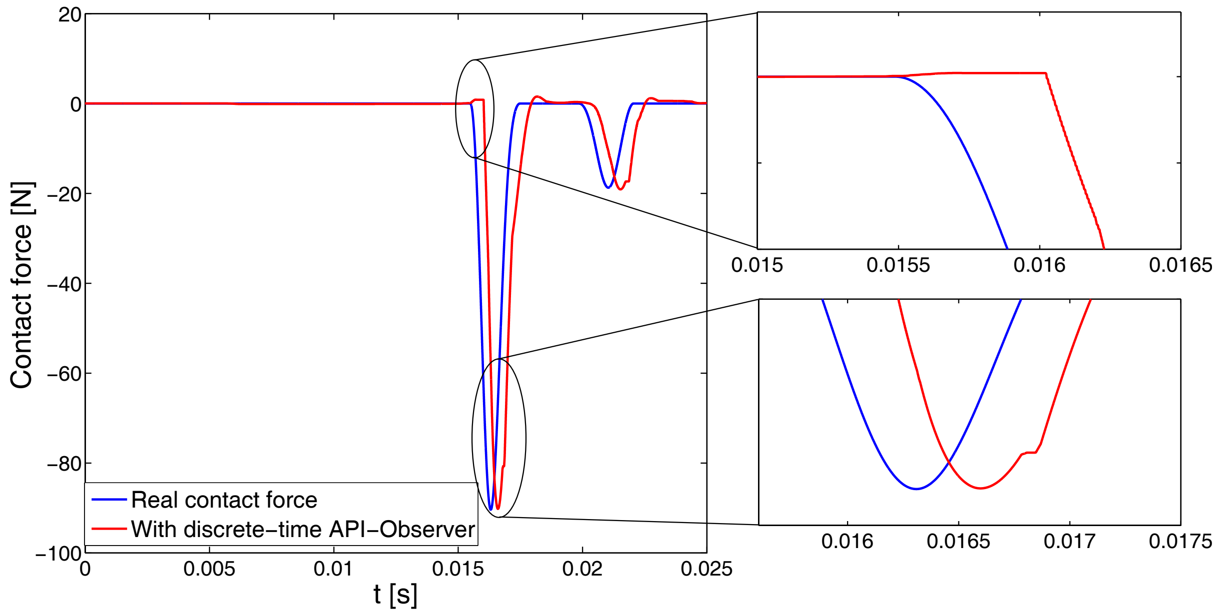

Figure 2.13: Estimation results of contact force (discrete-time)

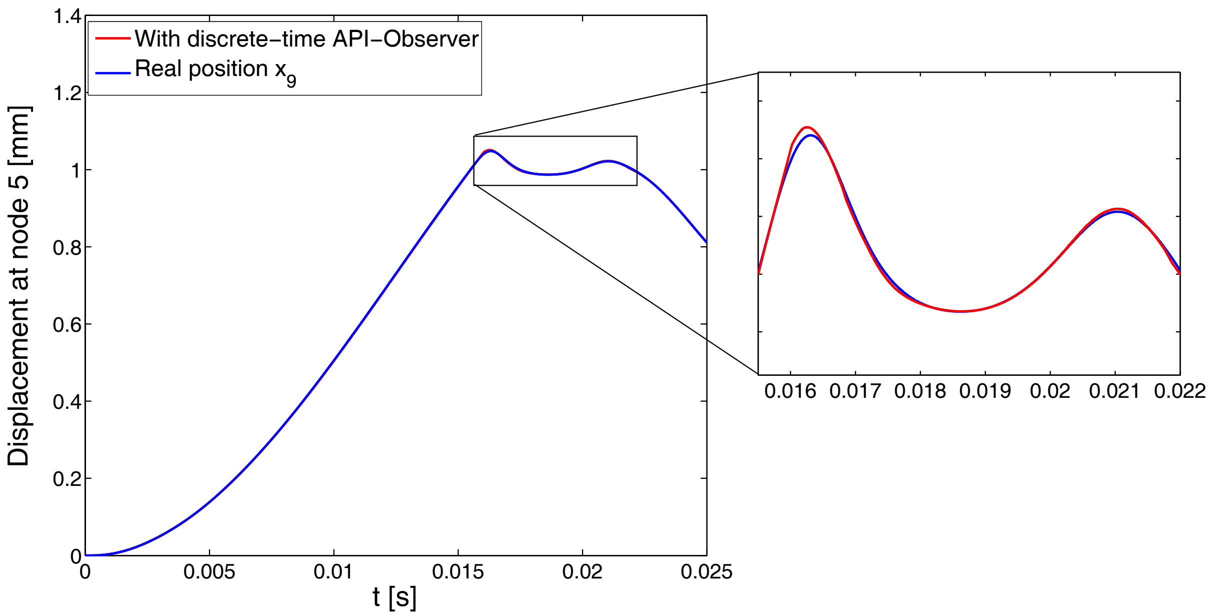

Figure 2.14: Estimation results of displacement (discrete-time)

2.5.2 Experimental results on an elastic beam test rig

An elastic beam test rig [69, 115] is shown in Figure 2.16.

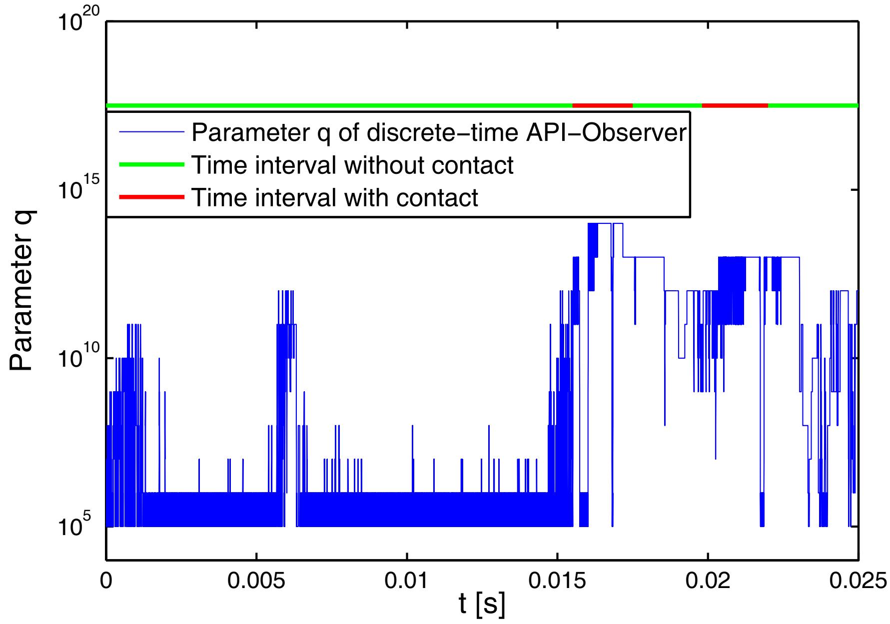

Figure 2.15: Online adapted parameter q (discrete-time)

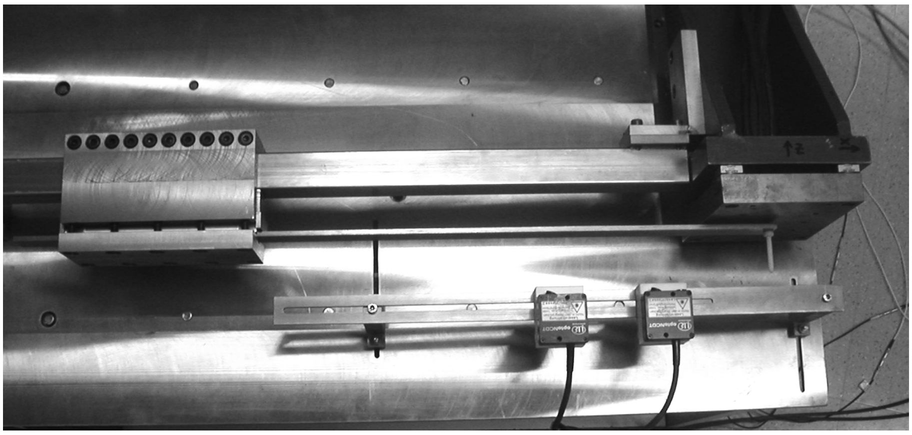

Figure 2.16: Test rig of an elastic beam

The elastic beam system is modeled using Finite Element Method as mentioned in Chapter 2.5.1. Two measurements, the displacements at the third and the fourth nodes ($y_1(t) = x_7(t)$, $y_2(t) = x_9(t)$), are taken. The task is to estimate the unknown and not measured contact force $\boldsymbol{d}(x,t)$ acting on the last node of the beam.

The relevant matrices are the system matrix $\boldsymbol{A} = \begin{bmatrix} \mathbf{0}_{10\times10} & \boldsymbol{I}_{10\times10} \\ -\boldsymbol{M}^{-1}\boldsymbol{K} & -\boldsymbol{M}^{-1}\boldsymbol{D} \end{bmatrix}$, input matrix $\boldsymbol{B} = \boldsymbol{N} = \begin{bmatrix} \mathbf{0}_{18\times1} \\ 1 \\ 0 \end{bmatrix}$, the output matrix $\boldsymbol{C} = \begin{bmatrix} \mathbf{0}_{1\times6} & 1 & \mathbf{0}_{1\times13} \\ \mathbf{0}_{1\times8} & 1 & \mathbf{0}_{1\times11} \end{bmatrix}$.

The contact moment in time is defined by the situation, when the displacement of the last node fulfills $x_9(t) \geq 2.15$. The contact is assumed as an elastic-plastic contact, so the contact force is nonlinear with respect to displacement and time. The goal is to estimate the unknown contact force and the force to initialize the beam. Here the discrete-time API-Observer is applied. The experimental results are shown in Figure 2.17.

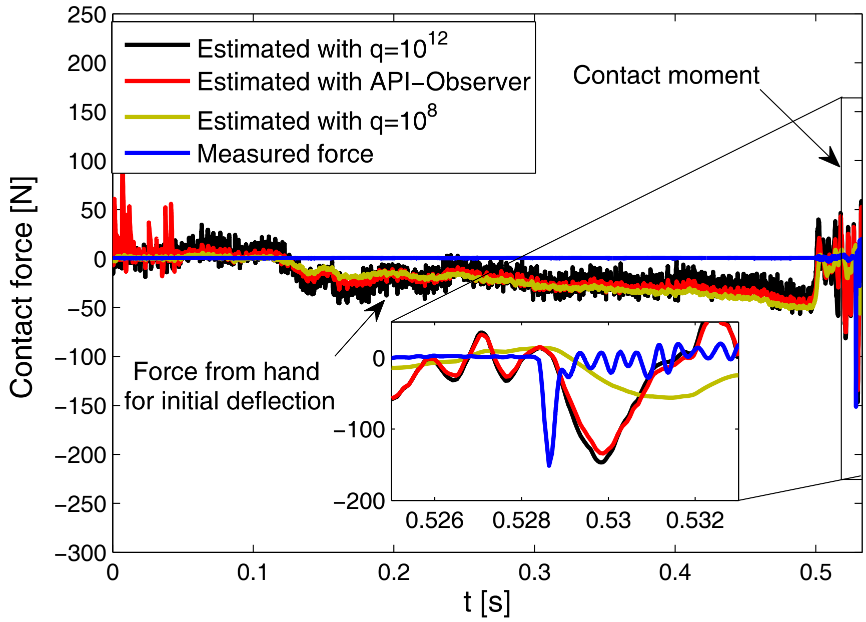

(a) Comparisons of estimated contact force

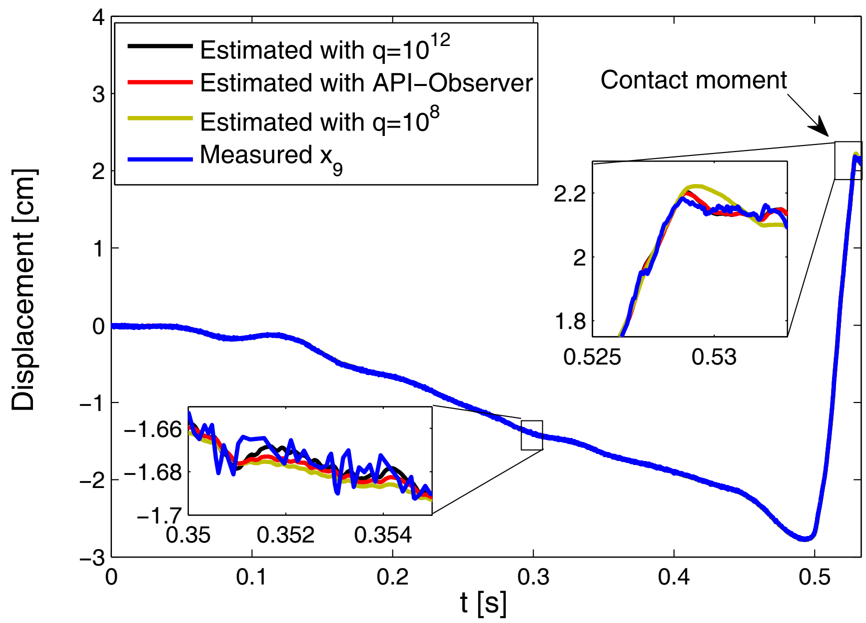

(b) Comparisons of estimated displacement x_9

Figure 2.17: Comparisons of estimations

In Figure 2.17(a), the comparison of the estimated contact force from different observers with the measured force is given to show at a glance the difference from three observers: a PI-Observer with $q = 10^8$, a PI-Observer with $q = 10^{12}$, and the API-Observer. The results show that the estimation quality using gains with $q = 10^8$ is not good, because the dynamics of the observer design with $q = 10^8$ is too slow to follow the fast dynamics of the contact force. On the other hand, the PI-Observer design with $q = 10^{12}$ is also not optimal due to the strong influence from measurement noise to the estimation results caused by the high gains with $q = 10^{12}$. From the comparison of measured and estimated displacement x_9 in Figure 2.17(b), it can be clearly seen that the displacement is almost perfectly reconstructed with high observer gains ($q = 10^{12}$) considering both the real displacement x_9 and the measurement noise as the behavior from the system. That exactly leads to the noisy estimation of the contact force with high observer gains. In contrast, the estimated force from the API-Observer follows rapidly the contact with a high design parameter q and shows not so strong influence from the measurement noise as with the constant parameter $q = 10^{12}$ when the contact is not taking place.

The changing design parameter q of API-Observer is given in Figure 2.18 to illustrate again the adaption of the design parameter q.

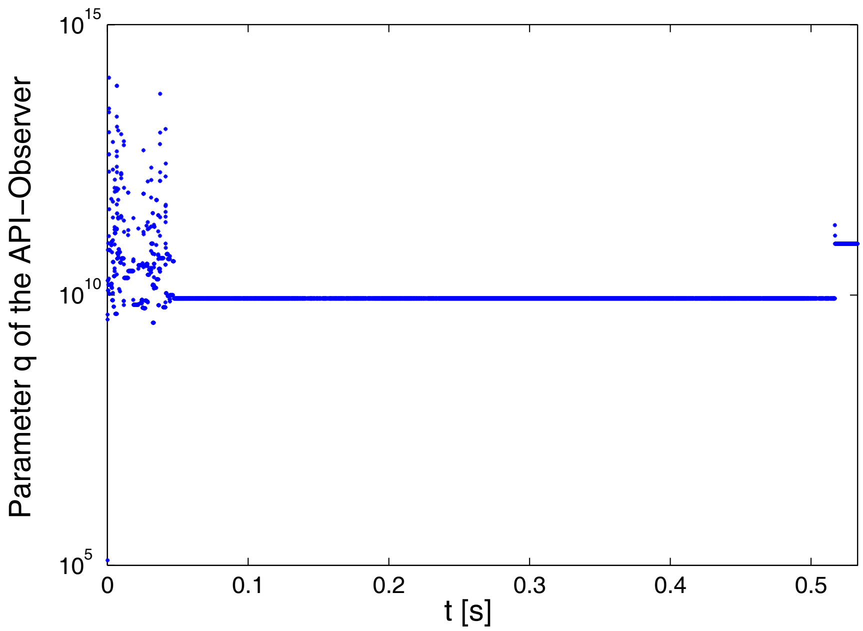

Figure 2.18: Parameter q of the API-Observer with experiment results

2.6 Summary

The Advanced PI-Observer (API-Observer) design is discussed in this chapter. The development of the PI-Observer is reviewed in the beginning, before the API-Observer is proposed. After that, the general PI-Observer design is briefly repeated and new discussions about the observer gain design are given to show the importance and possibilities for choosing suitable observer gains. Based on the discussion, the API-Observer design with one tunning parameter q is proposed to solve the problem of determining observer gains for unknown inputs estimation for the PI-Observer. In the API-Observer, the observer gains are adjusted according to the current situation and request. Furthermore, the suitable amplitude of observer gains from API-Observer is determined by the local minimization of the cost function. In contrast, the suitable observer gains for a general PI-Observer is chosen by trial and error method. Simulation and experiment results from an elastic beam are given to illustrate the implementation of the API-Observer. From the results, it can be concluded that the performance of the API-Observer for unknown input estimation is robust to the changes and differences of system behavior at different time, because it not strongly influenced by measurement noise and modeling errors in comparison with the general PI-Observer design with invariant observer gains.

3 Robust Nonlinear Control Design Based on PI-Observer Technique

For nonlinear systems, no general control theory has yet been developed. Different approaches have been proposed to realize robust control for nonlinear systems. Here, the PI-Observer can estimate the unknown inputs of a system as extended states and will be applied to combine with the classical input-output exact feedback linearization. The approach as the combination of exact feedback linearization and PI-Observer (named as EFL-PIO) will be shown in the sequel to realize a robust nonlinear control for a class of nonlinear systems. The lack of robustness in classical nonlinear control methods, like the exact feedback linearization method, strongly limits their application. In [28, 89, 91, 101, 104] different methods are developed and applied to solve the robustness problem. However, most of the methods [89, 101, 104] consider known bounds and/or dynamical properties of the modeling errors or the disturbances. In [28, 91], robust feedback linearization methods are proposed by improving the design of the nonlinear feedback. All of the methods are proposed to improve the robustness of exact feedback linearization when disturbances act on the considered system, but none of them can give the current information of the disturbances. The EFL-PIO approach discussed in this thesis takes no information or assumptions from the dynamics of the modeling errors and disturbances into consideration. Furthermore, the modeling errors and disturbances can be estimated as unknown inputs together with the system states by the high-gain PI-Observer.

3.1 Considered class of nonlinear systems

The considered class of nonlinear systems with unknown inputs is described by

$$\begin{aligned} \dot{\boldsymbol{x}}(t) &= \underbrace{\boldsymbol{f}(\boldsymbol{x}) + \boldsymbol{g}(\boldsymbol{x})\boldsymbol{u}(t)}_{\text{Nominal model}} + \boldsymbol{E}\boldsymbol{d}(\boldsymbol{x}, t), \\ \boldsymbol{y}(t) &= \boldsymbol{h}(\boldsymbol{x}), \end{aligned} \tag{3.1}$$

where $\boldsymbol{x}(t) \in \mathbb{R}^n$ denotes the state vector, $\boldsymbol{u}(t) \in \mathbb{R}^l$ the input vector, $\boldsymbol{y}(t) \in \mathbb{R}^m$ the output to be controlled. The vector $\boldsymbol{d}(\boldsymbol{x}, t) \in \mathbb{R}^s$ with $s \leq n$ together with the constant matrix $\boldsymbol{E} \in \mathbb{R}^{n \times s}$ represents the unknown inputs. Disturbances, modeling errors, parameter uncertainties, or other uncertainties to the nominal model can be summarized under $\boldsymbol{E}\boldsymbol{d}(\boldsymbol{x}, t)$, possibly in all the dynamical equations (when the rank of $\boldsymbol{E}$ equals n).

The problem to be solved is to design a controller, which can stabilize the system behavior or realize stable tracking and regulation control for the system in spite of the existence of disturbances $\boldsymbol{d}(\boldsymbol{x},t)$.

Several assumptions are considered:

- The vector fields $\boldsymbol{f}(\cdot)$ on $\mathbb{R}^n$, $\boldsymbol{d}(\cdot)$ on $\mathbb{R}^s$, $\boldsymbol{g}(\cdot)$ on $\mathbb{R}^{n\times l}$, and $\boldsymbol{h}(\cdot)$ on $\mathbb{R}^m$ are smooth[5)].
- The system has an equilibrium at $\boldsymbol{x}=0$.
- The unknown inputs $\boldsymbol{d}(\boldsymbol{x},t)$ and the corresponding derivatives are bounded, but the bounds and the related dynamical behavior are unknown.
- The nominal model of the system is available, input-output linearizable and the internal dynamics are stable.
- In MIMO cases, the number of the inputs equals the number of outputs, namely $l=m$.

A robust control approach is required to control the class of nonlinear systems in (3.1) due to the existence of unknown disturbances $\boldsymbol{d}(\boldsymbol{x},t)$.

3.2 Robust control approach based on exact linearization and PI-Observer

The proposed approach based on the contributions in [79, 81] shown in Figure 3.1 takes the advantages of the exact feedback linearization method to get a transformed (input-output linearized) description of the system and then applies the PI-Observer to estimate the transformed states together with the transformed unknown inputs. Using a state feedback control and a disturbance rejection, a robust control for the transformed system can be designed. With the assumption of the stability of the remaining zero dynamics, which is a typical assumption controlling mechanical system and which can be easily realized, the whole control loop with the proposed control design is stable and robust.

3.2.1 Input-output linearization of nonlinear system models

With the classical input-output linearization method as introduced in [47], the system model (3.1) can be transformed into the following form

$$\begin{bmatrix} y_1^{(r_1)}(t) \\ \vdots \\ y_m^{(r_m)}(t) \end{bmatrix} = \begin{bmatrix} v_1(t) \\ \vdots \\ v_m(t) \end{bmatrix} + \underbrace{\begin{bmatrix} \tilde{d}_1(\boldsymbol{x},t) \\ \vdots \\ \tilde{d}_m(\boldsymbol{x},t) \end{bmatrix}}_{\tilde{\boldsymbol{d}}(\boldsymbol{x},t)} \tag{3.2}$$

5) A smooth function is a function that has continuous derivatives up to some desired order over some domain.

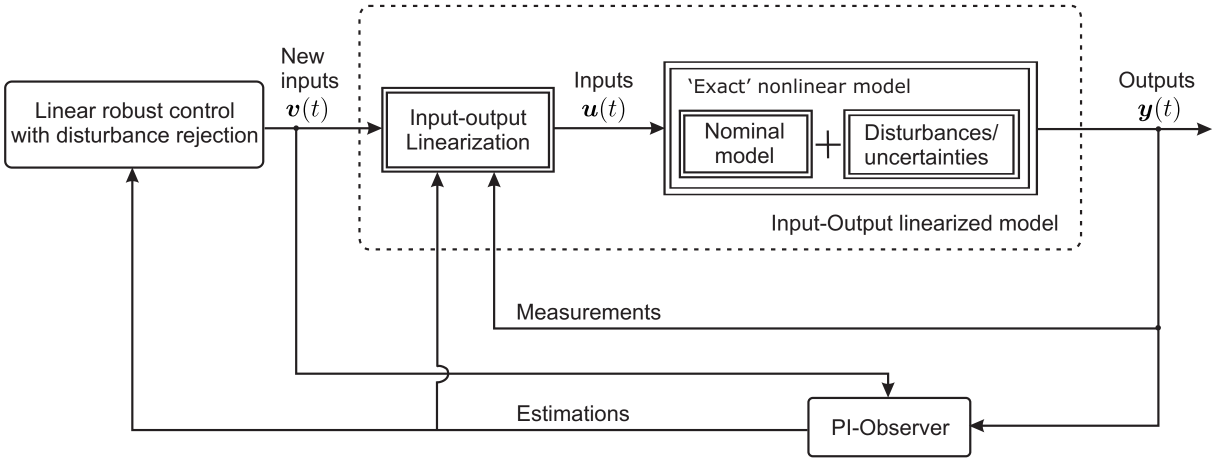

Figure 3.1: Sketch of the proposed approach

by feedback linearization with the input being defined as

$$\boldsymbol{u}(t) = -\boldsymbol{\Gamma}^{-1}(\boldsymbol{x}) \begin{bmatrix} \boldsymbol{L}_{\boldsymbol{f}}^{r_1} h_1(\boldsymbol{x}) \\ \vdots \\ \boldsymbol{L}_{\boldsymbol{f}}^{r_m} h_m(\boldsymbol{x}) \end{bmatrix} + \boldsymbol{\Gamma}^{-1}(\boldsymbol{x}) \begin{bmatrix} v_1(t) \\ \vdots \\ v_m(t) \end{bmatrix} {}^{6)}, \tag{3.3}$$

where the decoupling matrix

$$\boldsymbol{\Gamma}(\boldsymbol{x}) = \begin{bmatrix} \boldsymbol{L}_{g_1} \boldsymbol{L}_{\boldsymbol{f}}^{r_1-1} h_1(\boldsymbol{x}) & \cdots & \boldsymbol{L}_{g_m} \boldsymbol{L}_{\boldsymbol{f}}^{r_1-1} h_1(\boldsymbol{x}) \\ \vdots & \ddots & \vdots \\ \boldsymbol{L}_{g_1} \boldsymbol{L}_{\boldsymbol{f}}^{r_m-1} h_m(\boldsymbol{x}) & \cdots & \boldsymbol{L}_{g_m} \boldsymbol{L}_{\boldsymbol{f}}^{r_m-1} h_m(\boldsymbol{x}) \end{bmatrix}, \tag{3.4}$$

and the transformed unknown effects are

$$\tilde{\boldsymbol{d}}(\boldsymbol{x}, t) = \begin{bmatrix} \boldsymbol{L}_{\boldsymbol{Ed}}^{r_1-1} h_1 + \frac{d}{dt}(\boldsymbol{L}_{\boldsymbol{Ed}}^{r_1-2} h_1) + \frac{d^2}{dt}(\boldsymbol{L}_{\boldsymbol{Ed}}^{r_1-3} h_1) + \cdots + \frac{d^{(r_1-1)}}{dt}(\boldsymbol{L}_{\boldsymbol{Ed}} h_1) \\ \vdots \\ \boldsymbol{L}_{\boldsymbol{Ed}}^{r_m-1} h_m + \frac{d}{dt}(\boldsymbol{L}_{\boldsymbol{Ed}}^{r_m-2} h_m) + \frac{d^2}{dt}(\boldsymbol{L}_{\boldsymbol{Ed}}^{r_m-3} h_m) + \cdots + \frac{d^{(r_m-1)}}{dt}(\boldsymbol{L}_{\boldsymbol{Ed}} h_m) \end{bmatrix},$$

with r_i, $i = 1, \ldots, m$, the smallest integer such that at least and firstly one of the inputs appear in $y_i^{(r_i)}$. The total relative degree of the system is defined by $r = r_1 + r_2 + \cdots + r_m$. After the input-output linearization, the system model is transformed into a form with external dynamics (the input-output dynamics) and internal dynamics. Define new

[6] Here $L_{\boldsymbol{\mathcal{G}}}^i \boldsymbol{\mathcal{H}}$ denotes the $i-$th Lie derivative of $\boldsymbol{\mathcal{H}}$ with respect to $\boldsymbol{\mathcal{G}}$, where the Lie derivatives are defined by $L_{\boldsymbol{\mathcal{G}}}^0 \boldsymbol{\mathcal{H}} = \boldsymbol{\mathcal{H}}$, $L_{\boldsymbol{\mathcal{G}}}^i \boldsymbol{\mathcal{H}} = L_{\boldsymbol{\mathcal{G}}} L_{\boldsymbol{\mathcal{G}}}^{i-1} \boldsymbol{\mathcal{H}} = \nabla(L_{\boldsymbol{\mathcal{G}}}^{i-1} \boldsymbol{\mathcal{H}}) \boldsymbol{\mathcal{G}} (i = 1, 2, \ldots)$ with $\nabla \boldsymbol{\mathcal{G}} \triangleq \frac{\partial \boldsymbol{\mathcal{G}}}{\partial \boldsymbol{x}}$ and $\boldsymbol{\mathcal{H}} = \boldsymbol{\mathcal{H}}(\boldsymbol{x})$ and $\boldsymbol{\mathcal{G}} = \boldsymbol{\mathcal{G}}(\boldsymbol{x})$ are functions of $\boldsymbol{x}$.

coordinates for the external dynamics as

$$\begin{array}{llll}\mathcal{X}_1^1(t) = y_1(t) = h_1(\boldsymbol{x}), & \mathcal{X}_2^1(t) = L_f h_1(\boldsymbol{x}), & \cdots & \mathcal{X}_{r_1}^1(t) = L_f^{r_1-1} h_1(\boldsymbol{x}) \\ & & \vdots & \\ \mathcal{X}_1^m(t) = y_m(t) = h_m(\boldsymbol{x}), & \mathcal{X}_2^m(t) = L_f h_m(\boldsymbol{x}), & \cdots & \mathcal{X}_{r_m}^m(t) = L_f^{r_m-1} h_m(\boldsymbol{x}),\end{array} \tag{3.5}$$

where the states are the m outputs y_i and their derivatives up to order r_i with $i = 1, \cdots, m$. Choosing $n-r$ variables $\eta_1(t), \cdots, \eta_{n-r}(t)$, which are independent with respect to each other and to the coordinates $\boldsymbol{\mathcal{X}}(t)$ and the new state vector $\begin{bmatrix} \boldsymbol{\mathcal{X}}(t) \\ \boldsymbol{\eta}(t) \end{bmatrix}$ for the system is completed.

The external dynamics

$$\begin{array}{rcl}\dot{\mathcal{X}}_1^i(t) & = & \mathcal{X}_2^i(t) \\ & \vdots & \\ \dot{\mathcal{X}}_{r_i}^i(t) & = & v_i(t) + \tilde{d}_i(\boldsymbol{x}, t)\end{array} \tag{3.6}$$

for $i = 1, \cdots, m$ together with the internal dynamics (if $r < n$)

$$\dot{\boldsymbol{\eta}}(t) = \boldsymbol{w}(\boldsymbol{\mathcal{X}}, \boldsymbol{\eta}) + P(\boldsymbol{\mathcal{X}}, \boldsymbol{\eta})\boldsymbol{u}(t) + Q(\boldsymbol{\mathcal{X}}, \boldsymbol{\eta})\boldsymbol{d}(t) \tag{3.7}$$

describes the system dynamics. If $n = r$, no internal dynamics exists. The system is input-output linearized.

Based on the transformed form of the system with the external and internal dynamics in (3.6)-(3.7), linear control laws, e.g., state feedback with pole placement or LQR method, can be applied to control the transformed system (3.6). The performance of the control is apparently affected by the transformed unknown inputs, which makes classical nonlinear control ineffective. Additionally to realize the control design for the original system (3.1) with the classical nonlinear method, it has to be assumed that all the states $\boldsymbol{x}(t)$ are available (by measurements or reconstruction applying suitable observers assuming observability).

In the following paragraphs, a PI-Observer will be designed to estimate the states and the unknown disturbances in (3.2).

3.2.2 PI-Observer design for the transformed system

From the transformed system model (3.2), the transformed system dynamics are decoupled in m subsystems which can be described uniformly by

$$y_i^{(r_i)}(t) = v_i(t) + \tilde{d}_i(\boldsymbol{x}, t), \quad i = 1, \cdots, m, \text{ or} \tag{3.8}$$

$$\begin{array}{rcl}\dot{\mathcal{X}}_1^i(t) & = & \mathcal{X}_2^i(t) \\ & \vdots & \\ \dot{\mathcal{X}}_{r_i}^i(t) & = & v_i(t) + \tilde{d}_i(\boldsymbol{x}, t).\end{array} \tag{3.9}$$

Every subsystem can be written in an individual state space form

$$\begin{aligned}\dot{\boldsymbol{\mathcal{X}}}^{\boldsymbol{i}}(t) &= \boldsymbol{\mathcal{A}_i}\boldsymbol{\mathcal{X}}^{\boldsymbol{i}}(t) + \boldsymbol{\mathcal{B}_i}v_i(t) + \boldsymbol{\mathcal{N}_i}\tilde{d}_i(\boldsymbol{x},t),\\ y_i(t) &= \boldsymbol{\mathcal{C}_i}\boldsymbol{\mathcal{X}}^{\boldsymbol{i}}(t),\end{aligned} \tag{3.10}$$

with state vector $\boldsymbol{\mathcal{X}}^{\boldsymbol{i}}(t) = \begin{bmatrix} y_i(t) \\ \dot{y}_i(t) \\ \vdots \\ y_i^{(r_i)}(t) \end{bmatrix}_{r_i\times 1}$, system matrix $\boldsymbol{\mathcal{A}_i} = \begin{bmatrix} 0 & 1 & \cdots & 0 \\ \vdots & 0 & \ddots & 0 \\ 0 & \cdots & 0 & 1 \\ 0 & \cdots & \cdots & 0 \end{bmatrix}_{r_i\times r_i}$,
input matrix $\boldsymbol{\mathcal{B}_i} = \begin{bmatrix} 0 \\ \vdots \\ 0 \\ 1 \end{bmatrix}_{r_i\times 1}$, matrix $\boldsymbol{\mathcal{N}_i} = \begin{bmatrix} 0 \\ \vdots \\ 0 \\ 1 \end{bmatrix}_{r_i\times 1}$, output matrix
$\boldsymbol{\mathcal{C}_i} = \begin{bmatrix} 1 & 0 & \cdots & 0 \end{bmatrix}_{1\times r_i}$.

In this case, it is obvious that the system is fully controllable and fully observable according to the structure of $(\boldsymbol{\mathcal{A}_i}, \boldsymbol{\mathcal{B}_i})$ and $(\boldsymbol{\mathcal{A}_i}, \boldsymbol{\mathcal{C}_i})$.

The decoupled subsystems have an appropriate structure for the proposed PI- Observer design [118]. Therefore, PI-Observers can be constructed for each subsystem separately, for example

$$\begin{aligned}\begin{bmatrix} \dot{\hat{\boldsymbol{\mathcal{X}}}}^{\boldsymbol{i}}(t) \\ \dot{\hat{\tilde{d}}}_i(\boldsymbol{x},t) \end{bmatrix} &= \underbrace{\begin{bmatrix} \boldsymbol{\mathcal{A}_i} & \boldsymbol{\mathcal{N}_i} \\ \mathbf{0} & \mathbf{0} \end{bmatrix}}_{\boldsymbol{\mathcal{A}_{ei}}} \begin{bmatrix} \hat{\boldsymbol{\mathcal{X}}}^{\boldsymbol{i}}(t) \\ \hat{\tilde{d}}_i(\boldsymbol{x},t) \end{bmatrix} + \begin{bmatrix} \boldsymbol{\mathcal{B}_i} \\ \mathbf{0} \end{bmatrix} v_i(t) \\ &\quad + \underbrace{\begin{bmatrix} \boldsymbol{\mathcal{L}_{1i}} \\ \boldsymbol{\mathcal{L}_{2i}} \end{bmatrix}}_{\boldsymbol{\mathcal{L}_i}} (y_i(t) - \hat{y}_i(t)), \\ \hat{y}_i(t) &= \underbrace{\begin{bmatrix} \boldsymbol{\mathcal{C}_i} & \mathbf{0} \end{bmatrix}}_{\boldsymbol{\mathcal{C}_{ei}}} \begin{bmatrix} \hat{\boldsymbol{\mathcal{X}}}^{\boldsymbol{i}}(t) \\ \hat{\tilde{d}}_i(\boldsymbol{x},t) \end{bmatrix}.\end{aligned} \tag{3.11}$$

Furthermore, the requirement of a PI-Observer design [97, 118] is fulfilled: the extended system ($\boldsymbol{\mathcal{A}_{ei}}$, $\boldsymbol{\mathcal{C}_{ei}}$) is fully observable. With properly chosen observer gain matrices $\boldsymbol{\mathcal{L}_{1i}}$ and $\boldsymbol{\mathcal{L}_{2i}}$ with the corresponding dimension $r_i \times 1$ and 1×1, the transformed states $\boldsymbol{\mathcal{X}_i}(t)$ and the transformed disturbances $\tilde{d}_i(\boldsymbol{x},t)$ can be estimated with the PI-Observer as $\hat{\boldsymbol{\mathcal{X}}}_{\boldsymbol{i}}(t)$ and $\hat{\tilde{d}}_i(\boldsymbol{x},t)$.

3.2.3 Robust control design for the transformed system

Realizing a robust control, a state feedback control with a disturbance rejection

$$v_i(t) = -\boldsymbol{\mathcal{K}}^{\boldsymbol{i}}\hat{\boldsymbol{\mathcal{X}}}^{\boldsymbol{i}}(t) - \hat{\tilde{d}}_i(\boldsymbol{x},t) \tag{3.12}$$

can be taken to stabilize the transformed system dynamics, because the estimations $\hat{\boldsymbol{\mathcal{X}}}^{\boldsymbol{i}}(t)$ and $\hat{\tilde{d}}_i(\boldsymbol{x}, t)$ are available from the PI-Observer and the transformed system is assumed as fully controllable. The state feedback control (gain matrix $\boldsymbol{\mathcal{K}}^{\boldsymbol{i}}$) is designed by pole placement method with the characteristic polynomial to be a Hurwitz polynomial. Using the nonlinear feedback (3.3), the inputs to the original system dynamics can be constructed. At the same time, from the m PI-Observers the external unknown inputs $\tilde{\boldsymbol{d}}(\boldsymbol{x}, t)$ can be estimated in the transformed coordinations. Of course all the states $\boldsymbol{x}(t)$ and outputs $\boldsymbol{y}$(t) in the original coordinates should be available to realize the input-output linearization as usual.

3.2.4 Stability of the closed-loop system

The following theorem is addressed in order to analyze the stability and robustness of the closed-loop system.

Theorem 1. *Assume the system (3.1) has relative degree r and its zero dynamics is locally asymptotically stable. With state feedback matrices*

$$\boldsymbol{\mathcal{K}}^{\boldsymbol{i}} = \begin{bmatrix} \mathcal{K}_1^i & \mathcal{K}_2^i & \cdots & \mathcal{K}_{r_i}^i \end{bmatrix}$$

for every subsystem satisfying Hurwitz stability criterion and PI-Observers designed by LQR method with suitable chosen observer gains, the closed-loop system is locally asymptotically stable and robust against the unknown disturbances $\boldsymbol{d}$.

Proof. The external dynamics (3.6) is transformed with the control input designed by (3.12) into

$$\dot{\mathcal{X}}_{r_i}^i = -\mathcal{K}_1^i \hat{\mathcal{X}}_1^i - \mathcal{K}_2^i \hat{\mathcal{X}}_2^i - \cdots - \mathcal{K}_{r_i}^i \hat{\mathcal{X}}_{r_i}^i + \tilde{d}_i(\boldsymbol{x}, t) - \hat{\tilde{d}}_i(\boldsymbol{x}, t), \tag{3.13}$$

which can be analyzed after Laplace transformation in frequency domain

$$(s^{r_i} + \mathcal{K}_{r_i}^i s^{r_i - 1} + \cdots + \mathcal{K}_2^i s + \mathcal{K}_1^i)\mathcal{X}_1^i(s) = \underbrace{\boldsymbol{\mathcal{K}}^{\boldsymbol{i}} \left(\boldsymbol{\mathcal{X}}^{\boldsymbol{i}}(s) - \hat{\boldsymbol{\mathcal{X}}}^{i}(s) \right)}_{\boldsymbol{\mathcal{K}}^{\boldsymbol{i}} \boldsymbol{e}^i(s)} + \underbrace{\tilde{d}_i(s) - \hat{\tilde{d}}_i(s)}_{\boldsymbol{f_e}^i(s)}$$

with $\boldsymbol{e}^i(s)$ and $\boldsymbol{f_e}^i(s)$ as the estimation errors from the PI-Observer design in (3.11). The output $y_i(s) = \mathcal{X}_1^i(s)$ accordingly the external dynamics is stable, because the characteristic polynomial in (3.13) is Hurwitz stable and the inputs to the transfer behavior, the estimation errors of the PI-Observer, converge to an arbitrarily small value γ.

Due to the fact that the zero dynamics is assumed to be stable, it can be concluded that the whole control loop is stable and robust to the disturbances $\boldsymbol{d}$. □

3.3 Conditions for the application on mechanical systems

The proposed robust control approach in Chapter 3.2 has two requirements:
i) all the states in original coordinates should be either available or observable as transformed states in (3.10) and
ii) a nominal input-output linearizable model has to be available.

For mechanical systems, the limitations are not strong. In the following paragraphs, the conditions for the application of the proposed approach will be discussed.

3.3.1 Modeling of general mechanical systems

Without loss of generality, the discussed class of nonlinear mechanical systems is described by n second order differential equations

$$\begin{aligned}\begin{bmatrix} \ddot{q}_1(t) \\ \vdots \\ \ddot{q}_n(t) \end{bmatrix} &= \begin{bmatrix} f_1(q_1, \dot{q}_1, \cdots, q_n, \dot{q}_n) \\ \vdots \\ f_n(q_1, \dot{q}_1, \cdots, q_n, \dot{q}_n) \end{bmatrix} \\ &+ \begin{bmatrix} g_{11}(q_1, \dot{q}_1, \cdots, q_n, \dot{q}_n) & \cdots & g_{1l}(q_1, \dot{q}_1, \cdots, q_n, \dot{q}_n) \\ \vdots & \ddots & \vdots \\ g_{n1}(q_1, \dot{q}_1, \cdots, q_n, \dot{q}_n) & \cdots & g_{nl}(q_1, \dot{q}_1, \cdots, q_n, \dot{q}_n) \end{bmatrix} \boldsymbol{u}(t) \\ &+ \begin{bmatrix} d_1(q_1, \dot{q}_1, \cdots, q_n, \dot{q}_n, t) \\ \vdots \\ d_n(q_1, \dot{q}_1, \cdots, q_n, \dot{q}_n, t) \end{bmatrix}, \end{aligned} \tag{3.14}$$

namely

$$\ddot{\boldsymbol{q}}(t) = \underbrace{\boldsymbol{f}(\boldsymbol{q}, \dot{\boldsymbol{q}}) + \boldsymbol{g}(\boldsymbol{q}, \dot{\boldsymbol{q}})\boldsymbol{u}(t)}_{\text{Nominal model}} + \boldsymbol{d}(\boldsymbol{q}, \dot{\boldsymbol{q}}, t), \tag{3.15}$$

$$\boldsymbol{y}_m(t) = \boldsymbol{q}(t), \tag{3.16}$$

$$\boldsymbol{y}_c(t) = C_c\boldsymbol{q}(t), \tag{3.17}$$

with $\boldsymbol{q}(t) = \begin{bmatrix} q_1(t) \\ q_2(t) \\ \vdots \\ q_n(t) \end{bmatrix} \in \mathbb{R}^n$, input vector $\boldsymbol{u}(t) \in \mathbb{R}^l$, outputs to be controlled $\boldsymbol{y}_c(t) \in \mathbb{R}^m$ and measurement $\boldsymbol{y}_m(t) \in \mathbb{R}^n$. The vector fields $\boldsymbol{f}(\cdot)$ on $\mathbb{R}^n$ and $\boldsymbol{g}(\cdot)$ on $\mathbb{R}^{n\times l}$ are assumed as smooth. The assumed system structure (3.15) is typical for systems like mass-spring, multibody, or mechanical systems modelled by finite element method.

3.3.2 Conditions for the applications

Some assumptions are made here for mechanical systems to adopt the proposed robust control approach:

- all the displacements $\boldsymbol{q}$ are measurable, see (3.16),
- the outputs to be controlled are assumed as some of displacement, see (3.17),
- the number of inputs is equal to the number of outputs to be controlled, namely $l = m$ in Chapter 3.3.1, and

- the nominal system model in (3.15) is input-output linearizable.

With the assumptions mentioned above, the system (3.15) can be written in a general form with $2n$ first order differential equations

$$\begin{aligned} \dot{\boldsymbol{\phi}}(t) &= \begin{bmatrix} \phi_{n+1} \\ \vdots \\ \phi_{2n} \\ \boldsymbol{f}(\boldsymbol{\phi}) \end{bmatrix} + \begin{bmatrix} \mathbf{0}_{n\times 1} \\ \boldsymbol{g}(\boldsymbol{\phi}) \end{bmatrix} \boldsymbol{u}(t) + \begin{bmatrix} \mathbf{0}_{n\times 1} \\ \boldsymbol{d}(\boldsymbol{\phi}, t) \end{bmatrix}, \\ \boldsymbol{y}_{control}(t) &= \boldsymbol{C}_{contr}\boldsymbol{\phi}(t), \\ \boldsymbol{y}_{measure}(t) &= \boldsymbol{C}_{measure}\boldsymbol{\phi}(t), \end{aligned} \tag{3.18}$$

with the state vector $\boldsymbol{\phi}(t) = \begin{bmatrix} \boldsymbol{q}(t) \\ \dot{\boldsymbol{q}}(t) \end{bmatrix}$ and output matrices $\boldsymbol{C}_{contr}$ and $\boldsymbol{C}_{measure}$.

For such systems, the application of the proposed approach is feasible. The requirements of the approach are fufilled here.

Availability of all the states:

For the nonlinear feedback in the input-output linearization process in (3.3)-(3.5), usually all the system states, the outputs, and the derivatives of the outputs in the original coordinates are required. This includes for the application on mechanical systems:

- All the displacement as well as the outputs to be controlled are assumed as measurable.
- The velocities, which are also states in the original coordinates, can be estimated either by PI-Observers as the states in the transformed coordinates when the corresponding displacement are to be controlled, or by additional PI-Observers designed for estimation of the internal dynamics if the corresponding displacement do not appear in the outputs.
- The derivatives of the outputs can be obtained from the PI-Observers as the states in the transformed coordinates.

Possibility of full rank disturbance estimation:

Another important aspect is that the estimations of modeling errors and disturbances as unknown inputs possibly with full rank in the original coordinates in (3.14) are available based on the estimations of transformed unknown inputs by the PI-Observers.

3.4 Application examples

Two application examples of mechanical systems are given in this part to illustrate the application of the EFL-PIO method proposed in Chapter 3.2. One is a single link rigid manipulator depicted in Figure 3.2 with flexible joint (a single-input single-output (SISO) nonlinear benchmark system) and the other one is a multi-input multi-output (MIMO) nonlinear mass-spring system. The general implementation procedure of EFL-PIO is detailed with the application on the MIMO mass-spring system. The SISO robot system is chosen to show the application of EFL-PIO on the nonlinear systems in special cases where the nonlinear model is input-state-output linearizable.

3.4.1 Robust control of a SISO mechanical system

A well-known example of nonlinear mechanical systems, a single link rigid manipulator with flexible joint [119], is considered here. The system model is known input-state-output linearizable. The application condition of the proposed EFL-PIO method that the system model should be input-output linearizable is fulfilled naturally for an input-state-output linearizable system. Some details in the design have to be carefully considered for input-state-output linearizable systems. For instance, the limitation of displacement measurements mentioned in 3.3.2 may be relaxed, because the original states are available with back transformation from the transformed states estimated by PI-Observer. On the other hand, one possible problem is that the transformed matrix which indicates the acting position of the disturbances in the linearized model may not be constant. This can be solved by defining new variables in the linearized description of the system. Furthermore, the observability of the extended system should be verified and the required measurements should be therefore determined also circumstantially. The implementation of the EFL-PIO method will be shown in detail. The specific feature of EFL-PIO is the ability to give the estimation of the disturbances besides the robust feature.

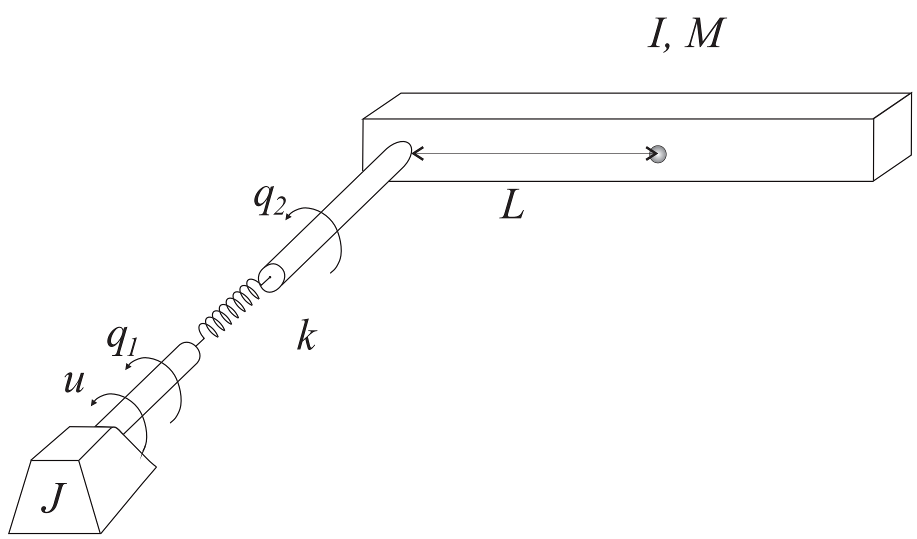

Figure 3.2: Single link robot with joint flexibility[119]

Modeling of single link rigid manipulator with flexible joint

A sketch of the well known example [119] is shown in Figure 3.2. The nominal input-state linearizable model of the system is defined as

$$\begin{aligned}\dot{\boldsymbol{x}} &= \begin{bmatrix} x_2 \\ -\frac{MgL}{I}\sin(x_1) - \frac{k}{I}(x_1 - x_3) \\ x_4 \\ -\frac{k}{J}(x_1 - x_3) \end{bmatrix} + \begin{bmatrix} 0 \\ 0 \\ 0 \\ \frac{1}{J} \end{bmatrix} u \\ &= \boldsymbol{f}(\boldsymbol{x}) + \boldsymbol{g}(\boldsymbol{x})u,\end{aligned}$$

with the states $\boldsymbol{x} = [q_1\ \dot{q}_1\ q_2\ \dot{q}_2]^T$. The variables q_1 and q_2 denote the angles of the movable and fixed part of the robot respectively and the variables $\dot{q}_1$, $\dot{q}_2$ are the corresponding angular velocities, see Figure 3.2. The variable u is the input torque from the motor. The unknown effects are taken as an external torque $M_{ex} = 3\,N \cdot mm$ acting on the free robot arm for time $t \geq 3s$. and a real moment of inertia $I_{real} = 0.75I$ (75% of the nominal one). Therefore, an extended model of the system can be described by

$$\dot{\boldsymbol{x}} = \boldsymbol{f}(\boldsymbol{x}) + \boldsymbol{g}(\boldsymbol{x})u + \boldsymbol{E}d(\boldsymbol{x}, t), \tag{3.19}$$

with $\boldsymbol{E} = [0\ 1\ 0\ 0]^T$ and $d(\boldsymbol{x}, t) = -\frac{1}{3}\left[\frac{MgL}{I}\sin(x_1) + \frac{k}{I}(x_1 - x_3)\right] + \frac{M_{ex}}{I_{real}}$. The measurements will be discussed later. The parameters from a test rig in [43] are used here and listed in Table 3.1.

Table 3.1: Parameters used in the simulation

Variable	Physical meaning	Value	Unit
M	Link mass	0.2	kg
g	Acceleration of gravity	9.81	m/s^2
L	Center of mass	0.02	m
I	Link inertial	1.35×10^{-4}	kg·m^2
J	Rotor inertia	2.16×10^{-3}	kg·m^2
k	Stiffness	7.47	N·m/rad

Input-state-output linearization

With the transformation

$$\boldsymbol{z} = \boldsymbol{T}(\boldsymbol{x}) = \begin{bmatrix} x_1 \\ x_2 \\ -\frac{MgL}{I}\sin(x_1) - \frac{k}{I}(x_1 - x_3) \\ -\frac{MgL}{I}\cos(x_1)x_2 - \frac{k}{I}(x_2 - x_4) \end{bmatrix},$$

a special input-state linearized model of the system (3.19) is described by

$$\dot{\boldsymbol{z}} = \boldsymbol{A}\boldsymbol{z} + \boldsymbol{b}v + \bar{\boldsymbol{N}}d, \tag{3.20}$$

where $\bar{\boldsymbol{N}} = \begin{bmatrix} 0 \\ 1 \\ 0 \\ -\frac{MgL}{I}\cos(x_1) - \frac{k}{I} \end{bmatrix}$, $\boldsymbol{A} = \begin{bmatrix} 0 & 1 & 0 & 0 \\ 0 & 0 & 1 & 0 \\ 0 & 0 & 0 & 1 \\ 0 & 0 & 0 & 0 \end{bmatrix}$, $\boldsymbol{b} = \begin{bmatrix} 0 \\ 0 \\ 0 \\ 1 \end{bmatrix}$, and

$$v = \frac{k}{IJ}u + a(\boldsymbol{x}),$$

with

$$\begin{aligned} a(\boldsymbol{x}) = {} & \frac{MgL}{I}\sin(x_1)\left[x_2^2 + \frac{MgL}{I}\cos(x_1) + \frac{k}{I}\right] \\ & + \frac{k}{I}(x_1 - x_3)\left[\frac{k}{I} + \frac{k}{J} + \frac{MgL}{I}\cos(x_1)\right]. \end{aligned}$$

PI-Observer and robust control design for the input-state-output linearized model

It can be seen that the linearized model in (3.20) is not suitable for a PI-Observer design because of the non-constant matrix $\bar{\boldsymbol{N}}$, which is a general problem in the application of EFL-PIO method to input-state-output linearizable systems. To solve this problem, two different possible solutions can be considered: one is to define a new input variable based on v; the other one is to define an additional unknown input besides d. In the latter one, the new unknown input will be dependent on the unknown input d which leads to a larger system dimension in the PI-Observer design and reduces the efficiency. Hence, the first possibility to solve the problem with non-constant matrix $\bar{\boldsymbol{N}}$ is considered. A new input variable is defined by

$$\tilde{v} = v + \left[-\frac{MgL}{I}\cos(x_1) - \frac{k}{I}\right]d.$$

Accordingly, the linearized model (3.20) is transformed into

$$\dot{\boldsymbol{z}} = \boldsymbol{A}\boldsymbol{z} + \boldsymbol{b}\tilde{v} + \tilde{\boldsymbol{N}}d, \tag{3.21}$$

where $\tilde{\boldsymbol{N}} = \begin{bmatrix} 0 \\ 1 \\ 0 \\ 0 \end{bmatrix}$.

With the measurements x_1 and x_3, the states $z_1 = x_1$ and $z_2 = -\frac{MgL}{I}\sin(x_1) - \frac{k}{I}(x_1 - x_3)$ in the linearized model (3.20) are available. It is proven with Kalman criterion that the extended system of the model (3.21) with

$$\boldsymbol{A_e} = \begin{bmatrix} 0 & 1 & 0 & 0 & 0 \\ 0 & 0 & 1 & 0 & 1 \\ 0 & 0 & 0 & 1 & 0 \\ 0 & 0 & 0 & 0 & 0 \end{bmatrix} \text{ and } \boldsymbol{C_e} = \begin{bmatrix} 1 & 0 & 0 & 0 & 0 \\ 0 & 0 & 1 & 0 & 0 \end{bmatrix}$$

is observable. Note that measuring x_1 and x_3 is the simplest way to have an observable model for (3.20), because the extended system is proven not observable using Kalman criterion with less measurements (e.g., with only one measurement x_1 or x_2) or other combinations with two measurements. The variables $\hat{\boldsymbol{z}}$, $\hat{d}$, and $\hat{\boldsymbol{x}} = \boldsymbol{T}^{-1}\hat{\boldsymbol{z}}$ can then be estimated and calculated by a suitable PI-Observer design for the system (3.21). A robust control for the system is then designed by $u = \frac{IJ}{k}\left[\tilde{v} - a(\hat{\boldsymbol{x}}) + \left(\frac{MgL}{I}\cos(\hat{x}_1) + \frac{k}{I}\right)\hat{d}\right]$, with a state feedback and disturbance rejection $\tilde{v} = -\boldsymbol{K}[\hat{\boldsymbol{z}} - \boldsymbol{z}_{ref}\ \hat{d}]^T$ for the linearized model.

Simulation results

Simulation results are given in Figure 3.3 and Figure 3.4. Here, control performance

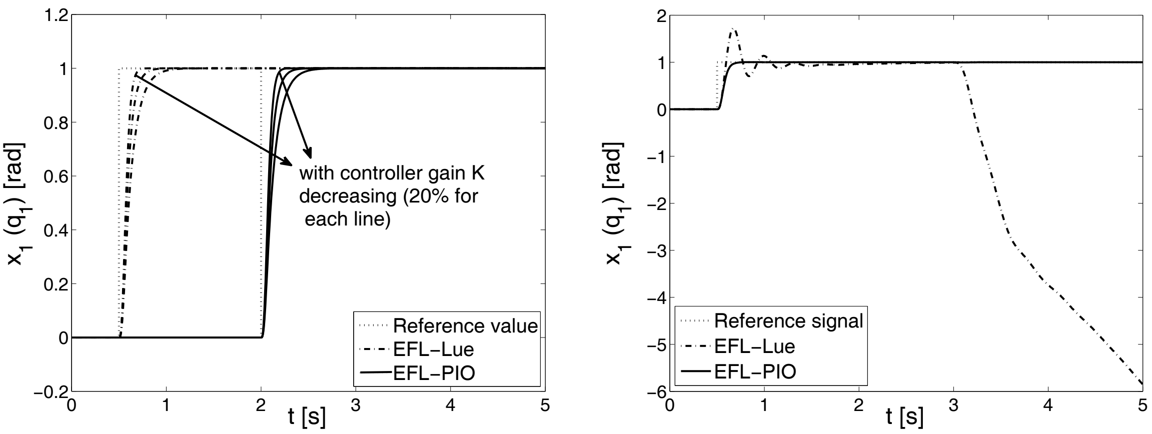

(a) Results without unknown effects (b) Results with unknown effects

Figure 3.3: Simulation results

from the proposed approach (EFL-PIO) and a nonlinear controller designed based on the classical exact feedback linearization and a Luenberger observer (EFL-Lue) are compared for the two cases with and without unknown/unmodeled effects. The same state feedback matrix is used in both of the methods. When the model and parameters are known and no disturbance exists, both of the EFL-Lue and EFL-PIO can achieve good control performance in the position control of x_1 as shown in Figure 3.3(a), where unit step functions at different time are taken as reference signal respectively for the two methods in order to get clear illustration of both methods. With the assumed unknown effects in the simulation, the EFL-Lue cannot stabilize the system, see Figure 3.3(b), because of the strong influence from the unknown effects, especially the external torque for $t \geq 3s$. The proposed EFL-PIO not only stabilizes the system in spite of the existence of the disturbance and uncertainties, but also gives an estimation of the unknown effects as shown in Figure 3.4.

It can be seen from the results that the proposed approach is robust to the considered parameter uncertainty and the disturbance torque.

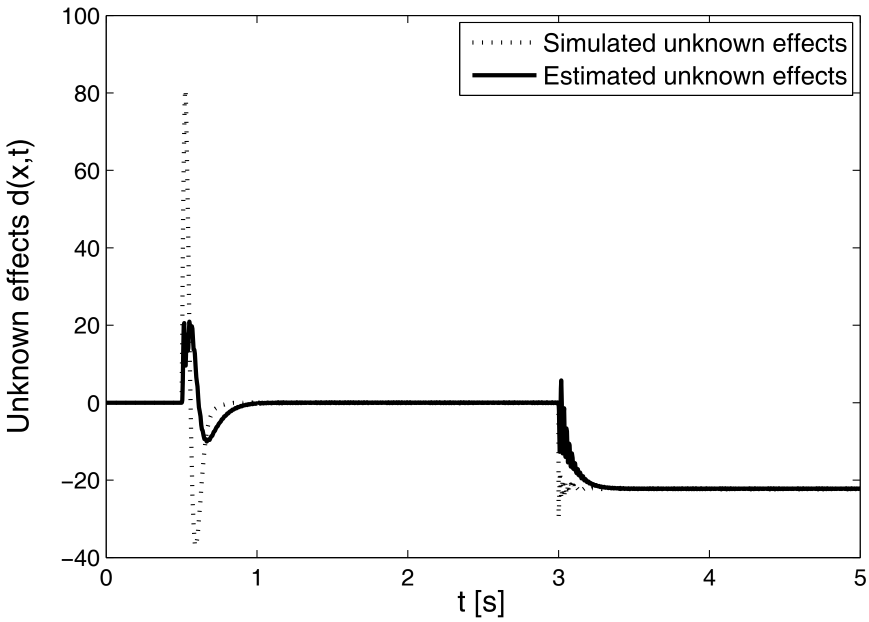

Figure 3.4: Estimation of unknown effects from PI-Observer

3.4.2 Robust control design of MIMO mass-spring system

A mechanical system will be used in this part to illustrate the general implementation process of the presented robust control method on input-output linearizable nonlinear mechanical systems as assumed.

Modeling of a nonlinear MIMO mass-spring system

An example of nonlinear MIMO mechanical systems, based on the system [3] shown in Figure 3.5, is given to illustrate the proposed method. The system is a mass-spring system

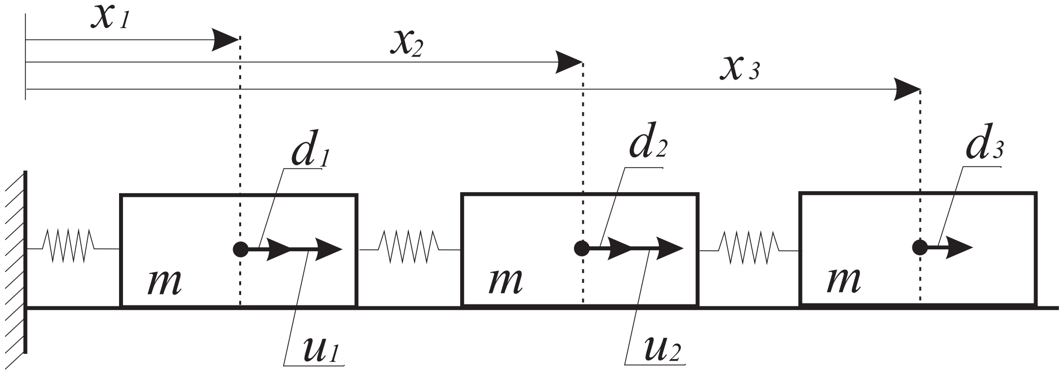

Figure 3.5: Nonlinear MIMO mechanical system

with nonlinear spring stiffness, which can be modeled as

$$\begin{aligned}
m\ddot{x}_1 &= k(-2x_1 + x_2) + k_p[-x_1^3 + (x_2 - x_1)^3] + u_1 + d_1,\\
m\ddot{x}_2 &= k(x_1 - 2x_2 + x_3) + k_p[(x_3 - x_2)^3 - (x_2 - x_1)^3] + u_2 + d_2,\\
m\ddot{x}_3 &= k(x_2 - x_3) + k_p(x_2 - x_3)^3 + d_3,\\
y_{meas} &= \begin{bmatrix} x_1 & x_2 & x_3 \end{bmatrix}^T, \text{and}\\
y_{contr} &= \begin{bmatrix} y_1 & y_2 \end{bmatrix}^T = \begin{bmatrix} x_1 & x_3 \end{bmatrix}^T.
\end{aligned} \tag{3.22}$$

The parameters used in simulation are $m = 0.5\ kg$, $k = 217.0\ N/m$, and $kp = 63.5\ N/m^3$. The dynamics of the disturbance forces d_1, d_2, and d_3 acting on the masses are assumed as unknown to the control design but considered in the simulation as $d_1 = 5$, $d_2 = 10sin(5t)$, and $d_3 = 20sin(10t)$ additionally to the nominal model presented in [3].

The input-output linearized form of the system can be written as

$$\ddot{y}_1 = v_1 + \frac{d_1}{m} = v_1 + \bar{\eta}_1, \tag{3.23}$$

$${y_2}^{(4)} = v_2 + [\frac{k}{m} + \frac{3k_p}{m}(x_2 - x_3)^2](\frac{d_2}{m} - \frac{d_3}{m}) = v_2 + \bar{\eta}_2, \tag{3.24}$$

if the inputs are chosen as

$$u_1 = m\left[v_1 - \frac{k}{m}(-2x_1 + x_2) - \frac{k_p}{m}\left[-x_1^3 + (x_2 - x_1)^3\right]\right] \text{ and} \tag{3.25}$$

$$\begin{aligned}
u_2 = {} & \frac{m}{\frac{k}{m} + \frac{3k_p}{m}(x_2 - x_3)^2} \times\\
& \{v_2 - \left[\frac{k}{m} + \frac{3k_p}{m}(x_2 - x_3)^2\right] \times\\
& \left[\frac{k}{m}(x_1 - 3x_2 + 2x_3) + \frac{k_p}{m}\left[2(x_3 - x_2)^3 - (x_2 - x_1)^3\right]\right] -\\
& 6\frac{k_p}{m}(x_2 - x_3)(\dot{x}_2 - \dot{x}_3)^2\}.
\end{aligned} \tag{3.26}$$

The remaining zero dynamics/internal dynamics

$$\ddot{x}_2 = \frac{1}{m}\left[k(x_1 - 2x_2 + x_3) + k_p[(x_3 - x_2)^3 - (x_2 - x_1)^3] + u_2 + d_2\right]$$

are stable, if the disturbance d_2 is bounded.

Two PI-Observers can be designed for the transformed decoupled dynamics (3.23) and (3.24)

$$\begin{aligned}
\dot{z}_a &= \begin{bmatrix} 0 & 1 \\ 0 & 0 \end{bmatrix} z_a + \begin{bmatrix} 0 \\ 1 \end{bmatrix} v_1 + \begin{bmatrix} 0 \\ 1 \end{bmatrix} \hat{\bar{\eta}}_1 + L_{1a}(y_1 - \hat{y}_1),\\
\dot{\hat{\bar{\eta}}}_1 &= L_{2a}(y_1 - \hat{y}_1),\\
\hat{y}_1 &= \begin{bmatrix} 1 & 0 \end{bmatrix} z_a,
\end{aligned} \tag{3.27}$$

and

$$
\begin{aligned}
\dot{z}_b &= \begin{bmatrix} 0 & 1 & 0 & 0 \\ 0 & 0 & 1 & 0 \\ 0 & 0 & 0 & 1 \\ 0 & 0 & 0 & 0 \end{bmatrix} z_b + \begin{bmatrix} 0 \\ 0 \\ 0 \\ 1 \end{bmatrix} v_2 + \begin{bmatrix} 0 \\ 0 \\ 0 \\ 1 \end{bmatrix} \hat{\bar{\eta}}_2 + L_{1b}(y_2 - \hat{y}_2), \\
\dot{\hat{\bar{\eta}}}_2 &= L_{2b}(y_2 - \hat{y}_2), \\
\hat{y}_2 &= \begin{bmatrix} 1 & 0 & 0 & 0 \end{bmatrix} z_b,
\end{aligned}
\tag{3.28}
$$

with the state vectors $z_a = \begin{bmatrix} \hat{y}_1 \\ \dot{\hat{y}}_1 \end{bmatrix}$ and $z_b = \begin{bmatrix} \hat{y}_2 \\ \dot{\hat{y}}_2 \\ \ddot{\hat{y}}_2 \\ \hat{y}_2^{(3)} \end{bmatrix}$, to estimate the transformed states and disturbances, namely $\hat{x}_1$, $\dot{\hat{x}}_1$, $\hat{\bar{\eta}}_1$, $\hat{x}_3$, $\dot{\hat{x}}_3$, $\ddot{\hat{x}}_3$, $\hat{x}_3^{(3)}$, and $\hat{\bar{\eta}}_2$. To construct the inputs in (3.25) and (3.26), besides the displacement x_1, x_2, and x_3 the velocities $\dot{x}_2$ and $\dot{x}_3$ are also required. As a transformed coordinate, the velocity $\dot{x}_3$ can be estimated by the PI-Observer (3.28). To estimate the velocity $\dot{x}_2$, a third PI-Observer can be designed by

$$
\begin{aligned}
\dot{z}_c &= \begin{bmatrix} 0 & 1 \\ 0 & 0 \end{bmatrix} z_c + \begin{bmatrix} 0 \\ 1 \end{bmatrix} v_3 + \begin{bmatrix} 0 \\ 1 \end{bmatrix} \hat{\bar{\eta}}_3 + L_{1c}(x_2 - \hat{x}_2), \\
\dot{\hat{\bar{\eta}}}_3 &= L_{2c}(x_2 - \hat{x}_2),
\end{aligned}
\tag{3.29}
$$

with state vector $z_c = \begin{bmatrix} \hat{x}_2 \\ \dot{\hat{x}}_2 \end{bmatrix}$,
$v_3 = \frac{k}{m}\left[(x_1 - 2x_2 + x_3) + k_p[(x_3 - x_2)^3 - (x_2 - x_1)^3] + u_2\right]$, and $\bar{\eta}_3 = \frac{d_2}{m}$.

With the estimations from the three PI-Observers (3.27), (3.28), and (3.29), the system (3.14) can be transformed into an input-output linearized form with nonlinear feedback (3.25) and (3.26). To realize a robust control loop, linear control methods can be applied to the linearized model (3.23) and (3.24), for example with linear state feedback control

$$
v_1 = -20\dot{\hat{x}}_1 - 100(x_1 - x_{1ref}) - \hat{\bar{\eta}}_1, \tag{3.30}
$$

$$
v_2 = -200\hat{x}_3^{(3)} - 15000\ddot{\hat{x}}_3 - 500000\dot{\hat{x}}_3 - 6250000(x_3 - x_{3ref}) - \hat{\bar{\eta}}_2. \tag{3.31}
$$

The desired values taken in the simulation are $x_{1ref} = 0.25$ and $x_{3ref} = 0.3$. The dynamics of the disturbances d_1, d_2, and d_3 are calculated from the estimations $\hat{\bar{\eta}}_1$, $\hat{\bar{\eta}}_2$, and $\hat{\bar{\eta}}_3$.

Simulation results

The simulation results considering a perfect nominal model of the system (no external disturbances $d_1 = d_2 = d_3 = 0$) with the proposed EFL-PIO method in comparison with classical input-output linearization method based on Luenberger observer (EFL-Lue) are given in Figure 3.6. It can be concluded that considering no disturbance both the proposed EFL-PIO method and the classical EFL-Lue result in good control performance (both the control errors converge). To illustrate the robustness of the control methods,

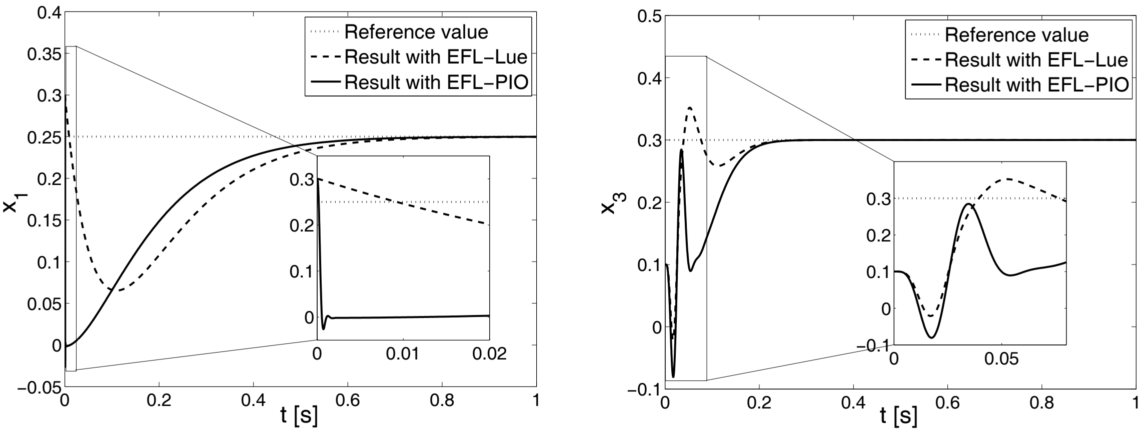

(a) (b)

Figure 3.6: Comparison of control results I

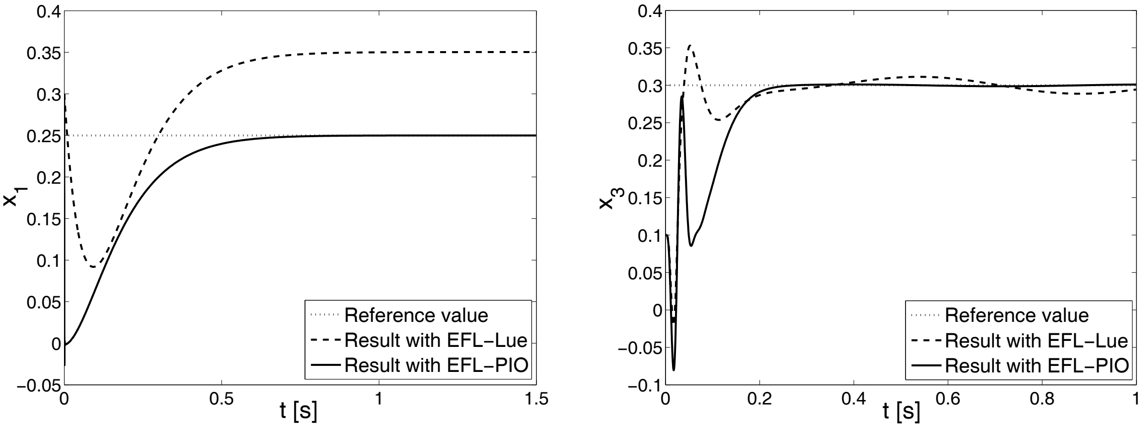

(a) (b)

Figure 3.7: Comparison of control results II

simulation results with consideration of external disturbances ($d_1 = 5$, $d_2 = 10sin(5t)$, and $d_3 = 20sin(10t)$) are shown in Figure 3.7.

The control performance from the proposed approach EFL-PIO has almost not been changed under the condition of existing external disturbances. In comparison, the classical EFL-Lue method is strongly influenced by the disturbances and the control results show a large remaining control error.

The only use of the control error to evaluate the performance of controllers is not a reasonable criterion, because the adjustable controller gains influence strongly the control results and result in different input energy required. Therefore, a criterion based on gains

$$P_{\boldsymbol{K}} = \left[\int_0^T \boldsymbol{u}^2 dt,\ \int_0^T \boldsymbol{e}^2 dt \right]_{\boldsymbol{K}}, \tag{3.32}$$

which considers both the control error $\int_0^T \boldsymbol{e}^2 dt$ and the input energy $\int_0^T \boldsymbol{u}^2 dt$ is used to evaluate the control performance, where $P_{\boldsymbol{K}}$ denotes the trajectory of the control input $\boldsymbol{u}$ as well as the control error $\boldsymbol{e}$ with changing $\boldsymbol{K}$. Here $\boldsymbol{K}$ defines the controller gains that can be tuned and T denotes the time window, where the performance is considered and compared. The performance of control design can be evaluated by judging the trends of the trajectories $P_{\boldsymbol{K}}$ with different methods. The one that reaches the same control error with lower input energy or uses the same energy to get smaller control error (i. e., closer to the origin) denotes the more effective control approach. Furthermore, the one with smaller change in the trajectory under uncertain conditions or with disturbances is robuster.

The criterion is applied for the detailed evaluation of the two control methods EFL-PIO and EFL-Lue as shown in Figure 3.8. The points are obtained in simulations with different set of control gains designed by pole-placement method. The time window $T = 10$ sec. is chosen. The trajectories of $P_{\boldsymbol{K}\_EFL-PIO}$ with and without disturbance are almost identical which implies to a strong robustness of the EFL-PIO method. In contrast, the trajectories $P_{\boldsymbol{K}\_EFL-Lue}$ show a large influence from the disturbance, although the EFL-Lue method is in the case without disturbance more effective than the proposed EFL-PIO method due to the lower location.

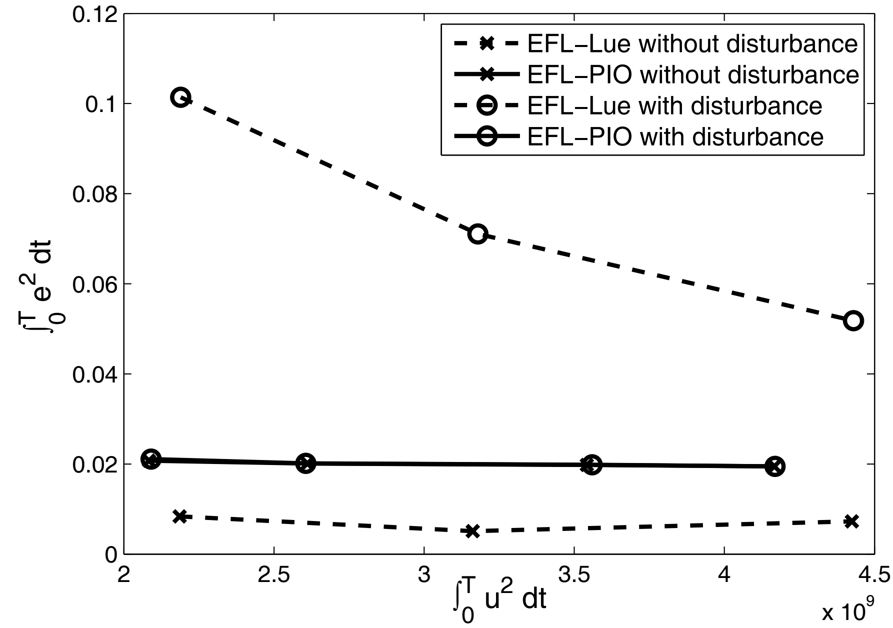

Figure 3.8: Comparison by means of criterion $P_{\boldsymbol{K}}$

Finally, the proposed approach not only realizes a robust control for the considered class of nonlinear MIMO systems, but also generates plausible estimations of the unknown disturbances/modeling error as shown in Figure 3.9. This may be in addition a suitable approach for extended Fault Detection and Isolation (FDI) and/or Structural Health Monitoring (SHM) technique supervising the condition and state of system by for example evaluating residuals.

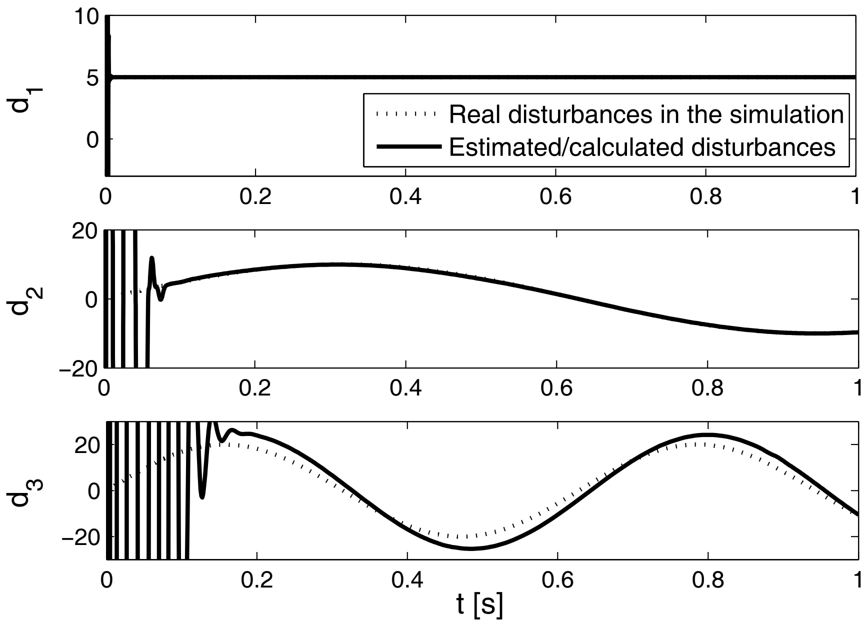

Figure 3.9: Estimation of disturbances

3.5 Summary

In this chapter, the robust control method based on PI-Observer and exact feedback linearization for nonlinear systems was introduced in detail. The nominal model of the considered class of system is assumed available and input-output linearizable. The unknown inputs or disturbances to the nominal system are assumed bounded, but no concrete bounds or dynamics of disturbances are known. Especially, the application of the proposed EFL-PIO method on nonlinear mechanical systems is discussed in Chapter 3.3, where the necessary conditions for the application are listed. Furthermore, two examples of typical nonlinear mechanical systems are given to illustrate the implementation of the proposed method. The general design process of the EFL-PIO method for systems with input-output linearizable system model is shown by a MIMO nonlinear mass-spring system in Chapter 3.4.2. The other example illustrates the application of the EFL-PIO on a nonlinear SISO mechanical system with input-state-output linearizable model. The control performance and the robustness of the EFL-PIO are compared for both examples with a classical exact feedback linearization method combined with a Luenberger observer (EFL-Lue). The improvement of robustness for the classical exact feedback linearization method is obvious. Additionally, the proposed EFL-PIO method offers plausible estimation of disturbances considered as unknown inputs.

4 Applications of PI-Observer Technique

The applications of PI-Observer on mechanical systems as introduced in Chapter 2.1 have been reported in many research publications. In the following parts, the PI-Observer-based control is implemented on a hydraulic differential cylinder to show its applicability on hydraulic systems. Here the nonlinear robust control approach (EFL-PIO) proposed in Chapter 3.2 with position measurement as well as a linear PI-Observer-based state feedback control and disturbance rejection without position measurement is used for the position control of the hydraulic cylinder. The design process and experimental results are given below to illustrate the PI-Observer-based control design for hydraulic systems.

4.1 Robust position control of a hydraulic cylinder with position sensor

Hydraulic cylinders are hydraulic systems with strongly nonlinear electro-mechanical behavior. They are widely used in several industrial areas, such as robots, heavy machines and so on. The dynamics of the hydraulic differential cylinder is described by nonlinear coupled differential equations (see [10, 121]). Many nonlinear control approaches have been developed for the position control of hydraulic differential cylinder, but most of them are based on the assumption, that the system model is perfectly known and related to the actual control situation (load, pressure, oil temperature, etc.), for example, the classical feedback linearization method developed by [10]. However, effective and safe nonlinear control approaches, which are robust to external disturbances and model uncertainties are required. In [28, 89, 91, 101, 104] different methods are developed and applied to solve the robustness problem of the exact feedback linearization approach. However, most of the methods like those published by [89, 101, 104] consider known bounds and/or dynamical properties of the modeling errors or the disturbances. On the other hand robust nonlinear controllers for hydraulic systems are also discussed except for the improved classical nonlinear control methods. A disturbance rejection-based control is introduced in [11], where the disturbance is successfully decoupled and its influence to the output is reduced. The approach requires the measurement of the disturbance force and its time derivative, which limits the application to those applications in which both measurements are available. To solve the same problem, an adaptive control method is presented in [121] also with requirements of several measurements, such as measurements of the time derivatives of the pressures. In contrast, the EFL-PIO approach proposed in this thesis combines the classical exact feedback linearization method and the PI-Observer to realize a robust nonlinear control for nonlinear systems with input-output linearizable nominal model. It utilizes PI-Observer to estimate the unknown effects instead of direct measurements of unknown disturbances or model uncertainties. With the introduction and illustration in Chapter 3.2, the EFL-PIO method is shown as an effective robust control method for mechanical systems, when the nominal system model is not precise and unknown external disturbances exist. In the following paragraphs, the EFL-PIO will be applied for a robust position control design for a hydraulic differential cylinder based on the contribution in [80].

4.1.1 Modeling of a hydraulic differential cylinder system

A nonlinear dynamical model of a hydraulic differential cylinder with a proportional control valve as shown in Figure 4.1 is given by

$$\begin{aligned}\dot{\boldsymbol{x}}(t) &= \begin{bmatrix} x_2 \\ \dfrac{1}{m(x_1)}\left[(x_3 - \dfrac{x_4}{\varphi})A_A\right] \\ \dfrac{E_{oil}(x_3)}{V_A(x_1)}(-A_A x_2) \\ \dfrac{E_{oil}(x_4)}{V_B(x_1)}\left(\dfrac{A_A}{\varphi}x_2\right) \end{bmatrix} + \begin{bmatrix} 0 \\ 0 \\ \dfrac{E_{oil}(x_3)}{V_A(x_1)}Q_A(x_3) \\ \dfrac{E_{oil}(x_4)}{V_B(x_1)}Q_B(x_4) \end{bmatrix} u(t) + \begin{bmatrix} 0 \\ d(t) \\ 0 \\ 0 \end{bmatrix}, \\ &= \boldsymbol{f}(\boldsymbol{x}) + \boldsymbol{g}(\boldsymbol{x})u(t) + \boldsymbol{d}(t),\end{aligned} \tag{4.1}$$

$$y(t) = x_1(t) = h(\boldsymbol{x}), \quad \boldsymbol{y}_m(t) = \begin{bmatrix} x_1(t) \\ x_3(t) \\ x_4(t) \end{bmatrix},$$

with the variant mass

$$m(x_1) = m_{basic} + \rho_{fl}(V_A(x_1) + V_B(x_1)),$$

the volumes in chambers A and B

$$V_A(x_1(t)) = V_{cA} + x_1(t)A_A, \quad V_B(x_1(t)) = V_{cB} + (H - x_1(t))A_B, \quad 0 \le x_1(t) \le H,$$

the disturbance as

$$d(t) = \frac{f_d(t)}{m(x_1)},$$

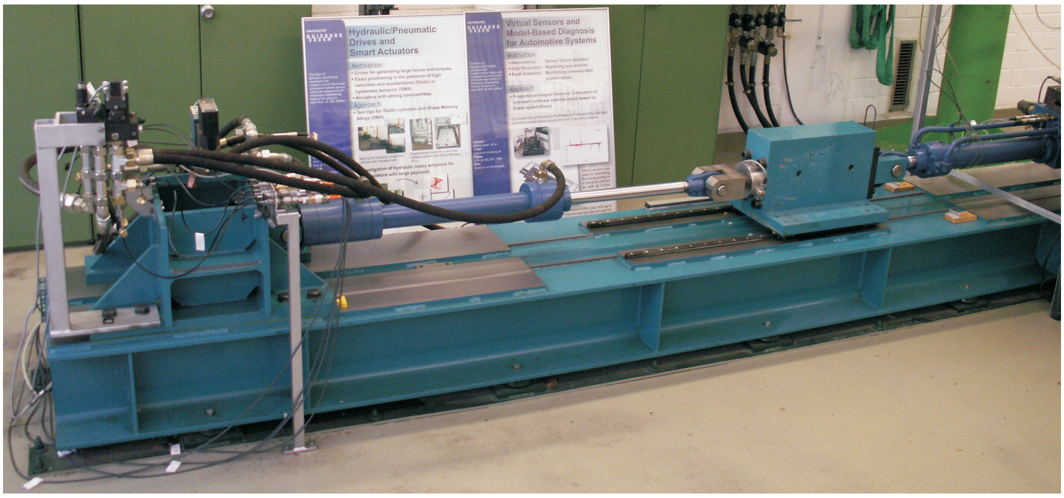

(a) Test rig of the used hydraulic differential cylinder system at the Chair of Dynamics and Control, University of Duisburg-Essen, Germany

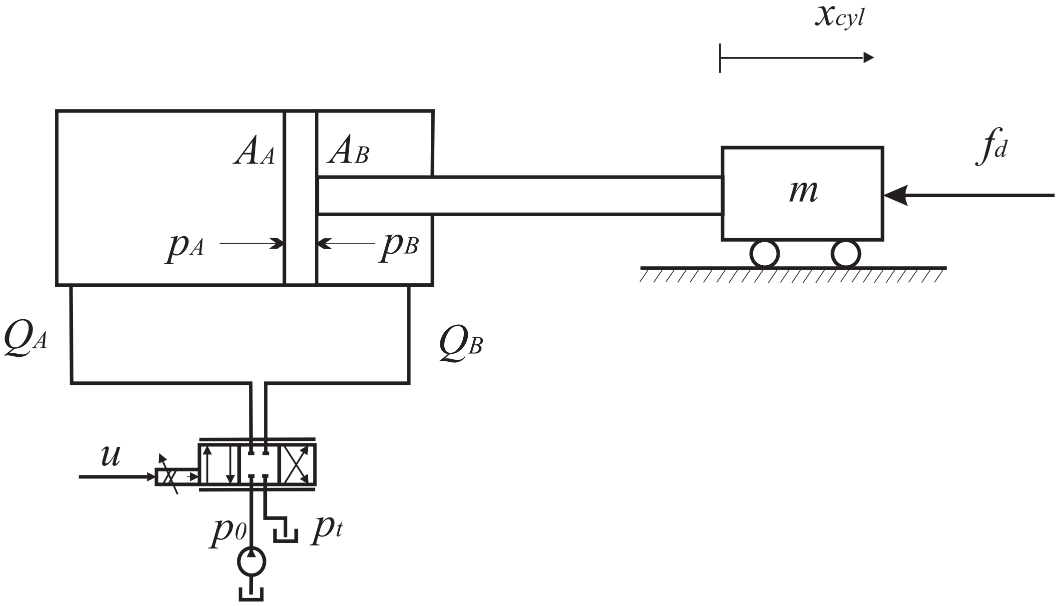

(b) Sketch of the used hydraulic differential cylinder system

Figure 4.1: Hydraulic differential cylinder system

the hydraulic flows

$$Q_A(x_3(t)) = \begin{cases} \dfrac{B_v}{x_{v,max}}\sqrt{|p_0 - x_3(t)|}, & u \geq 0 \\ \dfrac{B_v}{x_{v,max}}\sqrt{|x_3(t) - p_t|}, & u < 0 \end{cases},$$

$$Q_B(x_4(t)) = \begin{cases} -\dfrac{B_v}{x_{v,max}}\sqrt{|x_4(t) - p_t|}, & u \geq 0 \\ -\dfrac{B_v}{x_{v,max}}\sqrt{|p_0 - x_4(t)|}, & u < 0 \end{cases},$$

and the bulk modulus of elasticity

$$E_{oil}(p) = \frac{1}{2} E_{oil,max} \log_{10}(90 \frac{p}{p_{max}} + 3).$$

According to the characteristics of the proportional valve with the assumption of perfect electrodynamic behavior, the input $u(t)$ represents the effective position of the valve $x_{v,effect}(t)$, which can be calculated from the input voltage $u_v(t)$ by

$$x_{v,effect}(t) = \begin{cases} (u_v(t) - x_{v,deadzone+})^2, & u_v(t) \geq x_{v,deadzone+} \\ 0, & x_{v,deadzone-} < u_v(t) < x_{v,deadzone+} \\ -(u_v(t) - x_{v,deadzone-})^2, & u_v(t) \leq x_{v,deadzone-} \end{cases}.$$

Here $x_{v,deadzone-}$ and $x_{v,deadzone+}$ denote the negative and positive dead zone of the valve. The variables and constants are defined in Table 4.1.

Table 4.1: Definition of parameters and variables

Variable	Physical meaning	Value	Unit
$x_1(t) = x_{cyl}(t)$	Displacement of the mass cart	-	m
$x_2(t) = \dot{x}_{cyl}(t)$	Velocity of the mass cart	-	m/s
$x_3(t) = p_A(t)$	Pressure in chamber A	-	pa
$x_4(t) = p_B(t)$	Pressure in chamber B	-	pa
$f_d(t)$	External force acting on the piston	-	N
$u(t) = x_{v,effect}(t)$	Effective valve position	-	-
$u_v(t)$	Input voltage of the valve	-	V
$x_{v,max}$	Maximal valve position	2	mm
$x_{v,deadzone+}$	Valve dead zone (positive)	0.15	mm
$x_{v,deadzone-}$	Valve dead zone (negative)	-0.15	mm
m_{basic}	Basic mass of the cart	279.6	kg
ρ_{fl}	Density of the hydraulic oil	870	kg/mm^3
p_0	Supply pressure	8×10^6	pa
p_t	Tank pressure	5×10^5	pa
A_A	Cylinder piston area	3117.2	mm^2
A_B	Cylinder ring area	1526.8	mm^2
$\varphi = \frac{A_A}{A_B}$	Area ratio	2.042	-
B_v	Flow resistance	2.9e-7	$m^2 \cdot \sqrt{m/kg}$
$E_{oil,max}$	Max. bulk modulus of elasticity	2×10^9	pa
p_{max}	Max. supply pressure	3.15×10^7	pa
V_{cA}	Pipeline and dead volume (A)	198.6	cm^3
V_{cB}	Pipeline and dead volume (B)	297.8	cm^3
H	Stroke of the cylinder	0.5	m

4.1.2 Feedback linearization of the cylinder model

In this part, the nonlinear model of the hydraulic differential cylinder with proportional valve is linearized by the exact input-output linearization method. The system has one input $u(t) = x_{v,effect}(t)$ and one output to be controlled $y(t) = x_1(t)$.

For the nonlinear model (4.1), the input-output linearized model is described by

$$\dddot{y}(t) = v(t) + \tilde{d}(t), \tag{4.2}$$

with

$$\begin{aligned} v(t) &= L^3_{\boldsymbol{f}} h(\boldsymbol{x}) + L_{\boldsymbol{g}} L^2_{\boldsymbol{f}} h(\boldsymbol{x}) u(t) \\ &= \frac{A_A x_2}{\varphi^2 m^2(x_1) V_A(x_1) V_B(x_1)} \\ &\quad [\rho_{fl}(A_B - A_A)(x_3 \varphi^2 V_A(x_1) V_B(x_1) - x_4 \varphi V_A(x_1) V_B(x_1)) \\ &\quad - A_A \varphi^2 m(x_1) V_B(x_1) E_{oil}(x_3) - A_A m(x_1) V_A(x_1) E_{oil}(x_4)] \\ &\quad + \frac{A_A}{\varphi m(x_1) V_A(x_1) V_B(x_1)} \\ &\quad [\varphi V_B(x_1) E_{oil}(x_3) Q_A(x_3) - V_A(x_1) E_{oil}(x_4) Q_A(x_4)]\, u(t) \end{aligned} \tag{4.3}$$

and

$$\tilde{d}(t) = L_{\boldsymbol{d}} L^2_{\boldsymbol{f}} h(\boldsymbol{x}) + \frac{d^2}{dt} L_{\boldsymbol{d}} h(\boldsymbol{x}) + \frac{d}{dt} L_{\boldsymbol{d}} L_{\boldsymbol{f}} h(\boldsymbol{x}) = \dot{d}(t),$$

where $L_{\boldsymbol{f}}(\cdot)$, $L_{\boldsymbol{g}}(\cdot)$, and $L_{\boldsymbol{d}}(\cdot)$ denote Lie derivatives.

Due to the complexity of the nonlinear system model, it is difficult to analyze the internal dynamics of the system. The stability of the zero dynamics can be analyzed instead of the stability of the internal dynamics [114]. The zero dynamics of the system (4.1) can be written by

$$\dot{\xi}(t) = -\frac{m(x_1 = 0)}{A_A} \tilde{d}(t), \tag{4.4}$$

where $\xi(t) = x_3(t) - \dfrac{x_4(t)}{\varphi}$ and the input to guarantee zero output $u^*(t)$ is $u^*(t) = \dfrac{-L^3_{\boldsymbol{f}} h(\boldsymbol{x}) - \tilde{d}(t)}{L_{\boldsymbol{g}} L^2_{\boldsymbol{f}} h(\boldsymbol{x})}$. The zero dynamics is stable, if the transformed disturbance $\tilde{d}(t)$ is bounded. That means the disturbance in the original coordinates $d(t)$ should be differentiable, which can be assumed without loss of generality.

4.1.3 Estimation of the transformed coordinates and the disturbance

The linearized dynamics (4.2) can be described using state space representation as

$$\dot{\boldsymbol{\varsigma}}(t) = \begin{bmatrix} \dot{y}(t) \\ \ddot{y}(t) \\ \dddot{y}(t) \end{bmatrix} = \boldsymbol{A}\boldsymbol{\varsigma}(t) + \boldsymbol{B} v(t) + \boldsymbol{N} \tilde{d}(t), \tag{4.5}$$

with $\boldsymbol{A} = \begin{bmatrix} 0 & 1 & 0 \\ 0 & 0 & 1 \\ 0 & 0 & 0 \end{bmatrix}$, $\boldsymbol{B} = \begin{bmatrix} 0 \\ 0 \\ 1 \end{bmatrix}$, and $\boldsymbol{N} = \begin{bmatrix} 0 \\ 0 \\ 1 \end{bmatrix}$.

Based on (4.5), a PI-Observer is designed by

$$\begin{aligned} \dot{\hat{\boldsymbol{\varsigma}}}(t) &= \boldsymbol{A}\hat{\boldsymbol{\varsigma}}(t) + \boldsymbol{B}v(t) + \boldsymbol{N}\hat{\tilde{d}}(t) + \boldsymbol{L}_1(y(t) - \hat{y}(t)), \\ \dot{\hat{\tilde{d}}}(t) &= \boldsymbol{L}_2(y(t) - \hat{y}(t)), \\ \hat{y}(t) &= \begin{bmatrix} 1 & 0 & 0 \end{bmatrix} \hat{\boldsymbol{\varsigma}}(t). \end{aligned} \tag{4.6}$$

With suitable observer gain matrices $\boldsymbol{L}_1$ and $\boldsymbol{L}_2$, the transformed states $\boldsymbol{\varsigma}$ and the disturbance $\tilde{d}(t)$ can be estimated as $\hat{\boldsymbol{\varsigma}}(t)$ and $\hat{\tilde{d}}(t)$. All the states in the original coordinates are now available from measurements $\boldsymbol{y}_m(t)$ and the estimation of $\hat{\varsigma}_2(t) = \dot{\hat{x}}_{cyl}(t)$. The derivative of the disturbance in the original coordinate $\dot{d}(t) = \tilde{d}(t)$ is also estimated by Eq. (4.6).

4.1.4 Robust control design

From the Chapter 4.1.3, the prerequisites of the robust control design proposed in Chapter 3.2 are fulfilled. Namely all the states in the original coordinates are available and the nominal model of the system is input-output linearizable. A robust trajectory control with disturbance rejection can be designed by

$$v(t) = -\boldsymbol{K}\left[\hat{\boldsymbol{\varsigma}}(t) - \boldsymbol{\varsigma}_{ref}(t)\right] - \hat{\tilde{d}}(t), \tag{4.7}$$

where $\boldsymbol{\varsigma}_{ref}(t) = \begin{bmatrix} \varsigma_{1ref}(t) \\ 0 \\ 0 \end{bmatrix}$ is the desired trajectory of the position to be controlled based on $\varsigma_{1ref}(t)$.

4.1.5 Validation

The robust control design is validated on the test rig described in Figure 4.1. The conditions of the experiments, for instance the unknown inputs and disturbances considered, and the results are given in detail in the following parts.

Condition of the experiments

The disturbances and uncertainties modeled as unknown inputs are the friction force $f_{fric}(\boldsymbol{x}, t)$ between the mass and its bearing surface, the disturbance force $f_{syn}(\boldsymbol{x}, t)$ generated from a 2nd hydraulic cylinder with passive dynamics acting oppositely (see Figure 4.1) and with artificially added measurements noise etc. of different levels. An uncertainty of the moved mass Δm can also be considered additionally. Besides the considered disturbances and uncertainties, the experiments on the test rig for the validation of the robust control design are carried out using nominal working conditions, when the nominal model is established, for example, temperature of oil is kept constant (here as 40 degree Celsius). Eight different cases listed below in Table 4.2 are taken to analyze the behavior of controllers. The input to the proportional valve, the position of the mass, and the two

Table 4.2: Different experimental conditions considered for experiments

Case I: $\Delta m = 0$: no mass uncertainty, $f_{syn} = 0$: no disturbance force, and no measurement error	Case II: $\Delta m = 150\,kg$: mass uncertainty $150\,kg$, $f_{syn} = 0$, and no measurement error
Case III: $\Delta m = 0$, $f_{syn} \neq 0$, and measurement error (about $\pm 0\%$)	Case IV: $\Delta m = 150\,kg$, $f_{syn} \neq 0$, and measurement error (about $\pm 0\%$)
Case V: $\Delta m = 0$, $f_{syn} \neq 0$, and measurement error (about $\pm 2\%$)	Case VI: $\Delta m = 150\,kg$, $f_{syn} \neq 0$, and measurement error (about $\pm 2\%$)
Case VII: $\Delta m = 0$, $f_{syn} \neq 0$, and measurement error (about $\pm 5\%$)	Case VIII: $\Delta m = 150\,kg$, $f_{syn} \neq 0$, and measurement error (about $\pm 5\%$)

pressures p_A and p_B are measured. The goal is to make the position control robust to disturbances and measurement noise in different possible combinations.

Comparison of the experimental results

Three controllers (a P-controller, a nonlinear controller designed based on the classical exact feedback linearization approach and a Luenberger observer (EFL-Lue), and the proposed robust controller (EFL-PIO)) are compared with experiments in different cases respectively to illustrate the properties of the proposed method.

In Figure 4.2, the three control methods (P-Controller, EFL-PIO, and EFL-Lue) for the position control of the hydraulic system are compared using the criterion in (3.32) with the relation between input energy $\int_0^T \boldsymbol{u}^2 dt$ and estimation error energy $\int_0^T \boldsymbol{e}^2 dt$ for eight different situations as introduced in Table 4.2.

The first upper two pictures in Figure 4.2 show that the EFL-PIO is not the most effective method considering input energy request, when no disturbance force f_{syn} and no measurement error exist and only mass uncertainty is considered. On the other hand, the results indicate that the mass uncertainty has small influence on the position control. The results in the lower six illustrations in Figure 4.2 show that the proposed method EFL-PIO is more effective than the P-Controller and the EFL-Lue method, when the disturbance force f_{syn} acting on the system, because the trajectory of the EFL-PIO lies closer to the origin and the EFL-PIO requires always less input energy considering same control error.

This illustrates the proposed robustness properties resulting from the novel combined

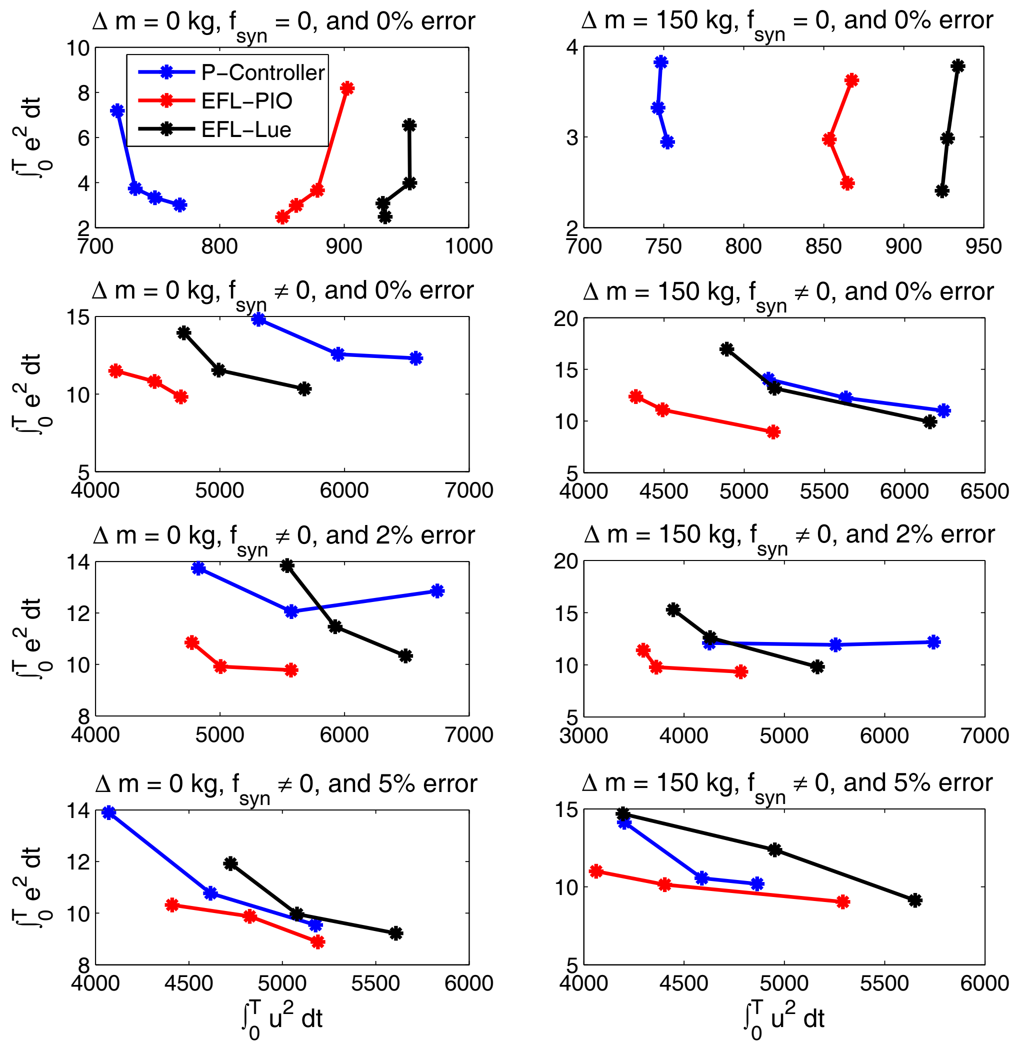

Figure 4.2: Comparison of different methods in eight cases

design approach. Additionally to the improved results, it should be noted that the better results do not require additional measurements or improved measurement quality. The opposite is the case, the robustness qualities allow less measurement quality (for the same control error/input energy result).

When all the trajectories are drawn in one figure (in Figure 4.3), it can be clearly seen that the change of the trajectory due to the strong disturbance force f_{syn} from EFL-PIO is the smallest among the three methods. It illustrates that the EFL-PIO is the most robust one among them.

To have a concrete view of the control performance, two representative control results under the conditions in cases I and VIII are shown in Figure 4.4 respectively.

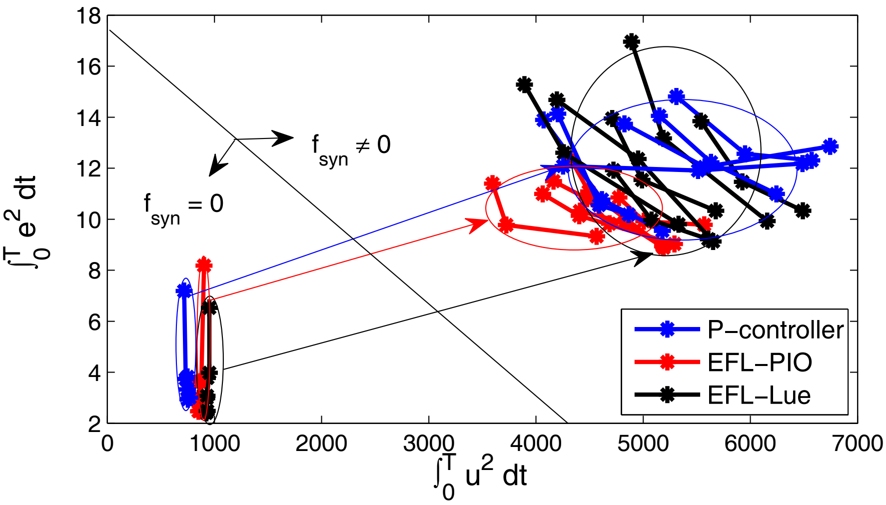

Figure 4.3: Comparison of all the situations

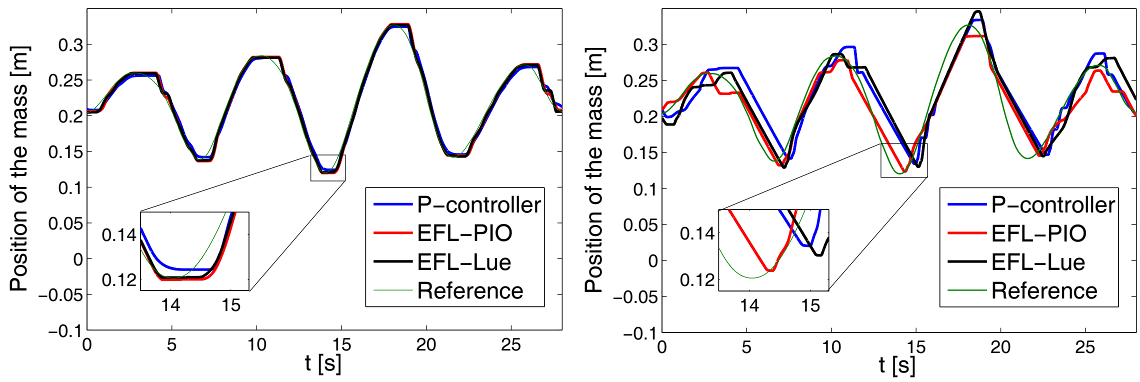

(a) Control results (Case I)

(b) Control results (Case VIII)

Figure 4.4: Control performance in two given situations

4.2 Robust position control with virtual sensor for position measurement

Besides the application of PI-Observer technique as a basis of robust control introduced in Chapter 4.1, the PI-Observer can also be applied as virtual measurement device to realize virtual measurement. In this part the application of PI-Observer as virtual sensor in [59] will be extended. The goal is to realize closed-loop position control only using the oil pressure measurements from the hydraulic cylinder system introduced in Chapter 4.1. The position information will be obtained from the estimated velocity and limitations of attachment points without a direct/physical measurement of the position. Hardware-in-the-Loop experiments based on a PC with Matlab/Simulink and dSPACE system are executed to validate the method and show its practicability. The experiment design is also compatible for an industrial Programmable Logic Controller (PLC).

4.2.1 Simplified model of the hydraulic differential cylinder

A simplified system model, which should have a suitable structure for the PI-Observer design discussed in Chapter 2.2 for linear system models with fully observability, is required to estimate the velocity with oil pressure measurements by PI-Observer. Hence, a linear model from the system with a reduced state vector to fulfill the observability condition is considered here.

State space representation of the simplified model

As introduced in [59], a simplified model of the hydraulic cylinder is considered

$$\begin{aligned} \dot{\boldsymbol{x}}(t) &= \boldsymbol{A}\boldsymbol{x}(t) + \boldsymbol{B}\boldsymbol{u}(t) + \boldsymbol{N} f_d(t), \\ \boldsymbol{y}(t) &= \boldsymbol{C}\boldsymbol{x}(t), \end{aligned} \tag{4.8}$$

where the states are the velocity and the pressures $\boldsymbol{x}(t) = \begin{bmatrix} v_{cyl}(t) \\ p_A(t) \\ p_B(t) \end{bmatrix}$, the measurements the pressures $\boldsymbol{y}(t) = \begin{bmatrix} p_A(t) \\ p_B(t) \end{bmatrix}$, the inputs the volumetric flow rates $\boldsymbol{u}(t) = \begin{bmatrix} Q_A(p_A(t), u_v(t)) \\ Q_B(p_B(t), u_v(t)) \end{bmatrix}$ with the input voltage of the valve $u_v(t)$. The variable $f_d(t)$ denotes the external force.

For simplicity, the volumes in the chambers, the mass, and the bulk modulus of elasticity are assumed as constant. Therefore, the first state in the model (4.1), the position of the mass, is no more involved in the dynamics of other states and it is not taken as a state in the simplified model (4.8). The matrices in (4.8) are described with the corresponding parameters.

The system matrix is $\boldsymbol{A} = \begin{bmatrix} 0 & \frac{A_A}{m} & -\frac{A_B}{m} \\ -\frac{A_A E_{oil}}{V} & 0 & 0 \\ \frac{A_B E_{oil}}{V} & 0 & 0 \end{bmatrix}$ with the area of the chambers A_A, A_B, the average mass of the cylinder system m, the average bulk modulus of elasticity E_{oil}, the average volume V; the input matrix $\boldsymbol{B} = \begin{bmatrix} 0 & 0 \\ \frac{E_{oil}}{V} & 0 \\ 0 & -\frac{E_{oil}}{V} \end{bmatrix}$; the output matrix $\boldsymbol{C} = \begin{bmatrix} 0 & c_{coef} & 0 \\ 0 & 0 & c_{coef} \end{bmatrix}$ with the sensor gain c_{coef}; and the input matrix of the external force $\boldsymbol{N} = \begin{bmatrix} \frac{1}{m} \\ 0 \\ 0 \end{bmatrix}$.

Due to the simplification, the model (4.8) can not describe the system behavior so well as the model (4.1). Some specific aspects are considered to make the model more accurate. The valve factor is for instance calculated by lookup table obtained experimentally, not based on empirical formula as in Chapter 4.1. Here, the volumetric flow rates are calculated according to the measured behavior of the proportional valve in use by the following equations

$$Q_A(p_A(t), u_v(t)) = \begin{cases} \operatorname{sgn}(x_v(t))\operatorname{sgn}(p_0 - p_A(t))B_v \sqrt{|p_0 - p_A(t)|}\, x_v(t), & x_v(t) \geq 0 \\ \operatorname{sgn}(x_v(t))\operatorname{sgn}(p_A(t) - p_T)B_v \sqrt{|p_A(t) - p_T|}\, x_v(t), & x_v(t) < 0 \end{cases},$$

$$Q_B(p_B(t), u_v(t)) = \begin{cases} \operatorname{sgn}(x_v(t))\operatorname{sgn}(p_B(t) - p_T)B_v \sqrt{|p_B(t) - p_T|}\, x_v(t), & x_v(t) \geq 0 \\ \operatorname{sgn}(x_v(t))\operatorname{sgn}(p_0 - p_B(t))B_v \sqrt{|p_0 - p_B(t)|}\, x_v(t), & x_v(t) < 0 \end{cases},$$

with the factor of the valve $x_v(t) = x_v(u_v(t), \dot{u}_v(t))$. The variables have the same meaning as introduced in the model (4.1).

Confirmation of the valve factor $x_v(t)$ The factor of the valve $x_v(t)$ is calculated with lookup tables, because the valve has a very complicated dynamical behavior which depends on the dynamics of the input.

For inputs with constant values, a simple lookup table shown in Figure 4.5 can be used and the factor can be obtained by $x_v(t) = f_1(u_v(t))$. For changing inputs, the combination of two lookup tables in Figure 4.5 and Figure 4.6 as well as the function $A_u = f(t, u_v(k))$ are applied. The factor $x_v(t)$ is then calculated by

$$x_v(t) = \begin{cases} f_1(u_v(t)), & -0.3 \leq x_v(t) \leq 0.3 \\ A_u f_2(u_v(t), \dot{u}_v(t)), & x_v(t) > 0.3 \text{ and } x_v(t) < -0.3 \end{cases},$$

where the function $A_u = f_3(t, u_v(t))$ is defined by $A_u = |5.5(u_v(t) - 0.56) + 1|$ and $0.3 \leq A_u \leq 3$. Linear interpolation is used to get the value from lookup tables.

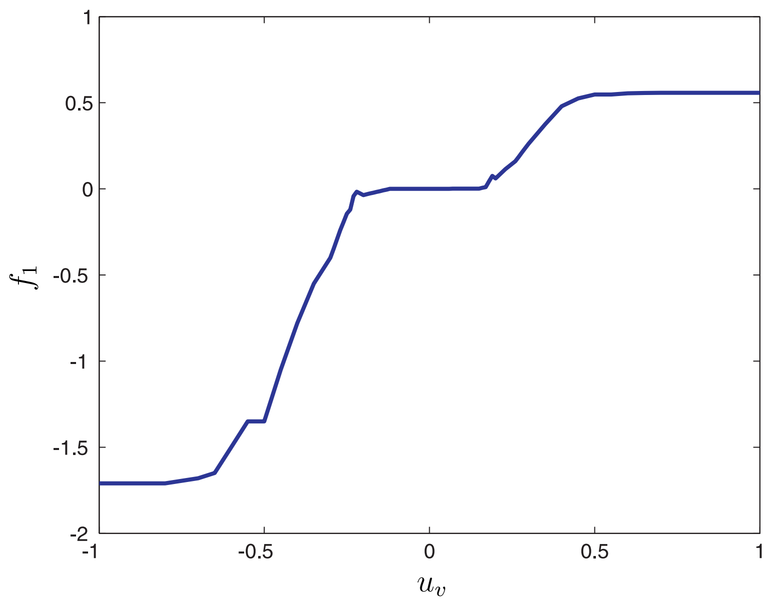

Figure 4.5: Lookup table 1 with $f_1(t) = f_1(u_v(t))$

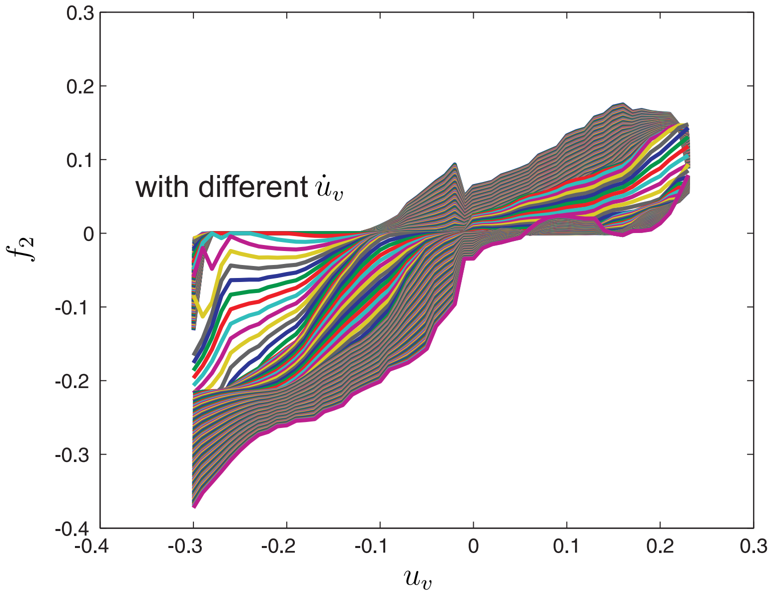

Figure 4.6: Lookup table 2 with $f_2(t) = f_2(u_v(t), \dot{u}_v(t))$

4.2.2 Position calculation from estimations of PI-Observer

The position calculation is realized by designing a PI-Observer as virtual sensor and the calculation is based on the estimation of velocity. In the following paragraphs, the calculation procedure will be illustrated in detail.

PI-Observer Design

Based on the simplified model (4.8), a PI-Observer can be designed in the following form

$$\dot{\boldsymbol{z}}(t) = (\boldsymbol{A}_e - \boldsymbol{L}\boldsymbol{C}_e)\boldsymbol{z}(t) + \boldsymbol{B}_e\boldsymbol{u}(t) + \boldsymbol{L}\boldsymbol{y}(t), \tag{4.9}$$

with the state vector $\boldsymbol{z}(t) = \begin{bmatrix} z_1(t) \\ z_2(t) \\ z_3(t) \\ z_4(t) \end{bmatrix}$ as the estimations of $\boldsymbol{x}(t) = \begin{bmatrix} v_{cyl}(t) \\ p_A(t) \\ p_B(t) \end{bmatrix}$ and $f_d(t)$ in (4.8), the system matrix $\boldsymbol{A}_e = \begin{bmatrix} 0 & \frac{A_A}{m}k_{b2p} & -\frac{A_B}{m}k_{b2p} & \frac{1}{m} \\ -\frac{A_A E_{oil}}{V} & 0 & 0 & 0 \\ \frac{A_B E_{oil}}{V} & 0 & 0 & 0 \\ 0 & 0 & 0 & f_{design} \end{bmatrix}$, input matrix $\boldsymbol{B}_e = \begin{bmatrix} 0 & 0 \\ \frac{E_{oil}}{V} & 0 \\ 0 & -\frac{E_{oil}}{V} \\ 0 & 0 \end{bmatrix}$, output matrix $\boldsymbol{C}_e = \begin{bmatrix} 0 & c_{coef} & 0 & 0 \\ 0 & 0 & c_{coef} & 0 \end{bmatrix}$, and the observer gain matrix $\boldsymbol{L}$. The variable f_{design} is one of the design parameters.

A discrete time observer design is required to realize the virtual sensor design compatible for an industrial PLC system. PI-Observer design for the system in discrete time is given by a recursion equation

$$\boldsymbol{z}(k+1) = \boldsymbol{A}_{ed}\,\boldsymbol{z}(k) + \boldsymbol{B}_{ed}\,\boldsymbol{u}(k) + \boldsymbol{L}_{d}\,\boldsymbol{y}(k). \tag{4.10}$$

The sampling time is chosen as 10 millisecond. The corresponding matrices in the discrete time model are calculated with the known model parameters and a suitable design of the observer gain matrix $\boldsymbol{L}$ using

$$\boldsymbol{A}_{ed} = \begin{bmatrix} \text{-3.9809e-015} & \text{-6.4115e-021} & \text{8.0812e-021} & \text{-9.4023e-022} \\ \text{1.0767e-014} & \text{1.7341e-020} & \text{-2.1857e-020} & \text{2.5430e-021} \\ \text{-1.3571e-014} & \text{-2.1857e-020} & \text{2.7549e-020} & \text{-3.2053e-021} \\ \text{1.2939e-008} & \text{2.4742e-014} & \text{-3.1186e-014} & \text{2.4278e-015} \end{bmatrix},$$

$$\boldsymbol{B}_{ed} = \begin{bmatrix} \text{1.0162e+003} & \text{-1.2809e+003} \\ \text{4.3665e+003} & \text{3.4644e+003} \\ \text{3.4644e+003} & \text{2.7486e+003} \\ \text{-1.4362e+000} & \text{-1.1466e+000} \end{bmatrix}, \quad \boldsymbol{L}_{ed} = \begin{bmatrix} \text{5.2088e-017} & \text{1.4441e-017} \\ \text{1.0000e+000} & \text{-3.9050e-017} \\ \text{1.7757e-016} & \text{1.0000e+000} \\ \text{1.9007e-003} & \text{-2.3956e-003} \end{bmatrix}.$$

The velocity and the external force(disturbance) can be estimated from the PI-Observer by measuring the two pressures p_A and p_B.

Correction of the calculated position

The position of the mass will be calculated by the integral of the estimated velocity and named $z_0(k)$. For the integration, some reset functions are considered to correct the integrated value and the estimation values online, because the integrated value is always influenced by the initial conditions and needs to be adjusted.

Reset of the calculated displacement Two reference points are taken to correct/reset the estimation and integration, namely the two attachment points at the minimal and maximal displacements. Since the two attachment points can be confirmed easily by using the information of the measured pressures, the following reset conditions are considered:

- reset the estimated position $z_0(k)$ to the far attachment point $0.5m$ when the pressures $p_A(k) \geq 70\%\, p_0(k)$ and $p_B(k) \leq 150\%\, p_T(k)$;
- reset the estimated position $z_0(k)$ to the near attachment point $0m$, when the pressures $p_B(k) \geq 70\%\, p_0(k)$ and $p_A(k) \leq 150\%\, p_T(k)$.

Reset of the estimated velocity When the cylinder is at one of the attachment points, the estimated velocity should also be corrected. The reset of the estimation of velocity is realized by resetting the estimated velocity $z_1(k) = 0$, when the estimated position $z_0(k) \geq 0.495$ and $u(k) \geq 0$, or $z_0(k) \leq 0$ and $u(k) \leq 0$.

Reset of the estimated force The estimated force/disturbance is adjusted to $z_4(k) = -1250\ N$ at the attachment positions $z_0(k) \geq 0.495$ and $z_0(k) \leq 0.05$ or with high pressures $p_A(k) \geq 70\%\ p_0(k)$ or $p_B(k) \geq 70\%\ p_0(k)$.

4.2.3 Experimental results

Some experiments on the test rig are executed with the PI-Observer design introduced in Chapter 2. At first, the situation considered in [59] with the PI-Observer as virtual sensor to estimate the position and external force is repeated. Related results are shown in Figure 4.7 and Figure 4.8.

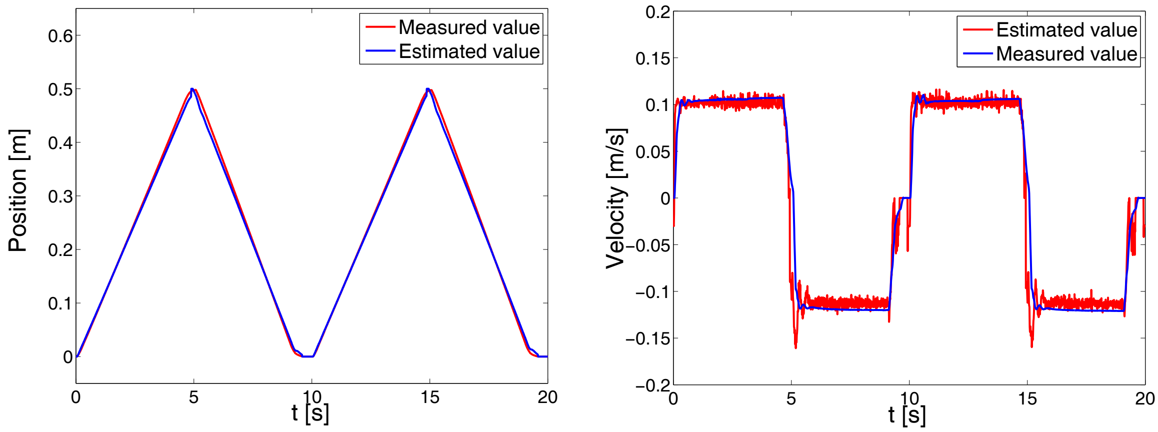

(a) Estimation of position (b) Estimation of velocity

Figure 4.7: Experimental results of position estimation I

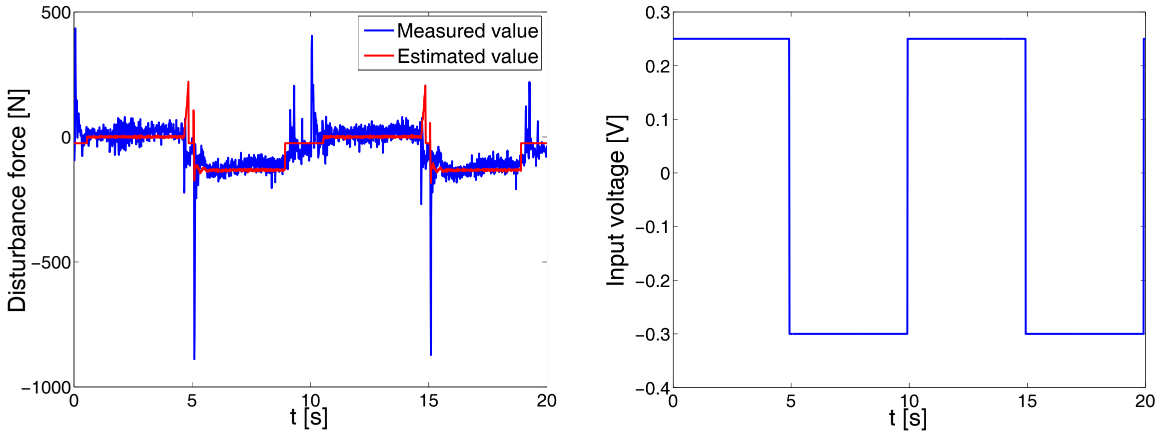

(a) Estimation of disturbance force (b) Applied input of the valve

Figure 4.8: Experimental results of position estimation II

Note that only the friction force is taken as the external force instead of a large external force considered in [59] to show the accuracy of the estimations. It can be seen clearly that the estimations of velocity and the external force as well as the calculated position from the PI-Observer are plausible.

The calculated position is used as virtual measurement to realize a position control with P-controller design. The corresponding results are given in Figure 4.9 and Figure 4.10. In Figure 4.9(a), the real (measured) position and the estimated position are compared with the reference value. The results show that the quality of position control without physical position measurement is not as good as with position measurement, but is acceptable for simple industrial application saving sensor costs.

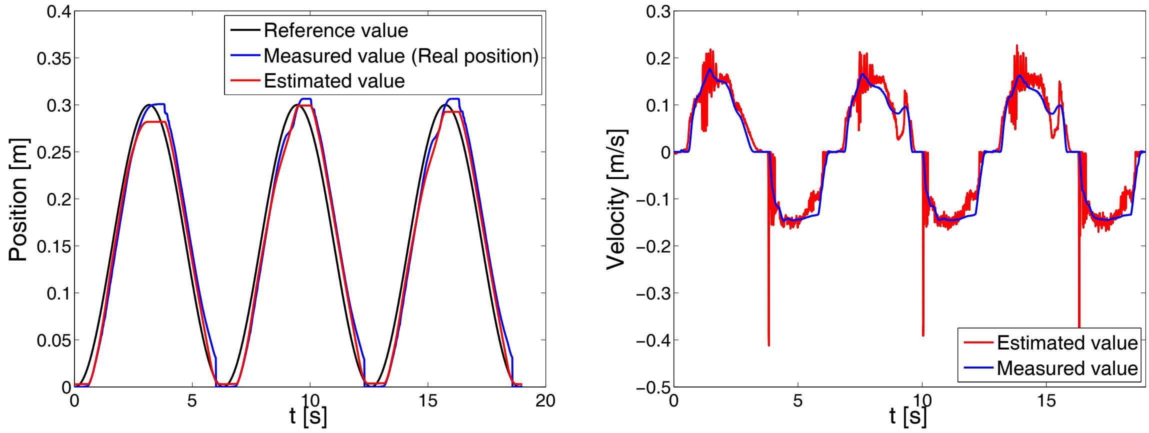

(a) Position control result (b) Estimation of velocity

Figure 4.9: Experimental results of position control I

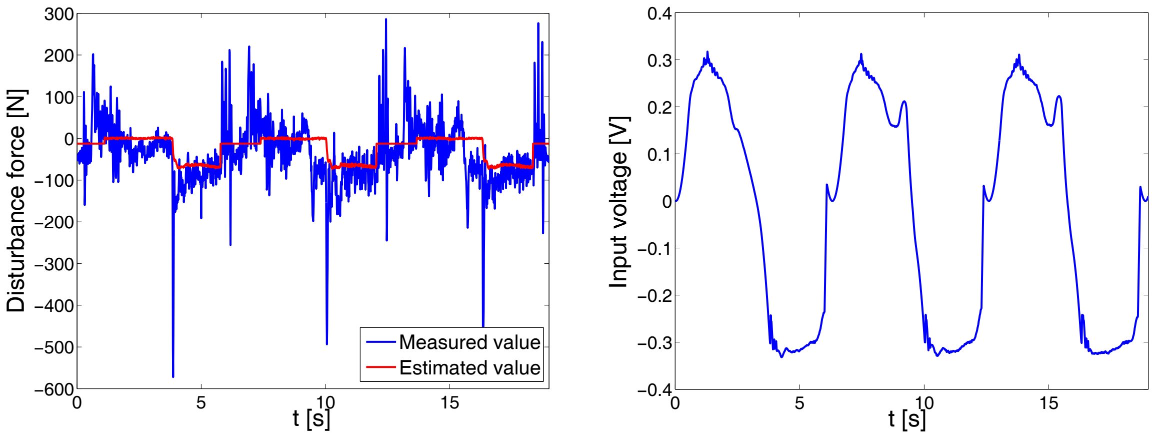

(a) Estimation of disturbance force (b) Applied input of the valve

Figure 4.10: Experimental results of position control II

4.3 Summary

In this chapter, the applications of PI-Observer-based control on hydraulic systems are discussed. A hydraulic differential cylinder system is considered. For the position control of the hydraulic differential cylinder, experiments show that the proposed EFL-PIO method has strong robustness properties compared with classical P-controller and exact feedback linearization with Luenberger observer (EFL-Lue) against disturbances or parameter uncertainties. Besides the robust control design for the hydraulic cylinder, the position control using PI-Observer as virtual sensor without position measurement is designed. The unmeasured position is calculated based on the estimations from the PI-Observer as virtual sensor. The calculated position is used as information to realize a position control. The experimental results show the applicability of the PI-Observer as a virtual sensor to realize control loop design.

5 Summary, Conclusion, and Outlook

In the first chapter of this thesis, the goals of this thesis are set as: analysis and improvement of the PI-Observer design with respect to the design of high observer gains and robust control design for nonlinear systems based on PI-Observer especially for nonlinear mechanical systems according to a careful study of the previous work. In the following chapters, the mentioned points are discussed in detail respectively. In this chapter, the whole thesis work is summarized, the important conclusions are repeated, and suggestions for future work are given.

5.1 Summary and conclusions

With a literature research of the observer design history, the advantages of the high gain PI-Observer as state and disturbance observer against state observers and other disturbance observers are listed and underlined in the beginning. After that, the further development of the PI-Observer is discussed. Based on the analysis and the development of PI-Observer design, two research directions are focused on in this thesis. One is the application of high gain PI-Observers on nonlinear systems and the other is the determination of high observer gains for PI-Observer based on an online adaption algorithm. Both of the two directions are discussed in detail and corresponding solution approaches are presented. An Advanced PI-Observer (API-Observer) design is proposed to solve the problem of choosing and adjusting observer gains for the high gain PI-Observer. Furthermore, the proposed PI-Observer based robust nonlinear control method (EFL-PIO) is argued as an alternative method, which can not only achieve strong robustness of control performance but also offer plausible estimations of disturbances, based on a review of robust nonlinear control. The contributions of the thesis work are summarized in the following points:

- For the advanced PI-Observer (API-Observer) design, the structure and design process of PI-Observer as a high gain state and disturbance observer is discussed and analyzed at first. Then, the trial and error method is detected as an inefficient and inconvenient way to determine the level for the high observer gains. The aspects that influence both the observer gain design and, indirectly, the estimation quality are discussed, based on which an adaption algorithm is defined. The adaption procedure and its implementation are detailed by an illustration example of an elastic beam, where a PI-Observer is required to estimate the contact force as unknown input to the system. The simulation results are given, showing the influence of the measurement noise and modeling errors on the choice of observer gains. It can be concluded from the simulation results that the API-Observer gains are changing with different situations and should be defined online according to the current situation. It can also be seen that the proposed algorithm can realize the automation of choosing suitable observer gains. The results based on real measurements from the test rig are given to show the applicability of the API-Observer on real systems both in continuous time and discrete time.

- The application of PI-Observer for nonlinear systems as the basis of robust control design is discussed next. Here the robust nonlinear control method based on PI-Observer and exact feedback linearization (EFL-PIO) is proposed for a class of nonlinear systems with input-output linearizable nominal model. For the EFL-PIO design, the unknown inputs or disturbances to the nominal system are assumed bounded, but no detailed bounds or dynamics of disturbances are known. Besides that, the conditions of the application of the proposed EFL-PIO method for nonlinear mechanical systems are listed in detail. To illustrate the implementation of the proposed EFL-PIO method, two typical nonlinear mechanical systems are chosen. Firstly, a nonlinear SISO mechanical system, a single link rigid manipulator with flexible joint, is discussed. Based on this SISO example, the application of EFL-PIO on input-state-output linearizable models and its accompanying problems, for example, a non constant matrix for the location of unknown inputs, are explained and solved in detail as an extension of the proposed EFL-PIO method, which is in general only for input-output linearizable system models discussed. After that, the general design process of the EFL-PIO method for systems with input-output linearizable system model is shown with a nonlinear mass-spring system. For both examples, the control performance and the robustness of the EFL-PIO are compared with a classical exact feedback linearization method combined with a Luenberger observer (EFL-Lue) using a novel criterion proposed in this thesis which considers both the control error and the corresponding input energy. Based on the comparisons, the improvement of robustness for the classical exact feedback linearization method is clearly evident. Additionally, the proposed EFL-PIO method offers sound estimation of disturbances considered as unknown inputs.

- The applications of PI-Observer-based control of a hydraulic differential cylinder are given to illustrate that the application of PI-Observer is not only suitable for classical mechanical systems (e.g., mass-spring systems) but also appropriate for hydraulic systems. Here the position control of a hydraulic differential cylinder system is considered as the control task. At first, the EFL-PIO method is applied to get a robust position control design for the system with the position as measurement. The experiment results show the strong robustness feature of the EFL-PIO method comparing with classical P-controller and the EFL-Lue method, when disturbances or parameter uncertainties are considered. Besides the robust control design for the hydraulic cylinder with position measurement, the position control is discussed using

PI-Observer as virtual sensor without position measurement. Here the unmeasured position is calculated based on the estimations from the PI-Observer, while the calculated position is used as information to realize a feedback for the position control. The control results show the applicability of the PI-Observer as a virtual sensor to realize control loop design, which was discussed already in literatures but firstly illustrated with experimental results in this thesis.

In brief, the thesis shows the feasibility of applying the PI-Observer in robust control of nonlinear and practical systems and the design of observer gains for the API-Observer realized by the presented adaption algorithm.

5.2 Outlook

For future work, the following points are considered and suggested:

- The proposed API-Observer design is based on a bank of PI-Observers for the comparison of cost functions. Therefore, the programming of the API-Observer is not as usual as for a normal observer or PI-Observer design. A basic understanding of the API-Observer structure and a special numerical integration including the adjustment algorithm have to be taken into account. In the future work, an API-Observer block can be programmed as a general platform for the designer.

- As mentioned in the thesis, the high gain PI-Observer can estimate unknown effects of a system and the API-Observer can make the estimation rational and adaptive for the current situation. Hence, an API-Observer-based control can be designed as robust control or fault detection method matching different situations, according to the special characteristics of the high gain PI-Observer and the API-Observer. On the other hand, the concept of the online adapted observer design could be applied in the design of controller gains.

- The applicability of the PI-Observer based robust control (the EFL-PIO approach) to nonlinear mechanical systems has been shown with simulation and experiment examples with unknown disturbances. However, the proposed EFL-PIO method is designed for the class of nonlinear systems with input-output linearizable models. Although the application for nonlinear systems with input-state-output linearizable models is also discussed with the single link manipulator example, it could still be further extended to more general systems.

Bibliography

[1] "Robust and Nonlinear Control Literature Survey (No.1-No.17)." *International Journal of Robust and Nonlinear Control* .

[2] Ahrens, J.H., and H.K. Khalil. "High-Gain Observers in the Presence of Measurement Noise: A Switched-Gain Approach." *Automatica* 45: (2009) 936–943.

[3] Astolfi, A., and L. Menini. *Further Results on Decoupling with Stability for Hamiltonian Systems*. London: Springer, 1999.

[4] Baş, Ö.Y., B. Shafai, and S.P. Linder. "Design of Optimal Gains for the Proportional Integral Kalman Filter with Application to Single Particle Tracking." In *Proceedings of the 38th IEEE Conference on Decision and Control*. Phoenix, AZ, United States, 1999, 4567–4571.

[5] Başpinar, C. *Robuste Kraft- und Positionsregelung von bewegungseingeschränkten Robotern mit idealen und elastischen Gelenken (Dissertation)*. Universität Wuppertal: Shaker, Aachen, 2005.

[6] Beale, S., and B. Shafai. "Robust Control System Design with a Proportional-Integral Observer." *International Journal of Control* 50: (1989) 97–111.

[7] Beard, R.V. *Failure Accommodation in Linear Systems Through Self-Reorganization (Dissertation)*. Massachusetts Institute of Technology, 1971.

[8] Bhattacharyya, S.P. "Observer Design for Linear Systems with Unknown Inputs." *IEEE Transactions on Automatic Control* 23, 3: (1978) 483–484.

[9] Boyd, S., L. El Ghaoui, E. Feron, and V. Balakrishnan. *Linear Matrix Inequalities in System and Control Theory*, volume 15 of *Studies in Applied Mathematics*. Philadelphia, PA: SIAM, 1994.

[10] Bröcker, M. "Nonlinear Disturbance Rejection of a Flexible Robot." In *European Control Conference (ECC'01)*. Porto, Portugal, 2001, 208–213.

[11] ———. "On Nonlinear Disturbance Attenuation for Hydraulic Cylinders via Tracking Control." In *Proceedings of the 15th Triennial IFAC World Congress*. Barcelona, 2002, 792f.

[12] Busawon, K.K., and P. Kabore. "Disturbance Attenuation using Proportional Integral Observers." *International Journal of Control* 74, 6: (2001) 618–627.

[13] Chang, J.L. "Robust Discrete-Time Model Reference Sliding-Mode Controller Design with State and Disturbance Estimation." *IEEE Transactions on Industrial Electronics* 55, 11: (2008) 4065–4074.

[14] ———. "Robust Discrete-Time Output Feedback Model Reference Control Design with State and Unknown Input Estimation." *International Journal of Robust and Nonlinear Control* 19, 8: (2009) 847–867.

[15] Chen, B.S., C.S. Tseng, and H.J. Uang. "Robustness Design of Nonlinear Dynamic Systems via Fuzzy Linear Control." *IEEE Transactions on Fuzzy Systems* 7, 5: (1999) 571–585.

[16] Chen, J., and R.J. Patton. "Optimal Filtering and Robust Fault Diagnosis of Stochastic Systems with Unknown Disturbances." *IEE Proc. Control Theory Appl.* 143, 1: (1996) 31–36.

[17] Ciccarella, G., M.D. Mora, and A. Germani. "A Luenberger-Like Observer for Nonlinear Systems." *International Journal of Control* 57, 3: (1993) 537–556.

[18] Coelingh, H.J. *Design Support for Motion Control Systems - a Mechatronic Approach - (Dissertation).* University of Twente: The Netherlands, 2000.

[19] Corless, M., and J. Tu. "State and Input Estimation for a Class of Uncertain Systems." *Automatica* 34, 6: (1998) 757–764.

[20] Cox, H. "On the Estimation of State Variables and Parameters for Noisy Dynamic Systems." *IEEE Transactions on Automatic Control* 9, 1: (1964) 5–12.

[21] Darouach, M. "On the Novel Approach to the Design of Unknown Input Observers." *IEEE Transactions on Automatic Control* 39, 3: (1994) 698–699.

[22] Ding, S.X. *Model-based Fault Diagnosis Techniques - Design Schemes, Algorithms, and Tools.* Berlin, Heidelberg: Springer, 2008.

[23] Duan, G.R., G.P. Liu, and S. Thompson. "Eigenstructure Assignment Design for Proportional-Integral Observers: Continuous-Time Case." *IEE Proceedings, Part D - Control Theory Application* 148, 3: (2001) 263–267.

[24] ———. "Eigenstructure Assignment Design for Proportional-Integral Observers: the Discrete-Time Case." *International Journal of Systems Scienc* 34, 5: (2003) 357–363.

[25] Efimov, D.V., and A.L. Fradkov. "Robust and Adaptive Observer-Based Partial Stabilization for a Class of Nonlinear Systems." *IEEE Transactions on Automatic Control* 54, 7: (2009) 1591–1595.

[26] Elbeheiry, E.M., and H.A. Elmaraghy. “Robotic Manipulators State Observation via one-time Gain Switching.” *Journal of Intelligent and Robotic Systems* 38: (2003) 313–344.

[27] Farza, M., M. MŚaad, and L. Rossignol. “Observer Design for a Class of MIMO Nonlinear Systems.” *Automatica* 40: (2004) 135–143.

[28] Franco, A.L.D., H. Bourlés, E.R.D. Pieri, and H. Guillard. “Robust Nonlinear Control Associating Robust Feedback Linearization and H_{inf} Control.” *IEEE Transactions on Automatic Control* 51, 7: (2006) 1200–1207.

[29] Gao, Y., Z. Liu, and H. Chen. “Robust H_∞ Control for Constrained Discrete-Time Piecewise Affine Systems with Time-Varying Parametric Uncertainties.” *IET Control Theory and Applications* 3, 8: (2009) 1132–1144.

[30] Guan, Y., and M. Saif. “A Novel Approach to the Design of Unknown Input Observers.” *IEEE Transactions on Automatic Control* 36, 5: (1991) 632–635.

[31] Ha, Q.P., A.D. Nguyen, and H. Trinh. “Simultaneous State and Input Estimation with Application to a Two-Link Robotic System.” In *Proceedings of the 5th Asian Control Conference*. Melbourne, Australia, July, 2004.

[32] Hagenmeyer, V., and E. Delaleau. “Exact Feedforward Linearization Based on Differential Flatness.” *International Journal of Control* 76, 6: (2003) 537–556.

[33] ———. “Robustness Analysis of Exact Feedforward Linearization Based on Differential Flatness.” *Automatica* 39, 11: (2003) 1941–1946.

[34] ———. “Continuous-Time Nonlinear Flatness-Based Predictive Control: An Exact Feedforward Linearisation Setting with an Induction Drive Example.” *International Journal of Control* 81, 10: (2008) 1645–1663.

[35] Heidtmann, F., and D. Söffker. “Virtual Sensors for Diagnosis and Prognosis Purposes in the Context of Elastic Mechanical Structures.” *IEEE Sensors Journal* 9, 11: (2009) 1577–1588.

[36] ———. “Numerical Optimizations in Observer-Based Monitoring of Elastic Mechanical Systems.” In *Proceedings of IEEE International Conference on Prognostics and Health Management*. Denver, USA, Oct., 2008, 1–8.

[37] ———. “Experimental-Modeling-Based Observer Approach for the Analysis of Structural Changes in Elastic Mechanical Systems.” In *Proceedings of the 9th International Conference on Motion and Vibration Control MOVIC 2008*. Munich, Germany, Sep., 2008.

[38] Hori, Y. “Disturbance Suppression on an Acceleration Control Type DC Servo System.” In *IEEE Power Electronics Specialists Conference ’88*. Kyoto, Japan, April, 1988.

[39] Hostetter, G., and J.S. Meditch. "Observing Systems with Unmeasurable Inputs." *IEEE Transactions on Automatic Control* 18, 3: (1973) 307–308.

[40] Hou, M., and P.C. Müller. "Design of Observers for Linear Systems with Unknown Inputs." *IEEE Transactions on Automatic Control* 37, 6: (1992) 871–875.

[41] Hu, J.S., F.R. Hu, and M.Y. Cheng. "A Partial Pole Placement Approach to Proportional-Integral Observer Design." *Proceedings of the Institution of Mechanical Engineers, Part I: Journal of Systems and Control Engineering* 223: (2009) 253–261.

[42] Hu, R. *Positionsregelung von Robotern mit der Methode der Nichtlinearitäten Schätzung und Kompensation (Dissertation).* Universität Wuppertal: VDI, Düsseldorf, 1999.

[43] Huang, A.C., and Y.C. Chen. "Adaptive Sliding Control for Single-Link Flexible-Joint Robot with Mismatched Uncertainties." *IEEE Transactions on Control Systems Technology* 12, 5: (2004) 770–775.

[44] Huang, L., and X. Mao. "SMC Design for Robust H_∞ Control of Uncertain Stochastic Delay Systems." *Automatica* 46, 2: (2010) 405–412.

[45] Hui, S., and S.H. Żak. "Low-Order State Estimators and Compensators for Dynamical Systems with Unknown Inputs." *Systems and Control Letters* 21, 6: (1993) 493–502.

[46] ———. "Observer Design for Systems with Unknown Inputs." *International Journal of Applied Mathematics and Computer Science* 15, 4: (2005) 431–446.

[47] Isidori, A. *Nonlinear Control Systems.* London: Springer Verlag, 1995, 3rd edition.

[48] ———. "H_∞ Control via Measurement Feedback for Affine Nonlinear Systems." *International Journal of Robust and Nonlinear Control* 4, 4: (2007) 553–574.

[49] Isidori, A., and A. Asolfi. "Disturbance Attenuation and H_∞ Control via Measurement Feedback in Nonlinear Systems." *IEEE Transactions on Automatic Control* 37, 9: (1992) 1283–1293.

[50] Johnson, C.D. "Optimal Control of the Linear Regulator with Constant Disturbances." *IEEE Transactions on Automatic Control* 13, 4: (1968) 416–421.

[51] ———. "Accommodation of External Disturbances in Linear Regulator and Servomechanism Problems." *IEEE Transactions on Automatic Control* 16, 6: (1971) 635–644.

[52] ———. "Theory of Disturbance-Accommodating Controllers." *Control and Dynamic Systems* 12: (1976) 387–489.

[53] Jones, H.L. *Failure Detection in Linear Systems (Dissertation).* Massachusetts Institute of Technology: Cambridge, MA, USA, 1973.

[54] Julier, S.J., and J.K. Uhlmann. "A New Extension of the Kalman Filter to Nonlinear Systems." In *11th International Symposium on Aerospace/Defense Sensing, Simulation and Controls*. 1997, 182–193.

[55] Jung, J., S. Han, and K. Huh. "Robust Proportional-Integral Kalman Filter Design Using a Convex Optimization Method." *Journal of Mechanical Science and Technology* 22, 5: (2008) 879–886.

[56] Jung, J., J. Hwang, and K. Huh. "Optimal Proportional-Integral Adaptive Observer Design for a Class of Uncertain Nonlinear Systems." In *Proceedings of the American Control Conference*. New York City, USA, 2007.

[57] Kaczorek, T. "Proportional-Integral Observers for Linear Multivariable Time Varying Systems." *Regelungstechnik* 27: (1979) 359–362.

[58] Kalman, R.E. "A New Approach to Linear Filtering and Prediction Problems." *Transactions of the ASME Journal of Basic Engineering* 82, Series D: (1960) 35–45.

[59] Kashi, K. *Development of a Fault Diagnosis System for an Active Roll Control System using Observers and Virtual Sensors (Dissertation)*. University of Duisburg-Essen, Shaker Verlag, 2006.

[60] Kashi, K., and D. Söffker. "Model-Based Estimation of Force and Displacement of a Hydraulic Cylinder." In *Proceedings of the 7th International Symposium on Advanced Vehicle Control KIVI-NIRIA*. Arnheim, Netherlands, 2004.

[61] Kazantzis, N., and C. Kravaris. "Nonlinear Observer Design Using Lyapunov's Auxiliary Theorem." *Systems and Control Letters* 34, 5: (1998) 241–247.

[62] Khalil, H.K. *Nonlinear Systems (3rd Edition.).* Prentice-Hall, 2002.

[63] Kim, K., B. Shafai, and E. Kappos. "Proportional Integral Estimator." In *Proceedings of the Meeting Signal and Data Processing of Small Targets*. Orlando, FL; United States, 1989, 187–208.

[64] Kirchenkamp, S. *PI-Observer Techniques Applied to Mechanical Systems (Dissertation).* University of Duisburg-Essen: Shaker Verlag, Aachen, 2010.

[65] Kopp, R.E., and R.J. Orford. "Linear Regression Applied to System Identification for Adaptive Control Systems." *AIAA Journal* 1, 10: (1963) 2300–2306.

[66] Krajcin, I. *Einsatz des PI-Beobachters zur modellbasierten Diagnose und Regelung elastischer mechanischer Strukturen (Dissertation).* University of Duisburg-Essen: Shaker Verlag, Aachen, 2006.

[67] Krajcin, I., and D. Söffker. "Model-Based Estimation of Contact Forces in Flexible Structures." *Mathematical and Computer Modelling of Dynamical Systems* 10: (2004) 303–316.

[68] ———. "Design of the Proportional Integral Observers for Unknown Input Estimation in Experimental Approaches." In *Proceedings of the 20th ASME Biennial Conference on Mechanical Vibration and Noise*. Long Beach, USA, 2005.

[69] ———. "Diagnosis and Control of 3D Elastic Mechanical Structures." In *Proceedings of the 12th SPIE Symposium on Smart Structures and Materials*. San Diego, CA, USA, 2005.

[70] Kravaris, C., V. Sotiropoulosa, C. Georgioua, N. Kazantzisb, M. Xiao, and A.J. Krener. "Nonlinear Observer Design for State and Disturbance Estimation." *Systems and Control Letters* 56, 11-12: (2007) 730–735.

[71] Krener, A.J., and M. Xiao. "Nonlinear Observer Design in the Siegel Domain." *SIAM Journal on Control and Optimization* 41, 3: (2002) 932–953.

[72] Lee, I., T. Kim, and S. Choi. "Hydraulic Servo System Using a Feedback Linearization Controller and Disturbance Observer - Sensitivity of System Parameters -." In *Proceedings of the 7th JFPS International Symposium on Fluid Power*. Toyama, Japan, Sep. 2008.

[73] Leu, Y.G., T.T. Lee, and W.Y. Wang. "Observer-Based Adaptive Fuzzy-Neural Control for Unknown Nonlinear Dynamical Systems." *IEEE Transactions on Systems, Man, and Cybernetics - Part B: Cybernetics* 29, 5: (1999) 583–591.

[74] Linder, S.P. *Robust Qualitative and Quantitative Methods for Disturbance Rejection and Fault Accommodation (Dissertation)*. Northeastern University, Boston, Massachusetts, United States, 1997.

[75] Linder, S.P., and B. Shafai. "Robust PFI Kalman Filters." In *Proceedings of the American Control Conference*. Philadelphia, Pennsylvania, 1998.

[76] Liu, C.S., and H. Peng. "Disturbance Observer Based Tracking Control." *ASME Journal of Dynamic Systems, Measurement, and Control* 122, 2: (2000) 332–335.

[77] ———. "Inverse-Dynamics Based State and Disturbance Observers for Linear Time-Invariant Systems." *ASME Journal of Dynamic Systems, Measurement, and Control* 124, 3: (2002) 375–381.

[78] Liu, Y., and D. Söffker. "Improvement of Optimal High-Gain PI-Observer Design." In *Proceedings of the European Control Conference ECC 2009 (ECC'09)*. Budapest, Hungary, Aug. 2009.

[79] Liu, Y., and D. Söffker. "Robust Control Approach for Input-Output Linearizable Nonlinear Systems with Modeling Errors based on High-Gain PI-Observer." In *Proceedings of the 6th Mathmod*. Vienna, Austria, Feb. 2009.

[80] Liu, Y., and D. Söffker. "Robust Approach for Position Control of Hydraulic Differential Cylinder." In *Proc. of the ASME IDETC/CIE 2007*. Las Vegas, Nevada, USA, Sep. 2007.

[81] ———. "A Robust Control Design Approach Combining Exact Linearization and High-Gain PI-Observer." In *Proc. of the ASME IDETC/CIE 2007*. Las Vegas, Nevada, USA, Sep. 2007.

[82] ———. "New Development of Optimal High-Gain PI-Observer Design." In *Proceedings of the 9th International Conference on Motion and Vibration Control (MoViC)*. Munich, Germany, Sep. 2008.

[83] Liu, Y., and J. Zhang. "Minimal-Order Observer and Output-Feedback Stabilization Control Design of Stochastic Nonlinear Systems." *Science in China Series F: Information Sciences* 47, 4: (2004) 527–544.

[84] Lückel, J., and P.C. Müller. "Verallgemeinerte Störgrößenaufschaltung bei unvollständiger Zustandskompensation am Beispiel einer aktiven Federung." *Regelungstechnik* 27: (1979) 281–288.

[85] Luenberger, D.G. "Observing the State of a Linear System." *IEEE Transactions on Military Electronics* 8: (1964) 74–80.

[86] ———. "Observers for Multivariable Systems." *IEEE Transactions on Automatic Control* 11, 2: (1966) 190–197.

[87] ———. "An Introduction to Observers." *IEEE Transactions on Automatic Control* 16, 6: (1971) 596–602.

[88] Lunze, J. "An Example for the Design of Switching Observers." *at - Automatisierungstechnik* 48: (2000) 556–562.

[89] Marino, R., and P. Tomei. "Robust Stabilization of Feedback Linearizable Time-Varying Uncertain Nonlinear Systems." *Automatica* 29: (1993) 181–189.

[90] Marx, B., D. Koenig, and D. Georges. "Robust Fault Diagnosis for Linear Descriptor Systems using Proportional Integral Observers." In *Proceedings of the 24th IEEE Conference on Decision and Control*. 2003, volume 1, 457–462.

[91] Mokhtari, A., A. Benallegue, and B. Daachi. "Robust Feedback Linearization and GH_{inf} Controller for a Quadrotor Unmanned Aerial Vehicle." *Journal of Electrical Engineering* 57: (2006) 20–27.

[92] Müller, P.C. "Control of Nonlinear Systems by Applying Disturbance Rejection Control Techniques." In *International Conference on Control 88*. Institution of Electrical Engineers, 1988, 734–737.

[93] ———. "Indirect Measurement of Nonlinear Effects by State Observers. in: W. Schiehlen (Ed.), Nonlinear Dynamics in Engineering Systems." *Springer* 205–215.

[94] ———. "Robust Independent Joint Control of Robots by Estimating and Compensation of Coupling, Uncertain, Nonlinear Effects." In *Proceedings of the 1st International Symposium Mathematical Models in Automation and Robotics*. Institute of Control Engineers, Technical University of Szczecin, 1994, 404–409.

[95] ———. *Anmerkungen zum sogenannten 'High-gain-Beweis' des PI-Beobachters.* Personal notes, 2008.

[96] Müller, P.C., and C. Başpinar. "Convergence of Nonlinearity Estimations by Linear Estimators." *Zeitschrift für Angewandte Methematik und Mechanik* 80: (2000) 325–326.

[97] Müller, P.C., and J. Lückel. "Zur Theorie der Störgrößenaufschaltung in linearen Mehrgrößenregelsystemen." *Regelungstechnik* 25: (1977) 54–59.

[98] Niemann, H.H., J. Stoustrup, B. Shafai, and S. Beale. "LTR Design of Proportional-Integral Observers." *International Journal of Robust and Nonlinear Control* 5, 7: (1995) 671–693.

[99] Nijmeijer, H., and T.I. Fossen. *New Directions in Nonlinear and Observer Design.* London, New York: Springer, 1999.

[100] O'Reilly, J., and M.M. Newmann. "Minimal-Order Observer-Estimators for Continuous-Time Linear Systems." *International Journal of Control* 22, 4: (1975) 573 590.

[101] Park, C. "Robust Stable Fuzzy Control via Fuzzy Modeling and Feedback Linearization with its Applications to Controlling Uncertain Single-Link Flexible Joint Manipulators." *Journal of Intelligent and Robotic Systems* 39: (2004) 131–147.

[102] Park, Y., and J.L. Stein. "Closed-Loop, State and Input Observer for Systems with Unknown Inputs." *International Journal of Control* 48, 3: (1988) 1121–1136.

[103] Petersen, I.R. "Robust H_∞ Control of an Uncertain System Via a Stable Output Feedback Controller." *IEEE Transactions on Automatic Control* 54, 6: (2009) 1418–1423.

[104] Polycarpou, M.M., and P.A. Ioannou. "Robust Adaptive Nonlinear Control Design." *Automatica* 32: (1996) 423–427.

[105] Profeta, J.A., W.G. Vogt, and M.H. Mickle. "Disturbance Estimation and Compensation in Linear Systems." *IEEE Transactions on Aerospace and Electronic Systems* 26, 2: (1990) 225–231.

[106] Rami, M.A., S.E. Faiz, A. Benzaouia, and F. Tadeo. "Robust Exact Pole Placement via an LMI-Based Algorithm." *IEEE Transactions on Automatic Control* 54, 2: (2009) 384–398.

[107] Rodrigues, L., and J.P. How. "Observer-Based Control of Piecewise-Affine Systems." *International Journal of Control* 76, 5: (2003) 459477.

[108] Schrijver, E., J. Dijk van, and H. Nijmeijer. "Equivalence of Disturbance Observer Structures for Linear Systems." In *Proceedings of the 39th IEEE Conference on Decision and Control*. Sydney, Australia, 2000, volume 5, 4518–4519.

[109] Shafai, B., S. Beale, H. Niemann, and J. Stoustrup. "LTR Design of Discrete-Time Proportional-Integral Observers." *IEEE Transactions on Automatic Control* 41, 7: (1996) 1056–1062.

[110] Shafai, B., and R.L. Carroll. "Design of Proportional-Integral Observer for Linear Time-Varying Multivariable Systems." In *Proceedings of the 24th IEEE Conference on Decision and Control*. Ft. Lauderdale, FL, 1985, volume 24, 597–599.

[111] Shafai, B., and H.M. Oloomi. "Output Derivative Estimation and Disturbance Attenuation using PI Observer with Application to a Class of Nonlinear Systems." In *Proceedings of the 35th Southeastern Symposium on System Theory*. 2003, 196–200.

[112] Shafai, B., C.T. Pi, and S. Nork. "Simultaneous Disturbance Attenuation and Fault Detection using Proportional Integral Observers." In *Proceedings of the American Control Conference*. Anchorage, AK, 2002, 1647–1649.

[113] Shafai, B., C.T. Pi, S. Nork, and S.P. Linder. "Proportional Integral Adaptive Observer for Parameter and Disturbance Estimations." In *Proceedings of the 41st IEEE Conference of Decision and Control*. 2002, volume 4, 4694–4699.

[114] Slotine, J.J.E., and W. Li. *Applied Nonlinear Control*. Englewood Cliffs, New Jersey: Prentice-Hall, 1991.

[115] Söffker, D. "New Results of the Development and Application of Robust Observers to Elastic Mechanical Structures, in: H. Ulbrich, W. Günthner (Eds.), Vibration Control of Nonlinear Mechanism and Structures, Solid Mechanics and its Applications." *Springer* 130: (2005) 319–330.

[116] Söffker, D., J. Bajkowski, and P.C. Müller. "Detection of Cracks in Turbo Rotors - A New Observer Based Method." *ASME Journal of Dynamic Systems, Measurement, and Control* 3: (1993) 518–524.

[117] Söffker, D., and P.C. Müller. "Control of Dynamic Systems with Nonlinearities and Time Varying Parameters." *ASME Proceedings of Dynamics and Vibration of Time-Varying Systems and Structures* 56: (1993) 269–277.

[118] Söffker, D., T. Yu, and P.C. Müller. "State Estimation of Dynamical Systems with Nonlinearities by using Proportional-Integral Observer." *International Journal of Systems Science* 26: (1995) 1571–1582.

[119] Spong, M.W., and M. Vidyasagar. *Robot Dynamics and Control*. New York: John Wiley and Sons, 1989.

[120] Stein, J.L., and Y. Park. "Measurement Signal Selection and a Simultaneous State and Input Observer." *ASME Journal of Dynamic Systems, Measurement, and Control* 110, 2: (1988) 151–159.

[121] Tar, J.K., J.F. Bitó, B. Pátkai, and A. Bencsik. "Non-linear Improvement of an Intelligent Adaptive Controller Designed for Hydraulic Differential Servo Cylinders." In *Proceedings of the 1st Slovakian-Hungarian Joint Symposium on Applied Machine Intelligence (SAMI 2003)*. Herlany, Slovakia, 2003, 75–86.

[122] Trumpf, J. "Observers for Linear Time-Varying Systems." *Linear Algebra and its Applications* 425: (2007) 303–312.

[123] Tsui, C. "Function-Observer Design for a Class of Linear Time-Varying System." *International Journal of Control* 44, 1: (1986) 277–282.

[124] Umeno, T., T. Kaneko, and Y. Hori. "Robust Servosystem Design with Two Degrees of Freedom and its Application to Novel Motion Control of Robot Manipulators." *IEEE Transactions on Industrial Electronics* 40, 5: (1993) 473–485.

[125] Vahedforough, E., and B. Shafai. "Design of Proportional Integral Adaptive Observers." In *Proceedings of the American Control Conference*. Washington, USA, 2008, 3683–3688.

[126] Wada, N., and M. Saeki. "An LMI Based Scheduling Algorithm for Constrained Stabilization Problems." *Systems and Control Letters* 57, 3: (2008) 255–261.

[127] Wang, S.H., E.J. Davison, and P. Dorato. "Observing the States of Systems with Unmeasurable Disturbances." *IEEE Transactions on Automatic Control* 20, 5: (1975) 716–717.

[128] Weinmann, A. *Uncertain Models and Robust Control*. Wein, New York: Springer, 1991.

[129] Wimmer, H.K. "Monotonicity of Maximal Solutions of Algebraic Riccati Equations." *Systems and Control Letters* 5: (1985) 317–319.

[130] Wojciechowski, B. *Analysis and Synthesis of Proportional-Integral Observers for Single-Input Single-Output Time-Invariant Continuos Systems*. Gliwice, Poland, 1978.

[131] Wu, Z., and W. Zhou. "Delay-Dependent Robust H_∞ Control for Uncertain Singular Time-Delay Systems." *IET Control Theory and Applications* 1, 5: (2007) 1234–1241.

[132] Yaz, E., and A. Azemi. "Observer Design for Discrete and Continuous Nonlinear Stochastic Systems." *International Journal of Systems Science* 24, 12: (1993) 2289–2302.

[133] Zeitz, M. "The Extended Luenberger Observer for Nonlinear Systems." *Systems and Control Letters* 9: (1987) 149–156.